

Lehrstuhl für Ernährungsphysiologie

Phenotypic characterization of peptide transporter PEPT2
deficient mice: assessing complex metabolic alterations by
profiling techniques

Isabelle Maria Anna Frey

Vollständiger Abdruck der von der Fakultät Wissenschaftszentrum Weihenstephan für
Ernährung, Landnutzung und Umwelt der Technischen Universität München zur Erlangung
des akademischen Grades eines

Doktors der Naturwissenschaften

genehmigten Dissertation.

Vorsitzender:	Univ.-Prof. Dr. Dirk Haller
Prüfer der Dissertation:	1. Univ.-Prof. Dr. Hannelore Daniel
	2. Univ.- Prof. Dr. Michael Schemann
	3. Univ.- Prof. Dr. Francois Verrey
	Universität Zürich / Schweiz
	(schriftliche Beurteilung)

Die Dissertation wurde am 29.08.2007 bei der Technischen Universität München
eingereicht und durch die Fakultät Wissenschaftszentrum Weihenstephan für
Ernährung, Landnutzung und Umwelt am 10.12.2007 angenommen.

Table of Contents

Table of Contents

Zusammenfassung	1
Summary	2
Introduction	3
1. Brief history of the discovery of peptide transport and peptide transporters	3
2. The PTR superfamily	5
3. Molecular and genetic attributes of mammalian peptide transporters	6
4. Determinants of substrate recognition and transport by PEPT1 and PEPT2	8
5. Localization, Function and Regulation of PEPT1 and PEPT2	10
6. The mouse as a model system for functional genomics	20
7. Application of profiling techniques for phenotyping of mutant mice	22
Aim of the Thesis	25
Materials	27
1. Laboratory animals	27
2. Chemicals and consumables	27
3. Instruments	27
Methods	28
1. Mouse husbandry, handling and sample collection	28
1.1 Mouse husbandry	28
1.2 Genotyping	28
1.3 Data sampling for weight, organ weight, litter size and lifespan	29
1.4 Collection of plasma, urine and tissue samples	29
1.5 Dietary intervention study	30
1.6 Blood pressure determination	31
2. Analysis of selected metabolites in body fluids and tissue	31
2.1 Protein, urea and creatinine concentration and osmolality of urine samples	31
2.2 Free and peptide bound amino acids in urine, plasma and tissue	31

Table of Contents

2.3	Clinical chemical parameters in plasma and urine	32
2.4	Glucagon in plasma	33
2.5	Thiol compounds in urine, plasma and tissue	33
3.	mRNA expression analysis of individual genes	34
3.1	Northern Blot analysis for mRNA expression of <i>Pept1</i> , <i>Pht1</i> and <i>Pht2</i>	34
3.2	Gene expression analysis by qPCR	34
4.	Characterization of kidney tissue by profiling techniques	35
4.1	Transcriptome analysis by cDNA microarrays	35
4.2	Proteome analysis by 2D-PAGE and MALDI-TOF-MS	36
4.3	Metabolite analysis by GC-TOF-MS	37
5.	Statistics	38
Results		39
1.	Basal phenotypic characterization of <i>Pept2</i> ^{-/-} mice	39
1.1	Body weight and organ weight	39
1.2	Litter size and weight at weaning	40
1.3	Lifespan	42
1.4	Urine parameters and amino acids in urine	42
1.5	Compensatory regulation of related peptide transporters in the kidney	45
1.6	Clinical-chemical parameters and free amino acids in plasma	46
1.7	Blood pressure	49
1.8	Glucagon	50
2.	Response to different dietary protein contents	51
2.1	Weight, food and water intake during the metabolic study	51
2.2	Clinical chemical plasma and urine parameters	52
2.3	Amino acids and dipeptides in urine	56
2.4	Additional ninhydrine positive metabolites in <i>Pept2</i> ^{-/-} urine samples	59
2.5	Gene expression in kidney tissue	61
3.	Characterization of kidney tissue by profiling techniques	64
3.1	Transcriptome analysis by cDNA microarrays and qPCR	64
3.2	Proteome analysis by 2D-PAGE and MALDI-TOF-MS	66
3.3	Metabolite analysis by GC-TOF-MS	70
3.4	Classification of processes and pathway analysis	72
4.	Analysis of constituents of glutathione metabolism	78
4.1	Urinary excretion of Cys-Gly	78

Table of Contents

4.2	GSH in urine, plasma and kidney tissue	79
4.3	Analysis of changes at mRNA level of genes involved in GSH-metabolism	80
Discussion		83
1.	Basal phenotypic characterization	83
2.	Response to different dietary protein contents	85
3.	Characterization of kidney tissue by profiling techniques	89
3.1	Methodological aspects of the applied profiling techniques	89
3.2	Integrated analysis of kidney tissue at mRNA, protein and metabolite level in combination with urine analysis reveals alterations in renal amino acid and glutathione metabolism	100
4.	Future perspectives	105
Appendix		109
1.	Complete lists of differentially expressed genes	109
2.	Oligonucleotide primers for qPCR	117
3.	List of abbreviations	119
References		123
Erklärung		141
Curriculum Vitae		143
Danksagung		147

List of Tables

List of Tables

Table 1: PTR family members in animals, bacteria, plants and fungi	5
Table 2: Molecular characteristics of the human POT genes and murine <i>Pept2</i>	7
Table 3: Relative organ weights	40
Table 4: Number and mean age of deceased animals during 2 years of follow-up	42
Table 5: Urine parameters in 24 h urine samples	43
Table 6: Free and dipeptide bound amino acids in urine of male and female mice	44
Table 7: Clinical chemical parameters in male and female mice	47
Table 8: Free amino acids in plasma of male and female mice	48
Table 9: Body weight and food and water intake in response to different protein content of the diet	52
Table 10: Clinical chemical parameters on diets with different protein content	53
Table 11: Urine parameters in response to diets with different protein content	55
Table 12: Free and dipeptide bound amino acids in urine	57
Table 13: Expression of genes involved in peptide and amino acid metabolism	62
Table 14: Changes in protein level in kidney tissue of PEPT2 deficient animals	67
Table 15: Metabolites in kidney tissue that contribute most to differentiation between genotypes	71
Table 16: Differentially expressed genes involved in amino acid metabolism	73
Table 17: Differentially expressed genes involved in fatty acid metabolism	74
Table 18: GSH in kidney tissue, urine and plasma	79
Table 19: Expression of genes involved in GSH metabolism	81
Table 20: Genes with elevated mRNA levels in <i>Pept2</i> ^{-/-} animals as identified by VarMixt	109
Table 21: Genes with decreased mRNA levels in <i>Pept2</i> ^{-/-} animals as identified by VarMixt	113
Table 22: Differentially expressed genes in <i>Pept2</i> ^{-/-} animals as identified by PAM	116
Table 23: Primers for housekeeping genes	117
Table 24: Primers for genes involved in peptide and amino acid transport and metabolism	117
Table 25: Primers for validation of microarray results	118
Table 26: Primers for genes involved in GSH metabolism	118

List of Figures

List of Figures

Fig. 1:	Main physiological function of mammalian PEPT1 and PEPT2	4
Fig. 2:	Structural elements defining substrate affinity (from (49))	9
Fig. 3:	PEPT1 and PEPT2 in the context of the epithelial cell	13
Fig. 4:	Renal accumulation of labelled model dipeptides	15
Fig. 5:	Relationship between different "omics" disciplines (from (55))	22
Fig. 6:	Monitoring of body weight over 25 weeks	39
Fig. 7:	Litter size at birth and surviving pups at weaning	41
Fig. 8:	Dipeptide bound glycine in male and female mice	45
Fig. 9:	Expression of PHT1 in kidney	46
Fig. 10:	Mean arterial blood pressure in male and female mice	49
Fig. 11:	Plasma glucagon levels in male and female mice	50
Fig. 12:	Dipeptide bound glycine and cystine in urine	58
Fig. 13:	Detection of additional ninhydrine positive metabolites in <i>Pept2</i> ^{-/-} urine samples	59
Fig. 14:	Peak area of compound Y in relation to creatinine	60
Fig. 15:	Expression of <i>Eaf2</i> and <i>Pept2</i> in the parental strains 129Sv and C57Bl/6	66
Fig. 16:	2D-PAGE analysis of proteins from kidney tissue samples (see next page)	68
Fig. 17:	Multivariate data analysis of metabolites	70
Fig. 18:	Biological processes (GO) affected by loss of PEPT2	72
Fig. 19:	Pathways affected by loss of PEPT2 (see next page)	76
Fig. 20:	Urinary cysteinyl-glycine in male and female mice	78
Fig. 21:	Schema of GSH metabolism in epithelial cells of the proximal tubule	104

Zusammenfassung

In Säugetieren wird die zelluläre Aufnahme von Di- und Tripeptiden durch die protonengetriebenen Transporter PEPT1 und PEPT2 vermittelt. PEPT2 ist in einer Vielzahl von Geweben lokalisiert mit einer besonders starken Expression in Epithelien der Niere und Lunge, jedoch ist bislang wenig über die physiologische Bedeutung des PEPT2 vermittelten Peptidtransports bekannt. In der vorliegenden Arbeit lieferte die Untersuchung eines *Pept2*-defizienten Mausmodells neue Erkenntnisse über die Funktion von PEPT2 und gab Einblicke in Adaptationsmechanismen, die durch das Fehlen des Transporters auftreten.

Eine erste grundlegende Phänotypisierung der *Pept2*^{-/-} Mäuse zeigte geringfügige Abweichungen bei den relativen Organgewichten, der Überlebensrate der Jungen aus homozygoten Verpaarungen und bei einzelnen klinisch-chemischen Parametern, jedoch keine Auswirkungen auf die Wurfgröße, Lebenserwartung, Blutdruck oder Glukagonspiegel. Obwohl die renale Akkumulation markierter Modellsubstrate in den *Pept2*^{-/-} Mäusen deutlich reduziert ist, war nur die Ausscheidung an peptidgebundenem Glycin und Cystin signifikant erhöht. Die Ausscheidung an peptidgebundenen Aminosäuren erhöhte sich mit zunehmendem Proteingehalt der Nahrung, während eine adaptive Überexpression der Aminosäuretransporter *Slc6a19* und *Slc7a7* bei niedriger und mittlerer Proteinzufuhr zu beobachten war. *Pept2*-defiziente Mäuse passen darüber hinaus ihre Futteraufnahme dem Proteingehalt der Nahrung an, mit höherer Aufnahme bei niedrigem Proteingehalt und niedrigerer Aufnahme bei hohem Proteingehalt.

Um einen umfassenden Überblick über die Mechanismen zu erhalten, die zum insgesamt unauffälligen Phänotyp der *Pept2*^{-/-} Tiere führen, wurde Nierengewebe auf Transkriptom-, Proteom- und Metabolom-Ebene untersucht. Eine Klassifizierung der differentiell exprimierten Genprodukte anhand der Gene Ontology (GO) Kategorien für biologische Prozesse zeigte, dass vor allem mRNA-Spezies und Proteine des Aminosäurestoffwechsels betroffen sind. Dementsprechend waren Aminosäuren die am stärksten veränderten Metabolite in Nierengewebe von *Pept2* defizienten Mäusen. Die niedrigeren Konzentrationen an Cystein, Glycin und Oxoprolin im Zusammenspiel mit veränderter Expression von Enzymen des Glutathion (GSH) Stoffwechsels auf mRNA und Proteinebene und drastisch erhöhter Ausscheidung des Dipeptids Cys-Gly lassen vermuten, dass PEPT2 vor allem für die Rückresorption von Cys-Gly aus dem GSH Abbau verantwortlich ist. Die PEPT2 vermittelte Rückresorption von Cys-Gly könnte einen wichtigen Beitrag zur Bereitstellung von Substraten für die epitheliale GSH Synthese leisten. Die umfassende Transkriptom-, Proteom- und Metabolom-Analyse hat somit neue Erkenntnisse über eine bislang unbekannt Funktion des Peptidtransporters PEPT2 in der Niere geliefert.

Summary

Cellular uptake of di- and tripeptides is mediated in mammals by the proton coupled peptide transporters PEPT1 and PEPT2. PEPT2 shows widespread expression throughout the organism, predominantly in epithelia of kidney and lung. Yet, little is known about the physiological relevance of PEPT2 mediated peptide transport. In the present thesis the characterization of a mouse model deficient in the PEPT2 transporter (*Pept2*^{-/-}) provided novel insights into the function of PEPT2 and the adaptive mechanisms that compensate for the loss of PEPT2.

Basal phenotypic characterization of *Pept2*^{-/-} mice revealed subtle differences with regard to relative organ weights, survival rate of pups from homozygotic litters, and selected clinical-chemical parameters, but no effects on litter size, lifespan, blood pressure, or glucagon levels were observed. Although renal accumulation of labelled model dipeptides is markedly reduced in the transporter deficient animals, urinary excretion of dipeptide bound amino acids was markedly increased for glycine and cystine, only. Peptide bound amino acid excretion in *Pept2*^{-/-} animals increased with protein content of the diet whereas in kidney the adaptive upregulation of the amino acid transporters *Slc6a19* and *Slc7a7* was observed on low and medium dietary protein levels. Transporter deficient animals adjusted their food intake to protein content of the diet with higher intake on the low protein diet and lower intake on the high protein diet.

In order to obtain a comprehensive overview over the alterations resulting in the silent phenotype of *Pept2*^{-/-} animals, we analyzed kidney tissue samples with transcriptome, proteome and metabolome profiling techniques. Classification of differentially expressed gene products according to gene ontology (GO) categories for biological processes revealed that predominantly amino acid metabolism is affected in the transporter-deficient animals. Accordingly, lower amino acid levels in *Pept2*^{-/-} kidneys constituted the most consistent changes of metabolite levels between genotypes. The lower concentrations of cysteine, glycine and oxoproline in kidney tissue together with altered expression of mRNA and proteins involved in GSH metabolism and a drastically increased excretion of the dipeptide cys-gly suggest that PEPT2 is predominantly a system for reabsorption of cys-gly originating from GSH breakdown. PEPT2 mediated uptake of cys-gly might constitute an important route of substrate delivery for GSH resynthesis. Application of profiling techniques thus provided evidence for a previously unanticipated novel function of PEPT2 in kidney.

Introduction

1. Brief history of the discovery of peptide transport and peptide transporters

Uptake of nutrients is essential in all kingdoms of life. As the lipid bilayer of the cell membrane is more or less impermeable to hydrophilic substances, specific carrier systems are needed to mediate the translocation of small water soluble molecules across the membrane. Today a wide range of different transmembrane transport proteins is known, that each conveys the specific transfer of a certain class of compounds. Carrier proteins and channel proteins form the two major classes of membrane transport proteins. Members of the latter form aqueous pores through the membrane that can be traversed by specific solutes along their concentration gradient whereas carrier proteins (often also called transporters) bind the compound and mediate its translocation across the membrane by a number of conformational changes. Apart from passive transport, carrier proteins can also mediate active transport against an electrochemical gradient either directly energized by ATP hydrolysis (primary active transport) or by coupling of the uphill transport of one solute to the downhill transport of another (secondary or tertiary active transport)(10, 130).

In mammals the main sites for absorption and reabsorption of nutrients are the small intestine and the kidney. Uptake of organic nutrients like sugars, amino acids and peptides is predominantly mediated by indirectly energized transporters of the solute carrier (SLC) gene series. At present it comprises 46 SLC families with 360 individual transporter genes identified, so far (1).

Uptake of amino acids in peptide bound form was first described in prokaryotes (118, 212) and it took more than 20 years until in vivo perfusion studies demonstrated in 1971 that intact dipeptides can also be absorbed in the human small intestine (2, 9). In the following years functional characterization of intestinal peptide transport described a transport system that is capable of the translocation of di- and tripeptides, but not free amino acids or tetrapeptides (7, 8). Accumulation of the hydrolysis resistant dipeptide glycyl-sarcosine in kidney tissue was a first indicator of a peptide transport system in the kidney (6). During this period it was hypothesized that the uptake of peptides against a concentration gradient is energized by sodium (Na^+), as at that time all mammalian transport systems for nutrient uptake were

driven by an electrochemical Na^+ gradient or solely by the substrate gradients via uniport or antiport processes. In contrast, nutrient flux across the cell membrane of bacteria, yeast and plants is predominantly driven by an electrochemical proton gradient. Thus it was a surprising finding when studies on rabbit intestinal brush border membrane vesicles in 1984 demonstrated that mammalian dipeptide transport is rather proton (H^+) than Na^+ dependent (83). Further studies provided evidence for the existence of two peptide transport systems one with high and one with low substrate affinity (210), the proton dependence could be assigned to the cotransport of H^+ with the substrate (53) and structural determinants of substrate affinity were explored (52) revealing that peptidomimetics like β -lactam antibiotics are also translocated by peptide transport systems (50). Detailed information about the functional characteristics will be given in later sections.

A new era in the research on peptide transport began in 1994 with the cloning of the low affinity peptide transporter (31, 71) from rabbit small intestine and the high affinity system was cloned little later from human and rabbit kidney (30, 204). In the order of their cloning the low affinity system was termed PEPT1 (Slc15a1) and the high affinity system PEPT2 (Slc15a2).

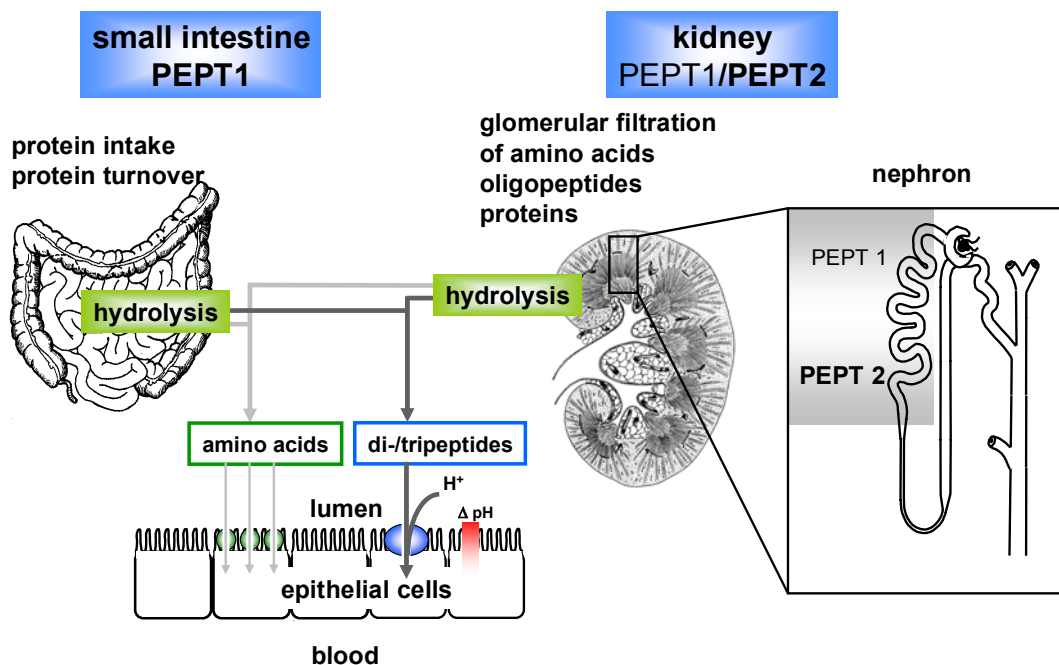


Fig. 1: Main physiological function of mammalian PEPT1 and PEPT2

The mammalian peptide transporters PEPT1 and PEPT2 mediate the uptake of di- and tripeptides driven by an inwardly directed electrochemical proton gradient. The highest expression of PEPT1 is found in the small intestine where it is responsible for the absorption of dietary peptides. Although PEPT1 is also expressed in the kidney, PEPT2 has been shown to be the predominant transporter for reabsorption of peptides from the glomerular filtrate.

PEPT1 represents the intestinal peptide transporter and PEPT2 is the predominant isoform in the kidney as depicted in Fig. 1. Two further mammalian peptide transporters PHT1 (Slc15a4) (257) and PHT2 (SLC15a3) (190) were later cloned from brain. They differ from PEPT1 and PEPT2 in that they transport the amino acid histidine in addition to peptides, but their functional characteristics have been explored much less so far.

2. The PTR superfamily

The mammalian peptide transporters belong to the **peptide transporter (PTR)** family (214) which is also called more precisely **proton coupled oligopeptide transporter (POT)** superfamily (167). Members of the family can be found in all kinds of living organisms and a variety of PTR transporters in different species is listed exemplarily in Table 1.

Table 1: PTR family members in animals, bacteria, plants and fungi

Species	Transporter	Gene	Protein	AA	Reference
<i>H. sapiens</i>	PEPT1	SLC15A1	NP_005064	708	(126)
<i>M. musculus</i>	PEPT1	SLC15A1	NP_444309	709	(75)
<i>R. norvegicus</i>	PEPT1	SLC15A1	NP_476462	710	(189)
<i>O. cuniculus</i>	PEPT1	SLC15A1	AAA17721	707	(71)
<i>D. rerio</i>	PEPT1	SLC15A1	NP_932330	718	(235)
<i>C. elegans</i>	PEP-2	pep-2 (opt-2)	NP_509087	835	(70)
<i>H. sapiens</i>	PEPT2	SLC15A2	NP_066568	729	(204)
<i>M. musculus</i>	PEPT2	SLC15A2	NP_067276	740	(184)
<i>R. norvegicus</i>	PEPT2	SLC15A2	NP_113860	729	(189)
<i>O. cuniculus</i>	PEPT2	SLC15A2	AAC48495	729	(31)
<i>D. rerio</i>	PEPT2	zgc: 152684	NP_001034917	719	(183)
<i>C. elegans</i>	PEP-1	pep-1(opt-1)	NP_502002	785	(70)
<i>D. melanogaster</i>	OPT1a	OPT1a (yin)	NP_477147	743	(182)
<i>H. sapiens</i>	PHT1	SLC15A4	NP_663623	577	(33)
<i>M. musculus</i>	PHT1	SLC15A4	NP_598656	574	(240)
<i>R. norvegicus</i>	PHT1	SLC15a4	NP_653359	572	(257)
<i>H. sapiens</i>	PHT2	SLC15A3	NP_057666	581	(33)
<i>M. musculus</i>	PHT2	SLC15A3	NP_075531	578	(217)
<i>R. norvegicus</i>	PHT2	SLC15A3	NP_647557	582	(190)
<i>S. cerevisiae</i>	Ptr2	PTR2	NP_013019	601	(63)
<i>L. lactis</i>	DtpT	dtpT	NP_266858	497	(32)
<i>E. coli</i>	TppB (ydgR)	tppB	NP_416151	500	(167)
<i>A. thaliana</i>	ATPTR2-B	ATPTR2-B	NP_178313	585	(213)
<i>A. thaliana</i>	NRT1.1(CHL1)	NRT1.1	NP_563899	590	(103)
<i>C. albicans</i>	PTR2	PTR2	P46030	623	(20)
<i>H. lixii</i>	PTR2	ThPTR2	CAI30793	557	(236)

Members of the PTR family vary in size from 450 to more than 800 amino acids. Generally the eukaryotic proteins are larger than bacterial transporters. The main substrates are di- and tripeptides, yet some bacterial transporters have been shown to accept tetrapeptides as well. POT members in plants e.g. NTR1.1 mediate the transport of nitrates, histidine and di- and tripeptides, and the PHT proteins appear to be phylogenetically similar to these representatives of the PTR family. For many of the PTR members identified yet, only limited data on functional characterization is available. So far it has not been possible to crystallize any member of the PTR family, thus the membrane topology of the transporters is mainly derived from hydropathy plots of the amino acid sequences. The proteins are predicted to contain 12 transmembrane domains (TMD) with the carboxy (C)- and amino (N)-termini facing the cytosol and a large extracellular loop between the TMDs 9 and 10. All members of the PTR family contain short amino acid sequence motifs that are highly conserved. The most conserved motif (PTR2-2) is located in TMD 5 (FYING-PTR-motif) consisting of 11 amino acids. Introduction of point mutations into this area of the transporters led to loss of transport or altered substrate preference indicating that the region is essential for substrate interaction (204, 260). Two further conserved motifs are found at the extracellular end of the first TMD reaching into the following extracellular loop (PTR2-1) and from the second half of the second TMD stretching into the first amino acids of the third TMD (PTR2-3).

3. Molecular and genetic attributes of mammalian peptide transporters

Within the mammalian peptide transporters human PEPT1 and PEPT2 share 50% sequence identity and about 70% sequence similarity (204). Only weak sequence similarity (20-25%) is found between the PEPT and PHT proteins whereas PHT1 and PHT2 show again 53% sequence identity (33). There is high sequence identity of 80-90% between the orthologues of a given transporter in human, mouse, and rat. *Pept2* maps to a region of mouse chromosome 16 that is syntenic to human chromosome 3q13.3-q21 (184). Further characteristics of the human POT genes and the murine PEPT2 gene are given in Table 2. For some of the POT genes alternative transcripts are predicted or have been verified experimentally. A splicing variant of PEPT1 *hPept1-RF* consists of 6 exons coding for 208 amino acids. When expressed alone

hPept1-RF does not show transport activity whereas coexpression with PEPT1 in *Xenopus* oocytes led to a shift in pH sensitivity of peptide transport (188). Several alternative transcripts can be deduced from the hPHT1 sequence, and an additional band has been observed in RT-PCR and Northern blot experiments (33). Of the four splicing variants predicted for hPht2 none has been verified experimentally so far.

Table 2: Molecular characteristics of the human POT genes and murine Pept2

Gene	<i>hPept1</i>	<i>hPept2</i>	<i>mPept2</i>	<i>hPht1</i>	<i>hPht2</i>
gene locus	13q33-q34	3q13.3-q21	between D16Mit11 and D16Mit99	11q12.1	12q24.32
Exons	23	22	22	8	8
cDNA (bp)	2127 bp	2846	3991	2807	2113
Sequence ID	NM_005073	NM_021082	NM_021301	NM_145648	NM_016582
splicing variants	<i>hPept1-RF</i>	-	-	≥ 1 alternative transcript	4 alternative transcripts predicted
amino acids	708	729	740	577	581
core protein mass (kD)	78,8	81,9	82,9	62	64,5
experimental protein mass (kD)	80	97	100	83	n.A.
N-linked glycosylation sites ¹	7	3	2	4	n.A.
PKC sites ¹	2	5	2	11	n.A.
PKA sites ¹	-	-	-	2	n.A.
Expression	intestine, kidney, bile	kidney, brain, lung, mammary gland, male/female reproductive tract, pancreas	kidney, brain, lung, mammary gland, male/female reproductive tract, pancreas	skeletal muscle, kidney, heart, liver, colon, brain	spleen, lung, placenta, leukocytes, heart, kidney, liver

1, putative, deduced from sequence

A number of N-linked glycosylation sites have been predicted for the mammalian POT transporters but have not been verified experimentally so far, apart from the observation of higher protein masses in Western blot analyses than predicted for the core protein. The role of the predicted protein kinase C (PKC) phosphorylation sites has likewise not been studied systematically for the human transporters, yet there is evidence from a porcine renal cell model (LLC-PK cells) that activation of PKC leads

to a decreased transport rate of PEPT2 (249) and that a likewise decrease in V_{\max} of PEPT1 mediated peptide transport is a consequence of PKC activation a human intestinal cell model (Caco-2 cells) (36). Protein kinase A (PKA) phosphorylation sites were identified in the PHT transporters and in the non-human peptide transporters, only, but their role in regulation of transport function has not been studied so far. A number of amino acids have been identified to be essential for substrate recognition or translocation in PEPT1 and PEPT2. His57 in PEPT1 and His87 in PEPT2 represent a conserved histidyl residue that is vital for transport function as mutants did not display any peptide transport (73). Due to the imidazole structure of the histidyl side chain it can be assumed that it is involved in the proton binding and/or translocation. Mutation of His142 to arginine in PEPT2 reduced transport activity to 30% of the wildtype transporter. Another mutation that leads to loss of transport function of PEPT2 is Arg57His, which is of special interest as this polymorphism has been reported to be present in *hPept2* in the public SNP database (<http://www.ncbi.nlm.nih.gov/SNP/>)(218). However, up to now there is no data available on the frequency of this SNP within the population. Recently a haplotype analysis of 27 SNPs located in *hPept2* revealed that there are two main variants which were referred to as *hPept2*1* and *hPept2*2* (170). The two haplotype variants differed in substrate affinity, pH sensitivity and expression levels of mRNA in the kidney and are both abundant in the population with a frequency of 44-47%. So far it is difficult to estimate the impact of the different biochemical properties of the two haplotypes on peptide handling in man. Yet, neither polymorphisms in PEPT2 nor in any of the mammalian POT transporters have been linked to disease so far.

4. Determinants of substrate recognition and transport by PEPT1 and PEPT2

Transport mediated by PEPT1 and PEPT2 is on the one hand very specific in that both transporters accept exclusively di- and tripeptides, but no free amino acids or tetrapeptides. On the other hand they accept a wide range of substrates as they generally transport all 400 dipeptides and all 8000 tripeptides that can be built from the 20 proteinogenic L-amino acids independent of sequence, size, charge or polarity (24). Transport is stereoselective thus that peptides composed of L-amino acids have higher affinity than peptides including D-enantiomers. In addition all kinds of

peptidomimetic compounds that resemble di- or tripeptides are recognized as substrates. The minimal structural requirements are represented for PEPT1 by ω -amino-pentanoic acid (60) whereas for PEPT2 an additional carbonyl group at a suitable distance to the C-terminal carboxyl group is necessary (225). These minimal structural requirements indicate that a peptide bond is not necessary, but if present it has to be in the *trans* configuration. Pharmacologically relevant peptidomimetic compounds like β -lactam antibiotics, angiotensin converting enzyme (ACE)-inhibitors, bestatin and prodrugs like val-acyclovir or peptidyl-bisphosphonates are substrates of PEPT1 and PEPT2, thus that peptide transporters contribute to the pharmacokinetics of peptidomimetic drugs by determining their intestinal uptake and renal reabsorption. PEPT1 as the intestinal carrier has been studied extensively as a target for oral drug delivery (for review see (185)) and for β -lactam antibiotics a correlation between affinity to PEPT1 and transepithelial uptake has been shown (38). Transport of δ -amino-levulinic acid (ALA) is also of pharmacological relevance as accumulation of this precursor of porphyrinesynthesis can be applied for photosensitizing in photodynamic therapy of tumours (60, 180). For both transporters high affinity inhibitors have been developed (26, 121, 226). The structural elements that determine the substrate affinity to PEPT1 and PEPT2 are summarized in Fig. 2

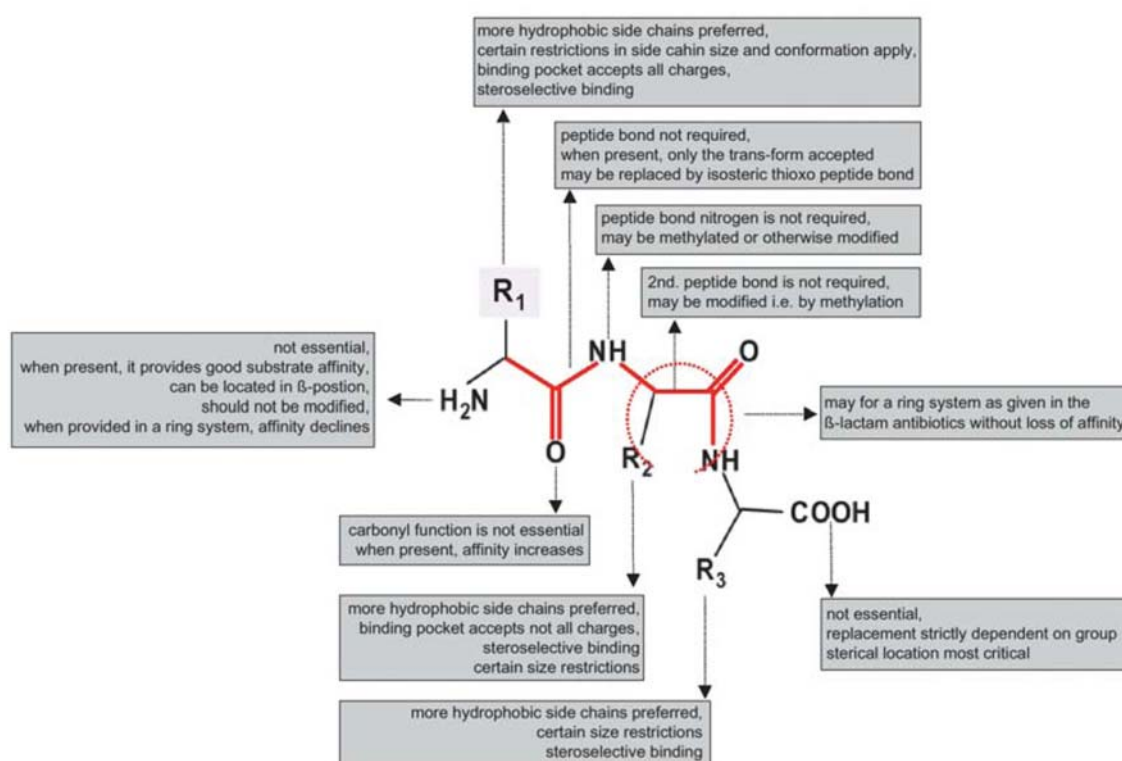


Fig. 2: Structural elements defining substrate affinity (from (49))

Although PEPT1 and PEPT2 transport the same set of substrates, they differ widely in substrate affinity and transport capacity. PEPT1 represents a low affinity, high transport capacity system with substrate affinities in the range of 200 μM – 10 mM whereas PEPT2 is a high affinity, low transport capacity system with substrate affinities approximately 15 times higher than for PEPT1 (5 – 500 μM) (51). β -lactam antibiotics without an α -amino-group like cefixime or ceftibuten are the rare examples of substrates with higher affinity to PEPT1 (82). High affinity substrates for PEPT2 consist of amino acids with hydrophobic side chains and tripeptides with an uncharged amino acid in position three (26).

PEPT1 and PEPT2 mediated transport is always electrogenic with a proton to substrate ratio of 1:1 for PEPT1 and 2:1 for PEPT2 (41) for neutral substrates and variable stoichiometry for charged substrates. The transporters strongly prefer zwitterionic substrates without net charge (14, 74). Their pH optimum lies in the range of pH 4.5 - 6.5 with higher affinity of anionic substrates at lower pH and higher affinity of cationic substrates at higher pH. At saturating substrate concentrations transport is independent of pH and transport rate is solely determined by membrane potential. The transmembrane domains (TMD) 1-6 seem to determine the pH dependence of the transporters whereas TMD 7-9 could define the substrate affinity (58, 72). As three-dimensional structures of PEPT1 and PEPT2 are still lacking not much more is known about the substrate binding site and affinity of substrates has to be tested experimentally which has been an active field of research over the past decades (for review see (26, 35)). Recently, 3D-QSAR models have been developed by comparative molecular similarity indices analysis (CoMSIA) based on 98 compounds tested for PEPT1 (25) and 83 compounds tested for PEPT2 (24). These models allow to explain some of the differences in substrate affinity between PEPT1 and PEPT2 and can be used to predict the binding affinity of novel substrates for rational drug design.

5. Localization, Function and Regulation of PEPT1 and PEPT2

Peptide transport had been identified functionally first in the small intestine and some years later in the kidney. After the cloning of PEPT1 and PEPT2 their localization in various organs and at cellular level has been studied in detail with different techniques. Localization of PEPT1-mRNA was detected in epithelial cells of rabbit

duodenum, jejunum and ileum by in situ hybridization with expression starting near the crypt-villus junction and continuous expression up to the villus tip (79). This localization was confirmed by immunohistochemistry in rat small intestine (158) and mouse small intestine and peptide uptake was visualized by the fluorescently labelled dipeptide D-Ala-Lys-AMCA (92). In human tissue, PEPT1-mRNA was detected in the same segments of the small intestine by RT-PCR with highest expression in the duodenum (101, 206, 221). The developmental expression of PEPT1 was studied in rat small intestine with highest levels of PEPT1 mRNA shortly after birth and a rapid decline around days 7-10. PEPT1 protein levels increased again between 3 and 12 weeks of age, but did not reach the levels observed on days 3-7 after birth (200). In this study expression of PEPT1 was also observed in colon shortly after birth whereas in human tissue no or very low levels of PEPT1 were found in healthy human colon (77, 101, 221), but definite expression during inflammatory bowel disease (143). Apart from the small intestine, PEPT1 is expressed in only few other tissues. In the kidney it is exclusively found in the convoluted proximal tubule (S1-Segment) (203). Further expression has been shown in the apical membrane of mouse cholangiocytes and the human bile duct epithelium cell line SK-ChA-1 (120) and functional peptide transport has been confirmed with δ -ALA uptake into tumor cells of the extrahepatic biliary duct (144). Recently low PEPT1 expression was observed by RT-PCR in thymus, male and female gonads and in the uterus of rat and mouse (204). In this study some differences in tissue distribution and expression level between rat and mouse were observed e.g. very low levels of PEPT1 in mouse kidney in comparison to rat kidney. A splice variant of PEPT1 that consists of only 150 amino acids of the PEPT1 C-terminus has been shown in the pineal gland and shows marked circadian variation in expression (81).

In contrast to PEPT1, PEPT2 is expressed in a wide variety of organs. Highest expression is found in the kidney. Its expression is confined to the outer medulla corresponding to the more distal, straight part of the proximal tubule (S2 and S3 segment) (203, 204). Peptide transporter expression in the kidney shows less developmental regulation with transporter levels reaching a plateau at about 2 weeks after birth (200). Medium levels of PEPT2 are found in the brain, where it has been localized by in situ hybridization to astrocytes, subependymal cells, ependymal cells and epithelial cells of the choroids plexus and satellite glial cells of dorsal root ganglia (23, 93). Although one study has shown PEPT2 expression in neurons but not in glial

cells by immunohistochemistry in adult rat brain (201), functional evidence for PEPT2 mediated peptide transport was shown in astroglia-rich primary cultures of neonatal rat brain (57, 61, 255) as well as in glial cells of adult rat brain but not in neuronal cells (97). PEPT2 mediated uptake into epithelial cells of the choroid plexus was further studied with different substrates (156, 157, 202, 222). Recently, PEPT2 expression has also been demonstrated in glial cells of the enteric nervous system of rat and mouse and in guinea pig a subclass of neurons was shown to possess PEPT2 mediated peptide uptake (187). In this study PEPT2 was further found to be expressed in residential macrophages of the enteric nervous system. PEPT2 mRNA has also been detected in Müller cells of the retina, but no evidence for functional peptide transport in retinal pigment epithelial cells could be shown (23, 154).

PEPT2 can be found in the lung with medium expression levels where the transporter is localized in tracheal and bronchial epithelia and in alveolar type II pneumocytes (96). Distribution and expression levels are unaltered during cystic fibrosis (95). Functional characterization of PEPT2 in lung primary cultures from different human individuals showed that donor-to-donor variation of transport does not correlate with PEPT2 haplotypes (18).

In the mammary gland PEPT2 can be found in epithelial cells of ducts and glands (94) and epithelial cells isolated from milk of lactating mammary gland displayed 4-fold higher PEPT2 mRNA levels in comparison to epithelial cells isolated from non-lactating mammary gland (11).

In the pancreas PEPT2 is expressed specifically in α -cells (150). RT-PCR screening of rat and mouse tissue suggests further expression of PEPT2 in the pituitary gland, male and female gonads, prostate and uterus (204). In this study PEPT2 was also found to be expressed in rat heart but not in mouse heart. Recently, another group identified PEPT2 by RT-PCR in guinea pig cardiomyocytes (143). Yet, the findings are somehow conflicting as the RT-PCR amplicon for PEPT2 from guinea pig kidney tissue displayed 100% sequence identity with that of rat PEPT2 whereas the RT-PCR amplicon from guinea pig cardiomyocytes had only 80% sequence identity with that of rat PEPT2.

In all but one study (77) where localization of PEPT1 and PEPT2 was studied at the subcellular level, the transporters were exclusively found in the apical membrane of polarized cells.

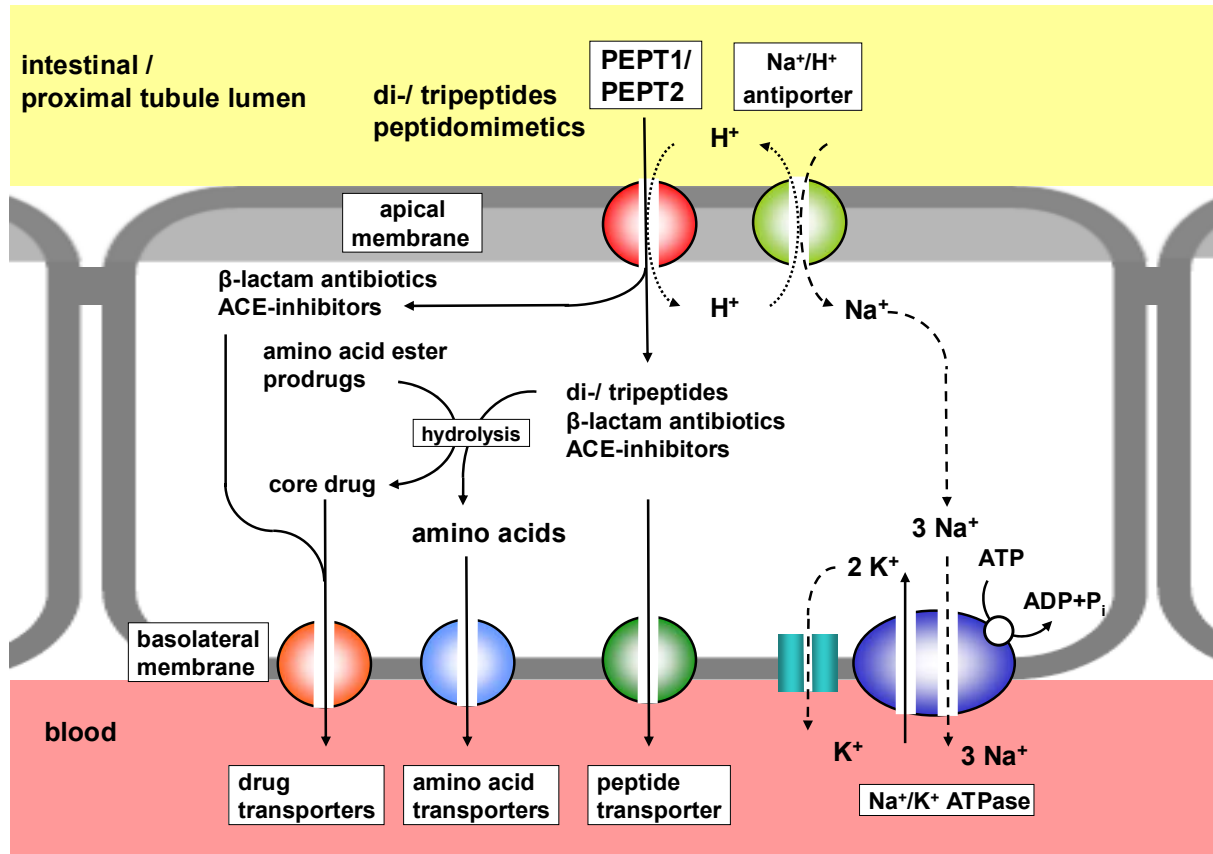


Fig. 3: PEPT1 and PEPT2 in the context of the epithelial cell

Transepithelial movement of peptides and peptidomimetics is mediated in cooperation by peptide, amino acid, and drug transporters and is energized by the proton gradient provided by ion transporters.

In Fig. 3 localization and functional coupling of PEPT1 and PEPT2 with other transporters in epithelial cells of the intestine and the renal proximal tubule are displayed. Both transporters are tertiary active carriers, as the proton gradient that energizes peptide transport is provided by sodium-proton exchangers (NHE) (229) which depend on the sodium gradient that is maintained by the sodium-potassium-ATPase.

Substrates that have been taken up via the apical membrane by PEPT1 or PEPT2 can leave the cell either unaltered at the basolateral membrane via a basolateral peptide transporter or a variety of drug transporters e.g. organic anion or cation transporters or they can be hydrolyzed by intracellular peptidases with amino acids leaving the cell by basolateral membrane amino acid transporters. The transporter that mediates the basolateral efflux of intact peptides has not been identified so far but characterized functionally with partly conflicting results for pH dependency (106, 219, 220, 227, 228). Little is known about the fraction of peptides that leaves the cell

intact via the basolateral peptide transport system, and although there is evidence that transepithelial uptake of intact peptides is possible (135, 178), the major fraction of peptides is probably hydrolyzed rapidly within the cell. Therefore basolateral peptide transport might be of importance for hydrolysis-resistant peptides, like those containing D-amino acids or C-terminal proline and hydroxyproline, only.

Only few studies are available on trafficking of the transporters to the apical membrane. A yeast-two-hybrid screen found interaction between PDZ-adaptor proteins and PEPT1 and PEPT2 (112) but for PEPT1 this finding was not further followed so far. Interaction of the last three amino acids of the C-terminus of PEPT2 – which form a PDZ-motif – with the PDZ2 and PDZ3 domain of the PDZK1 protein (153) does not seem necessary for apical targeting as a study of our group has shown that deletion of the last seven amino acids of the C-terminus (aa 723-729) does not impair apical sorting whereas mutation or deletion of leucine 722 or mutation of isoleucine 720 resulted in impaired apical expression and accumulation of the mutated proteins in endosomal and lysosomal vesicles (59). However, interaction of the PDZ-motif of PEPT2 with PDZK1 might play a role in coupling of PEPT2 to sodium proton exchangers that provide the proton gradient for peptide transport (114, 193, 237), as deletion of the PDZ-motif led to a reduction of Gly-Sar transport (153).

The main function of the intestinal peptide transporter PEPT1 is its contribution to protein nutrition by absorption of di- and tripeptides originating from breakdown of dietary protein in the gut. The impact of PEPT1 mediated peptide transport on protein nutrition has been demonstrated in a *C. elegans* model that is lacking the orthologue *pep-2* gene. Transporter-deficient worms show significantly retarded development, smaller body size, have a reduced number of progeny and the defects cannot be rescued by providing large quantities of free amino acids (136). Further evidence for the importance of peptide absorption for protein nutrition comes from patients suffering from Hartnup disease or cystinuria and the corresponding knockout mouse models. Hartnup disease originates from genetic defects in the amino acid transporter B⁰AT1 (SLC6A19) and cystinuria is caused by genetic defects in both subunits of the heteromeric amino acid transporter rBAT/b^{0,+}AT (SLC3A1/ SLC7A9) (119, 161, 198). Under both conditions some essential amino acids cannot be absorbed, yet patients as well as knockout mice rarely show signs of amino acid deficiency indicating that they can probably satisfy their needs for essential amino

acids by absorbing them in peptide bound form. In addition, liquid diets for enteral nutrition are well absorbed and better tolerated with small peptides as protein source instead of free amino acids (3).

In the kidney, peptides and amino acids are reabsorbed from the glomerular filtrate by the activities of peptide transporters and amino acid transporters acting in parallel in the apical membrane of tubular epithelial cells (for review see (5, 162)). The localization of PEPT1 in the S1 segment of the proximal tubule and PEPT2 in the S2 and S3 segment has led to the concept that the high capacity transporter PEPT1 is responsible for the reabsorption of bulk quantities of peptides in the more proximal part whereas PEPT2 as the high affinity transporter is acting in the more distal parts of the proximal tubule taking care of the remaining luminal substrates. Yet, early studies in rabbit brush border membrane vesicles indicated that mainly a high affinity system (PEPT2) is responsible for the bulk uptake of di- and tripeptides in the tubule (127). Initial characterization of a *Pept2*^{-/-} mouse model developed in the group of H. Daniel by I. Rubio-Aliaga revealed that after application of labelled hydrolysis-resistant model dipeptides significantly reduced accumulation in kidney tissue can be observed (186).

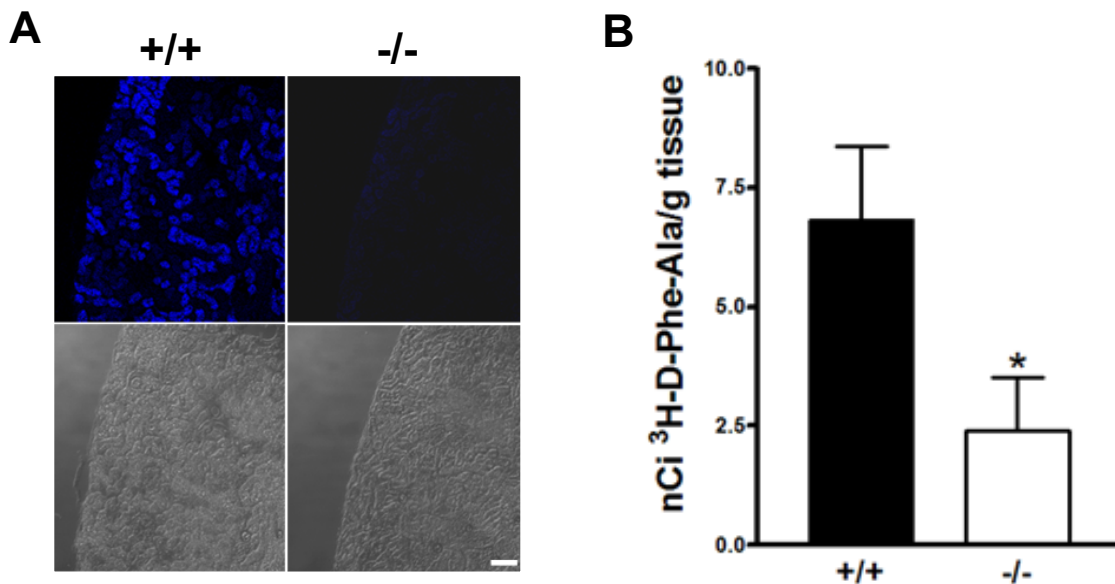


Fig. 4: Renal accumulation of labelled model dipeptides

Reduced renal accumulation of a fluorophore-conjugated dipeptide (A) and a radiolabeled-dipeptide (B) is observed in *Pept2* knockout mice. (A) In kidney slices obtained from wild type mice after intravenous injection of D-Ala-Lys-AMCA, fluorescence was detected in selected tubular structures of the cortex and outer medulla, whereas in slices from the *Pept2*^{-/-} mice, only very weak fluorescence was detectable in the outer cortex. Bottom, light microscopy pictures of the corresponding kidney sections. Bar, 80 μ m. (B) In kidney homogenates prepared from *Pept2*^{-/-} animals, accumulation of radioactivity after intraperitoneal administration of D-[³H]Phe-Ala was significantly reduced (* = $p < 0.05$)

During the course of this work clearance studies in a further PEPT2-deficient mouse line developed in the group of D.E. Smith confirmed that PEPT2 is the predominant transporter for peptide reabsorption in the proximal tubule accounting for approximately 86% of renal reabsorption of the hydrolysis resistant dipeptide glycyl-sarcosine (gly-sar) (155). It is assumed that the prime role of renal peptide reabsorption by PEPT2 is to minimize the loss of peptide-bound amino acids into urine thus contributing to the overall amino acid homeostasis of the body.

The function of PEPT2 in the central nervous system is still the subject of speculation. As astrocytes control the extracellular fluid composition in the brain and epithelial cells produce and control the cerebrospinal fluid (CSF) composition, it is assumed that PEPT2 contributes to these functions as a clearance mechanism to remove peptide fragments, neuropeptides and their breakdown products and also potentially harmful xenobiotics. Analogous function has been suggested for glial cells of the enteric nervous system (187). Studies with astroglia-rich primary cultures indicate that a further specific function of PEPT2 might be the uptake of the dipeptide cysteinyl-glycine (cys-gly). Cys-gly is a precursor of glutathione thus that PEPT2 may contribute to maintenance of adequate glutathione levels (61). Uptake studies performed with a number of substrates by the group of D.E. Smith suggest that PEPT2 is the predominant transporter for uptake of peptides and peptidomimetics into choroid plexus epithelium, as summarized in a recent review (204). In contrast to the small intestine and the kidney proximal tubule there is no pH gradient from CSF (~ pH 7.3) to epithelial cells of the choroid plexus (~ pH 7.0) and about an acidic microclimate at the brush boarder membrane can only be speculated so far.

PEPT2 mediated peptide transport in bronchial epithelium and type II pneumocytes might be involved in the uptake of surfactant breakdown products, contribute to the regulation of the thickness of the alveolar lining fluid layer, and be responsible for removal of peptides that could serve as nutrients for bacterial growth (100, 137), yet all these functions are mere speculation, up to date. On the other hand, PEPT2 expression in the lung has been identified as a pharmacologically interesting target for aerosolized drug formulations (18, 95).

Expression of PEPT2 in the apical membrane of epithelial cells of the terminal duct and glandules of the mammary gland indicates that the transporter does not contribute to the uptake of peptides from plasma for milk protein synthesis, but may rather mediate the reuptake of peptides from milk (94). It may further be responsible

for the relative low amounts of peptidomimetic drugs detected in milk after oral administration.

Expression of PEPT1 has been studied under various physiologic and pathophysiologic conditions (for review see (4)) whereas only little data is available on regulation of PEPT2. Peptide transport can be regulated at various steps in the sequence from induction of transporter expression up to the integration of the transport protein into the membrane. Expression levels of the transporter mRNA can be altered due to transcriptional induction/repression or altered mRNA-stability. Transporter protein levels can be influenced by altered mRNA-levels, changes in translation or alterations in protein stability. Changes in transport protein expression in the membrane need not be related to protein synthesis but can also reflect recruiting of transporters from preformed cytoplasmic pools to the apical membrane and activity of the transporter in the membrane can be influenced by changes in pH or membrane potential. Some recent studies investigated the PEPT1 promoter. The basal expression of PEPT1 seems to be dependent on a minimal promoter in the region -172/-35 that contains three SP1 binding sites. SP1 was shown to act as transcription factor for basal PEPT1 expression, but further transcription factors like SP3 or GKLf might also act at the same transcription factor binding sites (206). It was further shown that the transcription factor Cdx2 interacts with SP1 for trans-activation of the PEPT1 promoter (208). Cdx2 is known to be involved in differentiation and maintenance of intestinal epithelial cells, it is responsible for the intestinal expression of a variety of genes, and as PEPT1 and Cdx2-mRNA levels were found to be highly correlated in gastric samples it was hypothesized that it may be responsible for the intestine specific expression of PEPT1. Posttranslational regulation of PEPT1 mediated peptide transport might occur by regulation of NHE3 via changes in the proton gradient. NHE3 is a highly regulated protein. Downregulation of NHE3 by protein kinase A activation reduced peptide transport in Caco-2 cells (229) and expression of NHE3 in Hek293 cells led to an increase in PEPT1 mediated peptide transport that was linearly correlated to the NHE3 expression level (241).

A physiological condition with demand for increased PEPT1 expression is high substrate availability e.g. after a high protein meal. Indeed, exposure of Caco-2 cells to di- and tripeptides induced PEPT1 mRNA and protein expression whereas free amino acids had no effect (224, 238). This increase in PEPT1 expression induced by

substrates could also be observed in vivo in rats fed a high protein diet or a diet enriched in dipeptides (68, 209) and it was shown that the increase in PEPT1-expression was related to *de novo* protein synthesis from elevated levels of PEPT1-mRNA due to increased mRNA stability and transcriptional activation of the *Pept1* gene. On the other hand PEPT1 mRNA expression displays marked diurnal variation with highest expression in rats at the beginning of the dark period when animals are in the fasting state shortly before starting food intake (256). The diurnal variation of PEPT1 expression was suggested to be related to the fasting during the light period as short as well as prolonged fasting enhances PEPT1 expression (140, 159, 223, 256). Recently, it was demonstrated that the fasting induced increase in intestinal PEPT1 expression is mediated by the peroxisome proliferator-activated receptor α (PPAR α) (207), whereas PPAR α had no effect on renal PEPT1 expression.

Insulin and leptin have been shown to induce trafficking of PEPT1 protein to the membrane, insulin via binding to insulin receptors at the basolateral membrane (151) whereas leptin – probably derived from secretion in the stomach – acts at the apical membrane (4). In agreement are findings that PEPT1 expression and transport is reduced in a rat model of insulin-deficient diabetes and increased in a model of hyperinsulinemic type II diabetes (27, 243). Moreover, a recent study demonstrates that leptin can further induce PEPT1 expression by transcriptional mechanisms. The very high levels of leptin (15-fold increase (211)) that can be found in the colon during inflammation can trigger an increase in intracellular cAMP levels leading to activation of protein kinase A (PKA) and to an increase in the levels of the phosphorylated form of the cAMP-response element binding protein (Creb) (142). Cdx2 binding sites in the PEPT1 promoter have been shown to be crucial for the leptin induced PEPT1 transcription as Cdx2 and phosphorylated Creb (pCreb) interact in the leptin induced transcriptional activation. These recent findings might be one explanation for the expression of PEPT1 in the colon of patients with inflammatory bowel disease (IBD). On the other hand the inflammatory mediators tumour necrosis factor alpha (TNF α) and Interferon gamma (IFN γ) have been shown to induce the PEPT1 expression in the proximal and distal colon but to have no effect on its expression levels in the small intestine (234). As IFN γ (211) has been shown to induce leptin expression it can be hypothesized that its effects on PEPT1 expression might be mediated via leptin.

Long-term exposure to epidermal growth factor (EGF) has been observed to reduce

PEPT1 mRNA and protein levels in Caco-2 cells as well as of PEPT2 in SKPT cells (37, 152), whereas short term exposure to EGF led to increased PEPT1 mediated peptide transport and protein levels in Caco-2 cells without an effect at mRNA level (151). Hypothyroidism induced by thyroidectomy led to increased renal PEPT1 and PEPT2 mRNA levels and in a model of Methimazole induced hypothyroidism that represents a milder form of hypothyroidism renal PEPT2 mRNA and protein level were also increased (59, 204). Thyroid hormone is a key player in protein metabolism, malnutrition can be a cause of hypothyroidism and hypothyroidism is associated with reduced serum protein levels. It is therefore hypothesized that peptide transporter expression is upregulated during hypothyroidism to ensure protein homeostasis of the body by efficient peptide reabsorption in the kidney. The effect of hypothyroidism on PEPT1 expression in the small intestine has not been studied, so far, whereas hyperthyroidism was shown to reduce intestinal PEPT1 expression and peptide transport (16). Recently the effect of progesterone and norethisterone on PEPT1 expression in Caco-2 cells has been studied. Exposure of the cells to 30 μ M of progesterone or norethisterone led to decreased PEPT1 mRNA and protein levels, yet the effects of fluctuations of gestagen levels need further research as the applied hormone levels were about 50-fold higher than normal plasma levels (242).

Further pathophysiological conditions that have been studied are PEPT1 expression after intestinal resection, PEPT1 and PEPT2 expression in rat models of chronic renal failure like uninephrectomy or 5/6 nephrectomy and PEPT1 expression after traumatic brain injury. Intestinal resection did not induce PEPT1 expression in the ileum whereas it induced PEPT1 expression in the colon (261). Both models of reduced renal mass led to a profound induction of peptide transporter expression in the first 2-4 weeks after kidney resection (217, 233), whereas decreased PEPT2 expression was found in the 5/6 nephrectomy model after 16 weeks (141). Traumatic brain injury led to apoptosis in the mucosal epithelium and to significantly decreased villous height, crypt depth and surface area whereas PEPT1 mediated peptide transport was upregulated at the first 24 hours after the traumatic brain injury and remained at normal levels seven days later, despite mucosal atrophy (251).

6. The mouse as a model system for functional genomics

As explicated in the previous paragraphs little information is available on the function and regulation of the peptide transporter PEPT2. Particularly, it can be only speculated about its precise function in the various tissues it is expressed. A profitable and widely applied approach to gain insight into the function of a gene and its physiological relevance is to study model organisms with altered expression or deletion of the gene of interest. During the last decades the mouse has become the preferred mammalian model organism due to several reasons. First and most important, since the first generation of transgenic mice overexpressing a rat growth hormone gene generated by R. Palmiter and colleagues in 1982 (163) and the first generation of knockout mice for the hypoxanthine phosphoribosyl transferase (HPRT) gene by targeted disruption via homologous recombination in embryonic stem cells by K. Thomas and M. Capecchi in 1987 (109) the mouse has become the mammalian model of the first choice for induction of genetic alterations. The mouse is still the only mammalian organism in which the targeted inactivation of a gene is feasible and the widest array of genetic manipulations is possible. Today ample experience exists in the classic techniques and more sophisticated approaches like deleting gene function only at a certain time point or only in a certain cell type in conditional mouse models have been developed. The inducible expression or knockout of a gene came into focus on the one hand to study mouse models of genes that lead to a lethal phenotype in embryonic or early life if a conventional complete knockout is performed and on the other hand to ask and answer ever more detailed questions about the function of a gene in a certain context without the confounding effects that might occur in a conventional complete knockout of a gene (28, 124). The full sequencing of the human and mouse genome revealed that there is high homology between these species. Although the mouse genome is about 14% smaller than the human genome the genomes show a high degree of synteny: about 95% of the mouse and human genomes can be partitioned into syntenic regions in which the gene order on the chromosome is conserved. For 99% of the protein coding mouse genes a counterpart can be found in the human genome (244). Further advantages of the mouse as model organism are the availability of inbred animals that allow studying the function of a certain gene in an isogenic background, its short generation time, and easy maintenance and breeding. A recent survey of the Mouse Genome Informatics database (MGI; <http://www.informatics.jax.org>) revealed

that by targeted disruption nearly 4000 knockout mice have been created up to date. Due to the wide appreciation of knockout mouse models for the functional analysis of the now sequenced genomes of human and mouse, three large projects funded by the NIH (Knockout Mouse Project, KOMP), the EU (European Conditional Mouse Mutagenesis Program, EUCOMM) and Genome Canada and partners (North American Conditional Knockout Mouse Mutagenesis, NORCOMM) have been launched with the ambitious goal to create knockout mouse models for every single gene (91, 204). Even more challenging will be the phenotypic characterization of all these mouse models as even standardized high throughput phenotyping programs like the European Mouse Disease Clinic (EUMODIC) are currently aiming at analysing some hundred mouse lines (172). The ample information about the mouse as a model for human diseases and traits, including gene and gene function characterization, phenotype and disease model descriptions, DNA and protein sequences, polymorphisms, and much more can be accessed via the mouse genome database (MGD) (67) and various other resources for accession to certain mouse mutants or relevant information have been reviewed recently (168).

The knockout mouse model for the peptide transporter PEPT2 (*Pept2*^{-/-}) is the first mammalian knockout model for a peptide transporter. The usefulness of knockout animals to study transport protein physiology has been demonstrated in a number of knockout mice generated for amino acid transporters. The resulting animals reach from models for human disease like the mouse models for cystinuria type I (104) and cystinuria non-type I (76) over models that provide insight into the physiological function and relevance of transporters that have been characterized in heterologous expression systems previously, e.g. knockout mice for the cystine/glutamate transporter (xc⁻, Slc7a11) (191) or the cationic amino acid transporter CAT-2 (146) to knockout models that give the first information about the function and potential substrates of an orphan transporter of which no information about its substrates is available yet, like the knockout mouse for XT2/Slc6a18 (174).

7. Application of profiling techniques for phenotyping of mutant mice

The phenotypic characterization of a mouse model with altered or completely ablated expression of a gene can be a challenging task as often unexpected or seemingly silent phenotypes are encountered (193). It has been proposed to start with a primary level phenotypic assessment including monitoring of litter size, genotype distribution, visual observation, lifespan and general necropsy. Thereafter, a secondary level examination should be performed based on the results of the primary screen and on the assumptions which consequences the loss of a certain gene might have with regard to its localization and function as known at that time (253). The importance of elaborate hypothesis driven phenotypic characterization cannot be overestimated. Yet, it can be anticipated that the complex adaptation mechanisms that set in to compensate for the loss of a certain gene are out of reach for classical phenotyping strategies and very specific assays are inevitably prone to overlook changes related to previously unknown functions of the manipulated gene. In the last decade technologies have emerged that aim at the comprehensive analysis of all expressed biological entities of a functional level – transcriptome, proteome and metabolome - in a given sample. The corresponding technologies – transcriptomics, proteomics and metabolomics – are currently at various stages of development and have to cope with different levels of complexity as schematically depicted in Fig. 5:

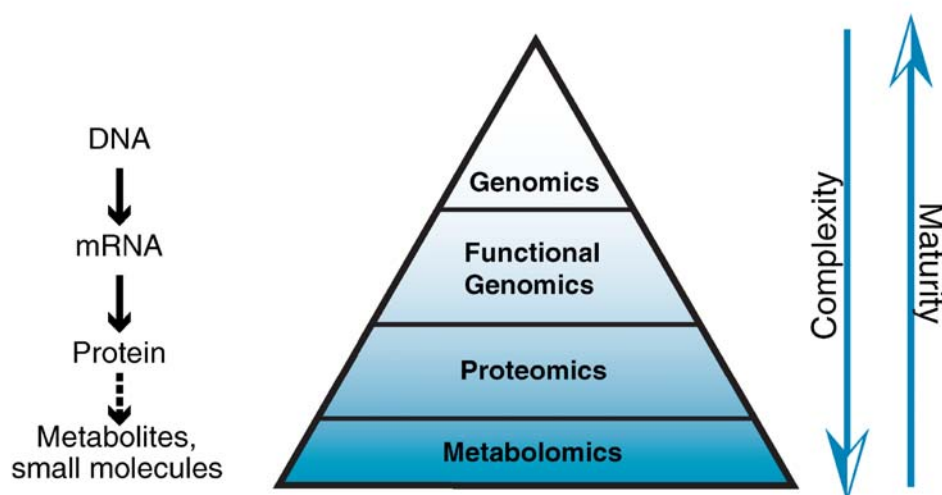


Fig. 5: Relationship between different "omics" disciplines (from (55))

Transcriptome analysis has come closest to the goal of comprehensive analysis as today it is possible to monitor in a single experiment the genome wide mRNA

expression of a sample by microarray hybridisation techniques. For an introduction and comparison of microarray technologies and emerging applications see (87, 107). The two major technologies are oligonucleotide arrays with single colour detection and spotted cDNA arrays with dual colour detection. In the former each array is hybridized with one sample allowing any array to be compared with any other array whereas in the latter the mRNA of two samples that are to be compared are labelled with two different fluorescent dyes and hybridized onto the same array. Reliability of microarray data within and between different platforms has been a matter of debate but seems to have improved considerably (204). Appropriate data analysis for identification of differentially expressed mRNAs has been identified as a crucial step in a microarray experiment (205) and development of statistical tools for microarray data analysis is a very active field of research (12). A current limitation of microarray technology is that only some platforms are able to resolve the alternative splicing products encoded by one gene. Transcriptome analysis has already been widely applied to mouse model phenotyping and has also been integrated into large scale phenotyping programmes like the German Mouse Clinic (21). Projects like definition of the normal variance of gene expression in different mouse tissues further enhance the power of transcript profiling in the characterization of mouse mutants (171).

Similarly, proteomics aims at the identification and quantification of all proteins expressed in a sample and in its wider sense also at the identification of their cellular localization, modifications (e.g. phosphorylation), 3D-structure and protein-protein interactions. An overview over current techniques and applications can be found in (55). The two main technologies for separation, quantification and identification of a sample proteome are two dimensional polyacrylamide gelelectrophoresis (2D-PAGE) in combination with mass spectrometry (MS) and liquid-chromatography in combination with mass spectrometry (LC-MS). Due to the very diverse qualities of proteins (e.g. mass, isoelectric point, solubility, stability, wide range of concentration level, etc.) it is not possible to measure the whole proteome of a sample so far. E.g. transmembrane proteins have been very resistant to proteomic analysis as they cannot be easily solubilised and separated by 2D-PAGE. Better coverage of the proteome can be achieved by fractionation e.g. according to cellular organelles or by removal of overabundant proteins e.g. removal of albumin and immunoglobulins for the analysis of the plasma proteome but renders the analysis more expensive, technically demanding and time consuming.

Metabolomics is the youngest of the three technologies and seeks to separate, identify and quantify all metabolites i.e. all the low molecular weight molecules, typically < 3000 m/z of a sample (102). The two main technologies applied are nuclear magnetic resonance (NMR) spectroscopy and liquid or gas chromatography (LC or GC) in combination with mass spectrometry (MS) and a detailed review on analytical techniques is given in (64). In general NMR is less sensitive than mass spectrometry techniques and gives a metabolic fingerprint of the high abundance metabolites but has proven to classify reliably e.g. disease states or mouse strains (90). At the moment the number and identity of the metabolites of a certain tissue or body fluid under normal conditions are not known but recent advances in mass spectrometry, that allow for exact mass determination necessary for compound identification and exact quantification at the same time, promote the construction of databases. In comparison to transcriptomics and proteomics techniques, metabolome analysis is much more rapid and much cheaper on a per sample basis rendering it a superior technique for high throughput screening.

The traditional central dogma of unidirectional information flow from genes to transcripts to proteins which then affect metabolic pathways and lead to changes of the phenotype has been replaced by a picture with multiple interactions and feedback-loops. Transcriptome, proteome and metabolome profiling are therefore complementary and should be combined for a comprehensive phenotyping approach that aims at capturing all changes related to mutation of the gene of interest and finally elucidating the function and relevance of a gene at the systems level.

Aim of the Thesis

Proton driven transmembrane transport of di- and tripeptides is mediated by highly conserved peptide transporters found throughout nature. The mammalian peptide transporter PEPT2 has been characterized in detail with regard to driving force, localization and substrate identification and affinity. Yet, little is known about the physiological relevance of PEPT2 mediated peptide transport. To further elucidate the function of PEPT2 a mouse model lacking a functional PEPT2 protein had been generated by I. Rubio-Aliaga by targeted disruption of the *Pept2* gene (186). She could show that renal accumulation of labelled hydrolysis resistant model dipeptides was markedly reduced in the transporter deficient animals.

The aim of the current thesis was to characterize the phenotypic alterations of the *Pept2* knockout mouse model to gain deeper insight into the physiological function of PEPT2. Since for most tissues with PEPT2 expression no precise functions of the transporter are known, we initiated a general phenotyping approach evaluating body weight, lifespan, reproductive performance and clinical chemistry in urine and plasma samples. In a more hypothesis driven approach we determined whether alterations in peptide transport have an effect on blood pressure or glucagon levels. Urine samples were analyzed for free and dipeptide bound amino acids to study whether loss of proximal tubule peptide reabsorption leads to amino acid losses that might affect overall amino acid homeostasis. Animals received diets with low (10%), medium (20%), or high (30%) protein content in a metabolic study as we hypothesized that perturbations of protein homeostasis due to loss of PEPT2 might vary depending on the protein supply to the organism.

Pept2 deficient animals displayed an overall silent phenotype with only subtle alterations. No compensatory regulation of related peptide transporters such as PEPT1 or PHT1 in the kidney was observed. We then characterized kidney tissue samples with profiling techniques at mRNA, protein and metabolite level to get a comprehensive overview over the alterations induced by loss of PEPT2. Integrated data analysis of results from the different biological levels provided evidence for a previously unanticipated role of PEPT2 in the delivery of substrates for epithelial glutathione (GSH) synthesis. We followed up on this hypothesis by determination of GSH in urine, plasma and kidney tissue and analysis of mRNA expression levels of enzymes involved in the metabolism of GSH.

Materials

1. Laboratory animals

PEPT2-deficient mice (*Slc15a2*^{tm1Dan}) have been generated in our lab by I. Rubio-Aliaga (186). Targeted disruption of the *Pept2* gene has been achieved by replacement of the coding region of exon 1 with the β -galactosidase gene via homologous recombination in ES cells. ES cells were derived from the 129X1 strain and blastocysts were of C57BL/6 origin. Breeding of the *Pept2*^{+/-} line was continued by mating of *Pept2*^{+/-} animals with a mixed genetic background of both strains. A backcross to C57BL/6 was pursued but the first *Pept2*^{-/-} animals with a pure genetic background of C57BL/6 became available at the end of this work, only. Mice with a pure genetic background of C57BL/6 or 129X1 were bought from Charles River (Charles River, Sulzfeld, Germany).

2. Chemicals and consumables

Unless otherwise specified all chemicals were from Sigma (Taufkirchen, Germany), Merck (Darmstadt, Germany) or Roth (Karlsruhe, Germany) and of pro analysis quality. Oligonucleotides for PCR were bought from MWG (Ebersberg, Germany)

3. Instruments

In addition to usual laboratory equipment the following specific analytical devices were used:

amino acid analyzer LC3000 (Eppendorf Biotronik, Hamburg, Germany), Biophotometer (Eppendorf, Hamburg, Germany), electronic pressure transducer type 5145 and four channel recorder (Schwarzer & Co., Munich, Germany), GC-TOF-MS system consisting of Hewlett Packard HP5890 gas chromatograph (Agilent, Waldbronn, Germany) and Pegasus II TOF mass spectrometer (LECO, St. Joseph, MI, USA), 1282 Compugamma GS γ -Counter (LKB Wallac, Freiburg, Germany), GenePix 4000A microarray scanner (Axon Instruments, Sunnyvale, CA, USA), HPLC system consisting of L-5000 LC-controller, 655-11 liquid chromatograph, F-1050 fluorescence spectrophotometer and D-2000 chromato-integrator (all Merck Hitachi, Darmstadt, Germany), IPGphor IEF system and Ettan Dalt II system for SDS PAGE (Amersham Biosciences Europe, Freiburg, Germany), PCR Sprinter, PCR Express and Hybridization oven Shake'n'stack (all from Hybaid, Middlesex, UK), Lightcycler

(Roche, Mannheim, Germany), MALDI-TOF Autoflex mass spectrometer (Bruker Daltonics, Leipzig, Germany), metabolic cages (in house custom design product), semi-micro osmometer (Knauer, Berlin, Germany), Microgrid TAS II spotter (Biorobotics Genomic Solutions, Huntingdon, U.K.) with Stealth SMP3 pins (Telechem, Sunnyvale, CA), PhosphorImager Cyclone (Packard, Mariden, CT, USA), Olympus AU400 auto analyzer (Olympus, Hamburg, Germany), spectrophotometer Uvikon 930 (Kontron Instruments, Neufahrn, Germany)

Methods

1. Mouse husbandry, handling and sample collection

1.1 Mouse husbandry

Animals were maintained at $22 \pm 2^\circ\text{C}$ and a 12:12 hrs light/dark cycle with access to tap water and a standard rodent diet (Altromin, 1320, Detmold, Germany) *ad libitum* unless stated otherwise. *Pept2*^{+/+}, *Pept2*^{+/-} and *Pept2*^{-/-} mice used for monitoring of body weight development, for analysis of lifespan, for urine parameters and free and dipeptide bound amino acids in 24h urine samples were littermates derived from a *Pept2*^{+/-} line. For all other experiments homozygous animals of the *Pept2*^{+/-} line were mated to yield litters of entirely *Pept2*^{+/+} or *Pept2*^{-/-} pups. All procedures applied throughout this study were conducted according to the German guidelines for animal care and approved by the state ethics committee under reference number 209.1/211-2531-41/03.

1.2 Genotyping

The genotype of an animal was identified by PCR screening with a primer pair directed against the first intron of the *Pept2* wildtype allele (forward Primer: m2F-147 5'-cca ctg aaa ctg aca ccc ac-3', reverse Primer: M2g1IB383 5'-gct ctg cac aca agg gaa ac-3'), which is replaced in the targeted allele, and with a primer pair directed against the lacZ cassette that is inserted in the targeted allele (forward Primer: lacZ1F 5'-cag gat atg tgg cgg at gag-3', reverse Primer: lacZ1R 5'-ggt caa cca ccg cac gat ag-3'). Tail biopsies were digested at 65°C with proteinase K (0.5 mg/ml proteinase K (Roche Diagnostics, Mannheim, Germany), 50 mM KCl, 10 mM Tris-HCl, 0.1 mg/ml gelatine, 0.45% Nonidet NP-40, 0.45% Tween 20, pH 8.3) over night. After digestion, proteinase K was heat inactivated at 95°C and PCR was performed

with a 1 μ l aliquot of the digested sample containing genomic DNA. PCR products were separated on a 1.5% agarose gel. A band of 632 bps indicates the amplification product of the wildtype allele and a band of 346 bps indicates the amplification product of the targeted allele.

1.3 Data sampling for weight, organ weight, litter size and lifespan

Body weight was monitored weekly starting from birth up to the age of 25 weeks with 14–50 mice per genotype, age and sex. For organ weight determination 12-14 week old animals were dissected and organ weights were determined on a precision balance with 12-20 mice per sex and genotype. Organ weight is expressed in relation to body weight. For analysis of litter size and development of pups from homozygous matings, pregnant mice were monitored every second day and the number of born pups was recorded as soon as birth was observed. Pups were weighed weekly and weaned at the age of 21 days. At weaning the number of pups that had survived was recorded again. To study whether lifespan is affected in transporter deficient animals, we monitored 10-12 littermates of each sex and genotype for 2 years. If an animal was found dead or had to be euthanized during this period due to obvious illness and suffering, the animal was dissected to identify the cause of death or illness.

1.4 Collection of plasma, urine and tissue samples

Blood samples were taken under ether anaesthesia by puncturing the retro-orbital sinus with heparin coated capillaries (Neolab, Heidelberg, Germany). To obtain plasma for the determination of clinical-chemical parameters and amino acids, blood was collected into Li-Heparin coated tubes (Sarstedt, Nuembrecht, Germany) and into Na-EDTA coated tubes (Sarstedt, Nuembrecht, Germany) with aprotinin (10.000 KIU/ml, Roche Diagnostics, Mannheim, Germany) for analysis of glucagon. Samples were centrifuged in a refrigerated centrifuge (4°C) at 2000 g for 15 minutes within 1 h of collection to prevent possible degradation. Haemolysis of the samples was avoided and excessively haemolytic samples were discarded.

For determination of thiols (GSH and cysteinyl-glycine) in plasma, blood was collected into precooled Na-EDTA coated tubes and centrifuged within 10 min at 2000 g and 0-2°C. An aliquot of plasma was immediately frozen at -20° for analysis of total thiols. For determination of free thiols 100 μ l plasma were deproteinized with 10 μ l sulfosalicylic acid (50% in aqua bidest). All plasma samples were stored at -20°C until analysed.

For collection of 24 h and 12 h urine samples mice were placed in metabolic cages that allow for separate collection of urine and feces. Containers for urine collection were cooled and 10 μ l of 10% thymol in isopropanol were added to avoid bacterial degradation of metabolites. Urine samples for determination of urea were collected separately without addition of thymol as thymol interferes with the urea assay according to the method of Berthelot. During urine collection mice had no access to food to avoid contamination of urine samples. 3-5 24h urine samples of each mouse were collected with at least 3 days in between to allow for recovery from food deprivation and pooled prior to analysis. 12 h urine samples were collected consecutively on the last five days of the dietary intervention studies and samples of each mouse were pooled prior to analysis.

For determination of thiols in urine, spot urine samples were collected on five consecutive days between 9.00 and 10.00 a.m. by mild pressure on the lower abdomen and immediately frozen to prevent degradation of metabolites. All urine samples were stored at -20°C until further analysis. Kidneys were removed after cervical dislocation, snap frozen in liquid nitrogen and stored at -80°C until further sample preparation.

1.5 Dietary intervention study

In the dietary intervention study, male mice received semi-synthetic purified diets with either a low protein (10%), medium (20%) or high (30%) protein content (w/w). For each diet and genotype 10 animals were studied. Diet formulation was identical with the AIN-93G diet (175, 176) except that protein was isocalorically replaced by carbohydrates and vice versa. Mice were placed in metabolic cages that allow for recording of food and water consumption. These diets were prepared in-house. Throughout the study mice had access to tap water *ad libitum*. During the first five days in the metabolic cages all animals received the medium protein diet *ad libitum* to allow for adaptation to the metabolic cages. The following fourteen days mice had free access to either the low, medium or high protein diet. Body weight and consumption of food and water were monitored daily between 8.00 and 9.00 a.m. On days 19-24 mice were placed in clean metabolic cages and food was removed for the 12 hours during the dark phase to allow for urine collection without contamination of urine by food. On day 24, blood and kidney tissue samples were taken.

1.6 Blood pressure determination

Blood pressure was determined under anesthesia with Midazolam (1.0 mg/kg), Medetomidin (0.05 mg/kg) and Fentanyl (0.02 mg/kg) i.p. (kindly provided by Dr. W. Erhardt, Institute of Experimental Oncology, Technical University of Munich, Munich, Germany) in 10 mice per sex and genotype at the age of 12-14 weeks. Heart rate and mean arterial blood pressure were measured by insertion of a catheter into the right common carotid artery and recorded with an electronic pressure transducer (Type 5145 Schwarzer & Co., Munich, Germany) connected to a four-channel recorder (Schwarzer & Co., Munich, Germany). The time span between administration of the anesthetic and the blood pressure determination was noted. There was no correlation between the duration of anesthesia and blood pressure over the period of observation. As the catheters that were inserted into the artery had to be prepared manually and thus differed slightly in diameter, we validated by blood pressure measurement with different probes in the same animal that the probe diameter did not influence the blood pressure determination.

2. Analysis of selected metabolites in body fluids and tissue

2.1 Protein, urea and creatinine concentration and osmolality of urine samples

Urinary protein content was determined with the Bio-Rad protein assay (Biorad, Munich, Germany) that is based on the method of Bradford (34) following the suppliers instructions and protein concentration was calculated from a standard curve generated with bovine serum albumine. Urea concentration of urine samples was determined with the Sigma Diagnostics Kit no. 640 (Sigma Diagnostics, St. Louis, MO, USA) and urinary creatinine levels were determined with the Sigma Diagnostics Kit no. 555 (Sigma Diagnostics) according to the manufacturers' instructions. Urine osmolality was determined with a semi-micro osmometer (Knauer, Berlin, Germany).

2.2 Free and peptide bound amino acids in urine, plasma and tissue

Urine samples were prepared for amino acid analysis in parallel with or without hydrolysis by renal membrane dipeptidase (EC 3.4.19.3) that was kindly provided by Dr. N. Hooper (University of Leeds, Leeds, UK). *In vitro* hydrolysis of urinary dipeptides was performed by incubation of 200 µl urine with 500 ng dipeptidase in 10 µl H₂O bidest for 30 min at 37°C. Urine samples for analysis of free amino acids were

incubated 30 min at 37°C after addition of 10 µl H₂O bidest as control. After incubation 290 µl of a Li-citrate sample dilution buffer pH 2.20 were added. For analysis of free amino acids in plasma 100 µl sample were diluted with 400 µl of the Li-citrate sample dilution buffer pH 2.20. For analysis of amino acids in tissue samples individual kidneys were homogenized in a mortar under liquid nitrogen and 25 mg of each tissue sample were extracted with 1 ml 5% sulfosalicylic acid by ultra sonification (30 strokes, low amplitude) on ice. Samples were centrifuged and 800 µl of the supernatant were neutralized with 200 µl 2M KHCO₃. All samples were filtered through centrifugal filter devices with 3 kD MWCO (Nanosep[®], Pall, East Hills, NY, USA) prior to analysis and the injection volume was 80 µl. Amino acids were separated by ion-exchange chromatography with a Eppendorf Biotronik LC3000 amino acid analyzer (Eppendorf, Hamburg, Germany) employing a lithium borate/acetate buffer system and ninhydrine postcolumn detection. The detection limit of the amino acids (defined as signal-to-noise ratio > 5) was around 1 µmol/l and the recovery of amino acids added at known concentrations to urine or plasma samples varied between 93% and 110%. Data were only used if duplicate analysis indicated reliable quantification. Urinary amino acids were normalized against creatinine in mmol/mol.

2.3 Clinical chemical parameters in plasma and urine

Determination of clinical chemical parameters in plasma was performed by Martina Klempt at the German Mouse Clinic (GSF, Neuherberg, Germany). Plasma samples were diluted with the same volume of deionized water and analyzed for the following parameters on an Olympus AU400 auto analyzer (Olympus, Hamburg, Germany) with adapted reagents for human samples from Olympus (Hamburg, Germany) and Roche (Mannheim, Germany): sodium, potassium, calcium, inorganic phosphorus, total protein, creatinine, urea, uric acid, cholesterol, triglyceride, creatine kinase, alanine amino transferase, aspartate amino transferase, alkaline phosphatase, alpha amylase, ferritin, transferrin. Quality control materials (Olympus, Hamburg, Germany) were analyzed on a daily basis.

Urine parameters of samples of the metabolic study were also analyzed by Martina Klempt at the German Mouse Clinic. Creatinine, urea, total protein and uric acid were analyzed on an Olympus AU400 auto analyzer (Hamburg, Germany) with adapted reagents from Olympus (Hamburg, Germany) and Roche (Mannheim, Germany).

2.4 Glucagon in plasma

For determination of glucagon, plasma was collected from 12 week old male and female animals either in fasted (17h) or postprandial (2h after a defined meal provided after 15 h fasting) state. N = 11-12 animals per sex, genotype and feeding state were studied. Glucagon was determined by a competitive radioimmunoassay (RIA) kit (Linco Research, St. Charles, MO, USA) according to the manufacturer's instructions with quantification of I¹²⁵-labelled glucagon on a γ -Counter

2.5 Thiol compounds in urine, plasma and tissue

Thiols (cysteinyl-glycine and GSH) in urine, plasma and tissue were determined by HPLC after derivatization with monobromobimane according to the method of Pastore et al. (164) with slight modifications. Briefly, 26 μ l of sample (urine, plasma or tissue extract prepared as described for amino acid analysis) were mixed with 26 μ l of 4 M NaBH₄ (dissolved in a solution of 333 ml/l DMSO and 66 mmol/l NaOH in water), 18.2 μ l EDTA (2 mmol/l)-dithiothreitol (DTT, 2 mmol/l), 5.2 μ l 1-octanol, 10.4 μ l HCl (1.8 mol/l) and 26 μ l HCl (0.1 mol/l) – DTT 0.1 (mmol/l). After incubation for 3 min at room temperature 39 μ l of N-ethylmorpholine buffer (2 mol/l, pH 8.0), 7.8 μ l monobromobimane (25 mmol/l in 1:1 acetonitrile/H₂O) and 156 μ l bidistilled H₂O were added. After incubation for 4 min at room temperature the reaction was stopped with 15.6 μ l of acetic acid. Samples were analyzed on a Merck Hitachi HPLC system consisting of a L-5000 LC-controller, 655-11 liquid chromatograph, F-1050 fluorescence spectrophotometer and a D-2000 chromato-integrator. 50 μ l of the derivatized sample were injected onto a 150 X 4.6 mm Hypersil-ODS column (3 μ m particle size, Thermo Electron, Dreieich, Germany), 30°C column temperature, equilibrated with eluent 1 (96% buffer A: ammonium nitrate (30 mmol/l), ammonium formate (40 mmol/l) pH 3,55; 4 % acetonitrile) and 3% eluent 2 (80% acetonitrile, 20% buffer A). The derivatized thiols were eluted with a gradient of eluent 2 (0-5 min, 3-5% eluent 2; 5 - 10 min, 5 - 6% eluent 2; 10 - 12 min, 6 - 14% eluent 2; 12 - 16 min, 14 - 100% eluent 2; 17 - 19 min, 100 - 3% eluent 2; 19 - 23 min, 3% eluent 2) at a flow rate of 1.5 ml/min. Fluorescence of the bromobimane adducts was determined at an excitation wavelength of 390 nm and an emission wavelength of 478 nm. The detection limit of thiols was around 200 nmol/l and the recovery of added cys-gly or GSH varied between 102% and 114%. The determination of thiols in urine and plasma was performed with the kind assistance of Anne Siewert as part of her final

year project.

3. mRNA expression analysis of individual genes

3.1 Northern Blot analysis for mRNA expression of *Pept1*, *Pht1* and *Pht2*

Total RNA of kidney samples was isolated with RNeasy (Qiagen, Crawley, UK) according to the manufacturer's instructions. 10 µg of RNA were separated by electrophoresis on a 1% denaturing agarose gel and transferred to a positively charged membrane (Hybond N, Amersham Biosciences, Piscataway, NJ, USA). cDNA fragments representing unique open reading frames of the following genes were used for hybridization: *Pept1* (accession no. NM 053079 nucleotide 1151-2139), *Pht1* (accession no. NM 023044 nucleotide 508-1130) or *Pht2* (accession no. NM 133895 nucleotide 6-599). The cDNA fragments were randomly labelled with [α - 32 P] dATP (MP Biomedicals, Eschwege, Germany) and hybridized for 1h in Express Hyb solution (Clontech, Mountain View, CA, USA) at 68°C, followed by a high-stringency wash step. For demonstration of RNA loading the blot was stripped and hybridized with a glyceraldehyde-3-phosphate dehydrogenase (GAPDH) cDNA probe. Hybridization signals were visualized by exposure to a phosphorimager screen and analyzed by densitometry.

3.2 Gene expression analysis by qPCR

Changes in transcript levels were studied by quantitative real-time reverse transcription PCR (qPCR) for genes involved in amino acid and peptide metabolism, for validation of cDNA microarray results and for genes involved in glutathione metabolism with RNA from kidneys of mice from the metabolic study (n = 5 animals per genotype and diet). Expression of *Eaf2* and *Pept2* was additionally studied by qPCR in kidney tissue samples of animals with a pure genetic background of C57BL/6 and 129X1 (n = 4 animals per strain). Total RNA of individual kidney tissue samples was isolated with the RNeasy Mini kit (Qiagen, Hilden, Germany) according to the manufacturer's protocol. 1 µg of total RNA from each individual kidney was transcribed into cDNA with MMLV-RT (Promega, Mannheim, Germany) and random hexamers (Fermentas, St. Leon-Rot, Germany). qPCR was performed on a LightCycler (Roche, Penzberg, Germany) with 3.3 ng cDNA per PCR reaction and the FastStart SYBR Green Kit (Roche, Mannheim, Germany). Cycle parameters were annealing at 62°C for 10 s, extension at 72°C for 20 s and melting at 95°C for 15 s.

Specificity of PCR products was controlled by melting curve analysis and by agarose gel electrophoresis. Primers were either designed using the Primer3 web interface (http://frodo.wi.mit.edu/cgi-bin/primer3/primer3_www.cgi) or the LightCycler Probe Design software Vers. 1.0 (Roche, Penzberg, Germany), or taken from the databases RTPrimerDB (166) or PrimerBank (239). Detailed information about the applied primer pairs and products is given in Table 23 Table 26. For relative quantification the geometric mean of crossing point (CP) values of the three housekeeping genes *Gapdh*, *Hprt* and *Sdha* was calculated for each sample as described in (169). This Bestkeeper Index was used as CP of the reference gene to calculate Mean Normalized Expression (MNE) values for each sample as described in (134).

4. Characterization of kidney tissue by profiling techniques

4.1 Transcriptome analysis by cDNA microarrays

All experiments for gene expression analysis by cDNA microarrays were performed by the group of Johannes Beckers (GSF, Neuherberg, Germany).

Isolation of total RNA, reverse transcription and fluorescent labelling: Individual kidneys were transferred into buffer containing chaotropic salt (RLT buffer, Qiagen, Hilden, Germany) and immediately homogenized with a Polytron homogenizer. Total RNA was obtained according to the manufacturer's protocols using RNeasy Midi kits (Qiagen). For each cDNA array, 20 µg total RNA was used for reverse transcription and indirect labelling with the fluorescent dyes Cy3 or Cy5 (Amersham Biosciences,, Freiburg, Germany) according to the TIGR protocol (99).

cDNA array expression profiling: cDNA-arrays employed and procedures for hybridization have been described previously (197). Briefly, probes were PCR amplified from the 20.000 (20k) mouse arrayTAG clone set (LION Bioscience, Heidelberg, Germany), dissolved in 3 x SSC and spotted on aldehyde-coated slides (CEL Associates, Pearland, TX) using the Microgrid TAS II spotter (Biorobotics Genomic Solutions, Huntingdon, U.K.) with Stealth SMP3 pins (Telechem, Sunnyvale, CA). Spotted slides were rehydrated, blocked, denatured and dried. Labelled cDNA was dissolved in 30 µl hybridization buffer (6 x SSC, 0.5 % SDS, 5 fold Denhardt's solution and 50% formamide) and mixed with 30 µl of reference cDNA solution labelled with the second dye. The hybridization mixture was placed on a prehybridized microarray and hybridized at 42°C for 18-20 hours. After

hybridization microarrays were immersed in 40 ml of 3 x SSC and then successively washed in 40 ml of 3 x SSC, 40 ml of 1 x SSC and 40 ml of 0.25 x SSC at room temperature and centrifuged for drying. Dried slides were scanned with a GenePix 4000A microarray scanner and the images were analysed using the GenePix Pro 3.0 image processing software (Axon instruments, USA). cDNA of each of the 5 *Pept2*^{-/-} mice was hybridized individually against an equimolar pool of the 5 *Pept2*^{+/+} animals. Additionally cDNA samples of four of the wildtype mice were hybridized individually against cDNA of the fifth wildtype mouse to account for biological variation within the control animals. Each hybridisation was repeated 4 times including 2 dye swaps.

Microarray data analysis: Data were formatted according to MIAME standards and submitted to the Gene Expression Omnibus (GEO) database as series GSE1585 and GSE1586. The data was first analyzed with the pattern analysis of microarrays (PAM) software developed by Alexei Drobyshv which is available at http://www.gsf.de/ieq/groups/expression/natural_variability.html, and the number of false significant genes among the top ranked genes was estimated by permutations. For the second analysis, intensity-dependent normalization was performed with the LOESS (259) procedure followed by subtraction of the log-ratio median calculated over the values for an entire block from each individual log-ratio using the *anapuce* package of R. Differential analysis was performed with the *varmixt* package of R (56). Variability of the variances was computed according to the number of available observations. A t-test was computed for each gene between both conditions (56). The variance was split between sub-groups of genes with homogeneous variance. The multiplicity of test was taken into account with False Discovery Rate (FDR) corrections (22).

4.2 Proteome analysis by 2D-PAGE and MALDI-TOF-MS

Sample Preparation for Two-Dimensional Gel Electrophoresis (2D-PAGE): Individual kidneys were homogenized in a mortar under liquid nitrogen, 50 mg tissue were transferred into 500 µl lysis buffer (7 M urea, 2 M thiourea, 2% CHAPS, 1% DTT, 2% Pharmalyte, Complete Mini proteinase inhibitor Roche Diagnostics, Mannheim, Germany) and homogenisation was achieved by ultrasonification (30 strokes, low amplitude) on ice. Lysed tissue samples were centrifuged for 30 min at 100 000 g at 4°C and protein concentrations were determined by a modified Bradford assay (Bio-Rad protein assay). Protein extracts were dialysed with the Plusone Mini Dialysis Kit (Amersham) against a modified lysis buffer (7 M urea, 2 M thiourea, 1% DTT) and

stored at -80 °C until analyzed.

2D-PAGE: 2D-PAGE was performed as described by Fuchs et al. (80). Briefly, 300 µg of protein were loaded by cuploading and IEF was performed on 18 cm IPG strips (pH 3-10, Amersham Biosciences, Freiburg, Germany) using an Amersham IPGPhor unit. 12.5% SDS-polyacrylamid gels were run on an Amersham Biosciences Ettan-Dalt II system in the second dimension. Gels were fixed and subsequently stained with Coomassie blue (CBB G-250, Serva, Heidelberg, Germany). Two gels were performed for every individual animal. Gels were scanned and analyzed using the ProteomWeaver software (Definiens Imaging GmbH, Munich, Germany), which combined the spot detection with automatic background subtraction and normalization of the spot volumes. Spots differing significantly ($p < 0.05$, Student's t-test) in density were picked for MALDI-TOF MS analysis.

Tryptic digestion of protein spots and peptide mass fingerprinting by Matrix-assisted laser desorption/ionization-time of flight-mass spectrometry (MALDI-TOF-MS): All methods applied here have been described in detail by Fuchs et al. (80). Briefly, CBB-stained spots were picked, destained and digested in gel with sequencing grade modified trypsin (Promega). The resulting peptide fragment extracts were analyzed by MALDI-TOF-MS with an Autoflex mass spectrometer (Bruker Daltonics, Leipzig, Germany). Proteins were identified with the Mascot Server 1.9 (Bruker Daltonics) based on mass searches with mouse sequences only. The criteria for positive identification of proteins were set as follows: (i) a minimum score of 63; (ii) mass accuracy of $\pm 0.01\%$ and (iii) at least two-fold analysis from four independent gels.

4.3 Metabolite analysis by GC-TOF-MS

The metabolome of kidney tissue samples was determined by Oliver Fiehn (Max Planck Institute of Molecular Plant Physiology, Golm, Germany). Metabolite levels in kidney tissue were analyzed as described in (246) with minor modifications. Briefly, individual kidneys were homogenized in a mortar under liquid nitrogen and 5 mg of tissue were extracted with a solvent mixture of methanol/chloroform/water 2.5:1:1 v/v/v kept at -20°C. Further fractionation of the extracts and derivatization of metabolites was performed as described previously (248). GC-TOF-MS analysis was performed using a HP5890 gas chromatograph with standard liners containing glass wool in a splitless mode at 230°C injector temperature with a liner exchange for every 50 samples. The GC was operated at constant flow of 1 ml/min helium on a 30 m, 0.25 mm ID, 0.25 µm RTX-5 column with a 10 m integrated precolumn. The

temperature gradient started at 80°C, was held isocratic for 2 min, and subsequently ramped at 15°C/min to a final temperature of 330°C which was held for 6 min. Data were acquired on a Pegasus II TOF mass spectrometer (LECO, St. Joseph, MI) and CHROMATOF 1.61 software at 20 s⁻¹ from m/z 85-500, R = 1, 70 kV electron impact (EI) and auto-tuning with reference gas CF 43. Samples were compared against reference chromatograms that had a maximum of detectable peaks at signal/noise >20. For identification and alignment, peaks were matched against a customized reference spectrum database, based on retention indices and mass spectral similarities. Relative quantification was performed on ion traces chosen by optimal selectivity from co-eluting compounds. Artifact peaks resulting from column bleeding, phthalates and polysiloxanes were removed. All data were normalized to tissue fresh weight (FW) and to internal references (ribitol and nonadecanoic acid methyl ester). Data were log-transformed, resulting in more Gaussian-type distributions. Differences between transporter-deficient and control animals were analyzed by principal component analysis (PCA) and partial least squares discriminant analysis (PLS-DA) after centering and unit variance (UV) scaling of the complete data set (identified and unidentified compounds) with SIGMA P 11 (Umetrics Ltd., Umeå, Sweden). PLS-DA was cross-validated by leaving out 20% of the samples, calculating a new model on the remaining samples and predicting the class membership of the left out samples. This process was repeated five times.

5. Statistics

Unless stated otherwise statistical analysis was performed by SPSS Versions 11.0-14.0 (SPSS, Chicago, IL, USA) and data are given as mean ± SD. The level of statistical significances was set at $p < 0.05$. All data was tested for normal distribution by Shapiro Wilk test. In case of normal distribution, data was analyzed by parametric tests. If normal distribution could not be assumed or if the sample size was $n < 5$, nonparametric tests were applied. Multiplicity of tests was accounted for by Bonferroni corrections for multiple comparisons.

Results

1. Basal phenotypic characterization of *Pept2*^{-/-} mice

1.1 Body weight and organ weight

Body weight of littermates was monitored over 25 weeks under standard housing and feeding conditions (Fig. 6). Male *Pept2*^{-/-} mice showed an apparent tendency for lower body weights, which became significant at weeks of life 13, 14 and 20 when compared to the heterozygous mice, only.

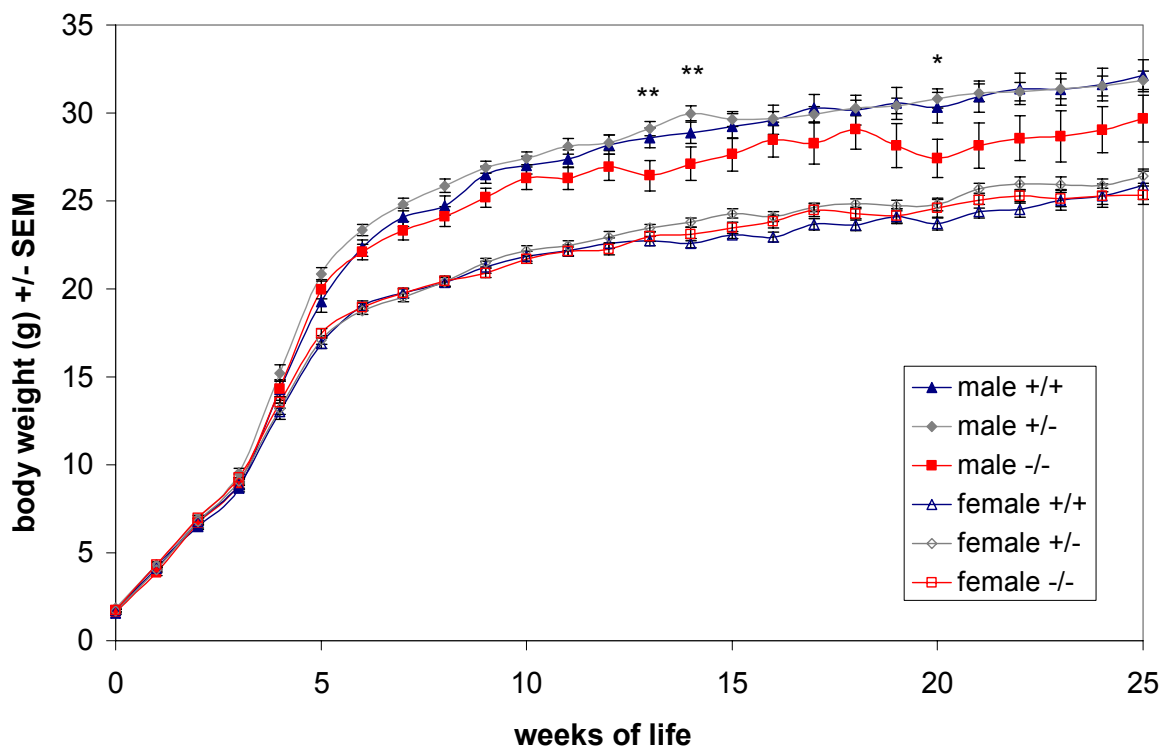


Fig. 6: Monitoring of body weight over 25 weeks

Body weight of male and female *Pept2*^{+/+}, *Pept2*^{+/-} and *Pept2*^{-/-} littermates was monitored over 25 weeks of life. N = 14-50 animals per sex and genotype were studied. Data from male and female mice were analyzed separately. Despite an apparent trend towards lower body weight for male *Pept2*^{-/-} animals, no significant difference could be observed between *Pept2*^{+/+} and *Pept2*^{-/-} mice. Significantly lower body weight was observed for *Pept2*^{-/-} vs. *Pept2*^{+/-} at week of life 13, 14 and 20 (* = p < 0.05, ** = p < 0.01, one way ANOVA).

To determine the origin of these differences, data on organ weights in relation to body weight of carcass, adipose tissue, intestine, liver, kidney, heart and brain (Table 3) were obtained. In male animals, relative heart weight was significantly lower in knockout animals. Female *Pept2*^{-/-} mice also displayed a tendency towards lower

heart weight that did not reach significance, yet. However, relative kidney weight was significantly lower in female *Pept2*^{-/-} mice.

Table 3: Relative organ weights

	male		female	
	+/+	-/-	+/+	-/-
carcass (%bw)	37.97 ± 0.95	37.54 ± 1.02	36.03 ± 1.22	36.30 ± 1.43
fat (%bw)	3.19 ± 1.16	3.82 ± 0.93	3.87 ± 1.46	3.28 ± 1.02
instestine (%bw)	5.33 ± 0.88	5.66 ± 0.82	7.13 ± 0.76	7.42 ± 0.60
liver (%bw)	5.49 ± 0.42	5.32 ± 0.31	5.03 ± 0.57	4.94 ± 0.24
kidney (%bw)	1.28 ± 0.07	1.24 ± 0.08	1.20 ± 0.13*	1.09 ± 0.09*
heart (%bw)	0.46 ± 0.07*	0.41 ± 0.03*	0.44 ± 0.42	0.42 ± 0.04
brain (%bw)	1.46 ± 0.12	1.43 ± 0.15	1.79 ± 0.11	1.78 ± 0.12

¹ bw = body weight (g)

All data represent the mean ± SD. Data from male and female animals were analyzed separately.

N = 16-20 male animals per genotype and n = 10-16 female animals per genotype were studied.

* = significant difference between genotypes determined by Mann-Whitney U-Test (p < 0.05)

1.2 Litter size and weight at weaning

PEPT2 is expressed in the male and female reproductive tract. LacZ staining performed in the targeted animals revealed that in the male reproductive tract PEPT2 is expressed in epithelial cells of the ejaculatory duct and in Leydig cells of the testes (unpublished data by I. Rubio-Aliaga). In the female reproductive tract LacZ staining could be observed in epithelial cells of uterine glands. We therefore hypothesized that reproductive performance might be impaired in the transporter deficient animals and compared the litter size of born pups in homozygotic wildtype and *Pept2*^{-/-} matings. Mean litter size was 7.4 ± 3.0 animals for *Pept2*^{+/+} litters and 6.6 ± 2.6 animals for *Pept2*^{-/-} litters. No significant difference between genotypes could be observed as shown in Fig. 7A. As PEPT2 is also expressed in the mammary gland, development of the pups might be affected in pups nursed by a *Pept2*^{-/-} mother. To

evaluate these effects we analysed the number of surviving pups at the age of weaning. As dams occasionally have difficulties in nursing the first litter, the first litter was omitted from the analysis. The number of surviving pups at weaning was marginally, yet significantly lower for *Pept2*^{-/-} litters as for wildtype litters as is shown in Fig. 7B with a mean number of 7.9 ± 2.8 surviving pups in *Pept2*^{+/+} litters and 6.2 ± 2.2 in *Pept2*^{-/-} litters.

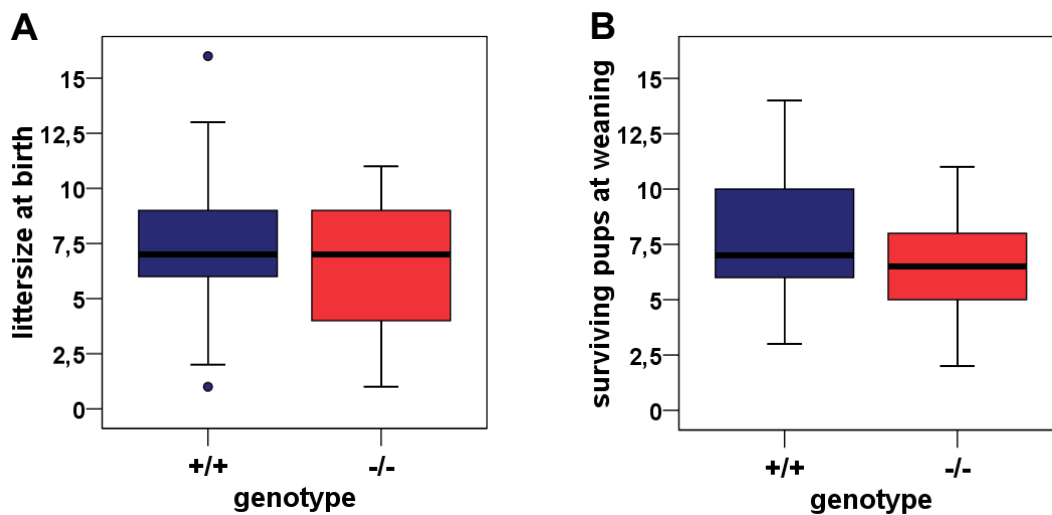


Fig. 7: Litter size at birth and surviving pups at weaning

The Boxplots represent the median, the quartiles and extreme values.

A, For the littersize at birth $n = 43$ *Pept2*^{+/+} litters and $n = 55$ *Pept2*^{-/-} litters were analyzed. There is no significant difference between genotypes.

B, For the number of surviving pups at weaning $n = 25$ *Pept2*^{+/+} and $n = 34$ *Pept2*^{-/-} litters were analyzed. The number of surviving pups is significantly lower ($p = 0.025$, Mann-Whitney-U-Test) in *Pept2*^{-/-} litters.

On the other hand, no differences in body weight from birth up to the age of weaning between litters nursed by wildtype or knockout dams were observed. Mean weight of male mice at weaning in *Pept2*^{-/-} litters was 13.9 ± 2.8 g in *Pept2*^{-/-} litters and 13.6 ± 2.8 g in *Pept2*^{+/+} litters and the mean weight of female mice was 12.8 ± 2.0 g and 11.7 ± 2.5 g in *Pept2*^{-/-} and *Pept2*^{+/+} litters, respectively. To further study whether the impaired survival of the *Pept2*^{-/-} pups is due to the nursing by the *Pept2*^{-/-} dams or whether *Pept2*^{-/-} pups have intrinsically a lower survival rate during their first weeks of life, litters of homozygotic matings could be swapped thus that the *Pept2*^{-/-} pups are nursed by a *Pept2*^{+/+} dam and vice versa.

1.3 Lifespan

To study whether the loss of the PEPT2 protein impairs vital functions in a way that the lifespan of the knockout animals is affected, we followed a group of littermate animals of each sex and genotype, including heterozygote animals. When the animals had reached a mean age of two years no obvious differences could be observed for the number and age of deceased animals or animals that had to be killed due to illness (mainly tumours) as shown in Table 4 and the animals were not further followed.

Table 4: Number and mean age of deceased animals during 2 years of follow-up

gender and genotype	n ¹	number of deceased animals	number of animals killed due to illness	age at death (Mean \pm SD in weeks)
male +/+	14	4	2	99.5 \pm 16.0
male +/-	16	2	2	74.5 \pm 29.7
male -/-	10	4	2	82.7 \pm 13.9
female +/+	12	5	1	83.8 \pm 16.2
female +/-	18	5	1	89.8 \pm 24.8
female -/-	11	5	2	102.6 \pm 11.9

¹ n = Number of animals studied

1.4 Urine parameters and amino acids in urine

As the highest expression of PEPT2 is found in the proximal tubule of the kidney we studied in urine samples whether urine composition differs between wildtype and knockout animals. Urine samples were collected during a 24 hour fasting period. As shown in Table 5, the volume of urine excreted per day by the *Pept2*^{-/-} mice was not statistically different from heterozygous or wildtype animals. Urine creatinine levels as well as the total protein to creatinine ratio and urea to creatinine ratio did not differ significantly among the different genotypes.

Table 5: Urine parameters in 24 h urine samples

gender / genotype	urine parameters			
	volume (ml/day)	creatinine (mmol/l)	total protein (mg/mmol creatinine)	urea (g/mmol creatinine)
male +/+ n = 8-10	1.30 ± 0.70	2.96 ± 0.61	204.4 ± 38.3	5.10 ± 0.64
male +/- n = 9-10	1.26 ± 0.44	3.12 ± 0.86	189.5 ± 37.3	5.85 ± 3.26
male -/- n = 7-9	0.86 ± 0.30	3.44 ± 0.84	168.5 ± 20.4	6.24 ± 1.58
female +/+ n = 7-10	0.80 ± 0.19	2.83 ± 0.67	97.3 ± 35.3	5.97 ± 1.30
female +/- n = 9-11	0.98 ± 0.48	2.82 ± 0.86	104.4 ± 16.4	5.08 ± 0.95
female -/- n = 9-10	1.25 ± 0.63	2.51 ± 0.61	112.3 ± 14.87	4.85 ± 0.86

All data represent the mean ± SD. Data from male and female animals were analyzed separately. There is no significant difference between genotypes.

As PEPT2 is responsible for the reabsorption of di- and tripeptides, we further analyzed the urine samples for free and dipeptide bound amino acids to study whether reduced reabsorption of peptides due to loss of PEPT2 does indeed lead to higher excretion. Dipeptides were determined indirectly by analyzing the urine samples for amino acids prior to and after digestion of the samples with purified membrane bound dipeptidase (EC 3.4.13.19). Progressive hydrolysis of di- and tripeptides by renal peptidases along the nephron might also lead to higher concentrations of free amino acids in urine samples of the transporter deficient animals. In Table 6 values are given for all proteinogenic amino acids that could be quantified reliably. For aspartate and asparagine, glutamate and glutamine the concentration of the sum of these amino acids is given, as asparagine and glutamine are not stable and can be hydrolyzed to aspartate or glutamate. Moreover the peaks of asparagine, glutamate and glutamine could not be separated completely in all samples. Although there is a tendency towards higher excretion of free amino acids in the transporter deficient animals no significant difference was observed for any of the amino acids studied.

Table 6: Free and dipeptide bound amino acids in urine of male and female mice

	male			female		
	+/+	+/-	-/-	+/+	+/-	-/-
free amino acids (mmol/mol creatinine)						
threonine	26.8 ± 7.7	31.0 ± 14.5	30.4 ± 10.1	34.5 ± 8.3	39.5 ± 10.3	42.0 ± 7.4
serine	23.8 ± 7.2	24.9 ± 9.4	25.7 ± 5.8	34.8 ± 10.8	37.2 ± 11.6	39.9 ± 8.6
glycine	98.1 ± 41.8	96.1 ± 32.7*	141.0 ± 40.7**	99.3 ± 24.7*	99.5 ± 22.7*	117.7 ± 25.7*
alanine	25.4 ± 10.2	30.3 ± 15.7	34.1 ± 10.8	49.4 ± 20.9	49.3 ± 20.0	58.9 ± 18.8
isoleucine	17.1 ± 5.9	17.9 ± 3.0	19.1 ± 4.2	36.3 ± 10.8	37.0 ± 10.0	45.6 ± 13.6
leucine	24.1 ± 7.6	24.6 ± 11.1	34.0 ± 8.8	29.5 ± 12.0	29.7 ± 13.2	42.3 ± 8.4
asp+asn +glu+gln	118.2 ± 38.4	153.4 ± 64.5	140.3 ± 47.0	168.7 ± 67.8	161.6 ± 63.4	153.3 ± 38.5
amino acids after dipeptidase digestion (mmol/mol creatinine)						
threonine	30.0 ± 11.7	33.8 ± 11.0	30.2 ± 4.4	36.9 ± 7.7	42.8 ± 8.4	42.9 ± 4.7
serine	17.2 ± 5.3	23.1 ± 8.5	20.5 ± 5.8	33.4 ± 11.7	34.3 ± 13.1	36.6 ± 9.6
glycine	114.0 ± 35.1 ^a	127.2 ± 30.8 ^{b*}	198.5 ± 38.5 ^{a,b**}	109.4 ± 28.0*	118.9 ± 36.6*	143.6 ± 28.6*
alanine	26.1 ± 9.3	31.3 ± 16.3	28.7 ± 12.5	50.6 ± 21.9	52.6 ± 18.4	55.0 ± 18.9
isoleucine	23.2 ± 6.8	24.0 ± 6.4	27.7 ± 5.0	36.7 ± 10.6	44.0 ± 11.5	45.0 ± 12.7
leucine	24.3 ± 5.8 ^a	28.6 ± 6.9	36.0 ± 5.6 ^a	31.7 ± 13.3 ^a	32.4 ± 11.2	47.3 ± 5.1 ^a
asp+asn +glu+gln	121.9 ± 26.7	155.4 ± 68.4	130.6 ± 62.1	177.7 ± 69.6	187.1 ± 60.7	163.7 ± 40.4

All values represent the mean ± SD. N = 7-9 male animals and n = 9-11 female animals per genotype were studied for free amino acids. N = 6-8 male animals and n = 8-10 female animals per genotype were studied for amino acids after dipeptidase digestion.

Data from male and female animals were analyzed separately.

All data were analyzed by Kruskal-Wallis and Mann-Whitney U-Test with Bonferroni correction for differences in respect to genotype. Values bearing identical superscripts (^{a, b}) indicate significant differences between genotypes (p < 0.05). Analysis for differences between analysis prior to and after dipeptidase hydrolysis was performed by Wilcoxon test for paired samples. * significant difference between free amino acid concentration and amino acid concentration after dipeptidase digestion (* = p < 0.05. ** = p < 0.01)

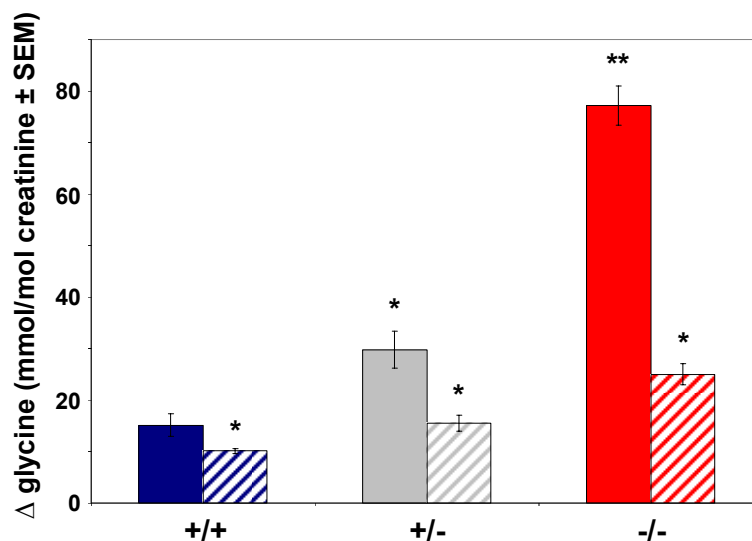


Fig. 8: Dipeptide bound glycine in male and female mice

Dipeptide bound glycine (Δ glycine) was calculated as the difference between glycine prior to and after dipeptidase digestion. N = 6-8 male animals (filled bars) and n = 8-10 female animals (striped bars) per genotype were studied. Data from male and female animals were analyzed separately. Analysis for differences between analysis prior to and after dipeptidase hydrolysis was performed by Wilcoxon test for paired samples. (* = $p < 0.05$, ** = $p < 0.01$)

A significant amount of dipeptide bound amino acid was observed for glycine, only. In male animals dipeptidase digestion led to a significant increase in glycine detected in urine of heterozygous and knockout mice and in female animals a significant amount of dipeptide bound glycine was observed for all genotypes (Fig. 8).

Yet, the fraction of dipeptide bound glycine was larger in the transporter deficient animals, thus that after dipeptidase digestion male knockout animals had a significantly higher glycine concentration in comparison to heterozygous and wildtype animals. Moreover, urine of *Pept2*^{-/-} animals contained more dipeptide bound leucine. Although the increase in free leucine due to dipeptidase digestion was not significant, overall leucine concentration was significantly higher after dipeptidase hydrolysis in *Pept2*^{-/-} in comparison to *Pept2*^{+/+} mice in male as well as in female animals.

1.5 Compensatory regulation of related peptide transporters in the kidney

As related peptide transporters might assume peptide reabsorption in kidneys of PEPT2 deficient animals, we investigated whether loss of PEPT2 leads to the compensatory upregulation of expression levels of other members of the PTR family. mRNA expression levels were analyzed by Northern blot for *Pept1*, *Ph1* and *Ph2*.

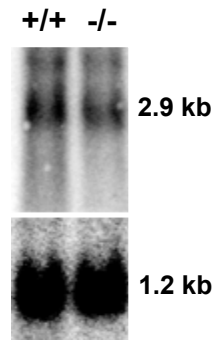


Fig. 9: Expression of PHT1 in kidney

Northern Blot analysis of PHT1 mRNA expression in kidney. No differences were detected in the intensity of the 2.9-kb band which corresponds to the PHT1 RNA. The blot was striped and rehybridized with a GAPDH probe as a loading and quality control (1.2-kb fragment).

As shown in Fig. 9 *Ph1* displays no differential expression between wildtype and transporter deficient animals. For *Pept1* and *Ph2* no signal could be detected in kidney tissue by Northern blot (data not shown). It appears that our probe for *Pept1* was not sufficiently sensitive to detect the low level of expression of *Pept1* in the kidney as only in samples from small intestine specific hybridization could be observed (data not shown). Yet, Rubio-Aliaga *et al.* could show by Western blot, that there is no difference in PEPT1 protein level between *Pept2*^{+/+} and *Pept2*^{-/-} animals (186). mRNA levels of *Pept1* were later analyzed by qPCR in samples from the metabolic study (see below). Whether *Ph2* is actually localized in mouse kidney has not been studied in detail so far. Northern blot analysis for *Ph2* with human samples has been shown to give a weak signal (33) whereas Northern blot analysis of rat kidney did not detect *Ph2* and RT-PCR of rat kidney mRNA with primers for *Ph2* revealed only a very faint signal (190)

1.6 Clinical-chemical parameters and free amino acids in plasma

Standard clinical chemistry performed in plasma samples at the German Mouse Clinic (GSF, Neuherberg, Germany) by Martina Klempt revealed a number of significant differences between genotypes as shown in Table 7. We furthermore calculated a reference range for each parameter by addition or subtraction of 2 standard deviations from the mean of the values for the control group (wildtype animals). None of the parameters in any group of animals was outside of the corresponding reference range suggesting that the observed differences – although in some cases significant when compared between genotypes – are not representing a pronounced pathophysiological alteration.

Table 7: Clinical chemical parameters in male and female mice

	reference range	male		reference range	female	
		+/+	-/-		+/+	-/-
sodium (mmol/l)	153 - 166	160 ± 3.1	159.5 ± 4.2	151 - 165	157.0 ± 4.5	158.2 ± 3.4
potassium (mmol/l) [‡]	3.5 - 5.3	4.4 ± 0.5	4.5 ± 0.3	3.8 - 5.7	4.5 ± 0.4	4.7 ± 0.5
calcium (mmol/l)	1.9 - 2.3	2.1 ± 0.1	2.2 ± 0.1	1.8 - 2.3	2.0 ± 0.2	2.0 ± 0.1
chloride (mmol/l)	109.7 - 126.5	118.1 ± 4.2	118.1 ± 3.3	111.9 - 128.6	121.8 ± 2.3	120.3 ± 4.2
phosphorus (mg/dl)	1.6 - 2.8	2.2 ± 0.3	2.3 ± 0.3	1.9 - 3.2	2.4 ± 0.3	2.5 ± 0.3
total protein (mg/dl)	4.7 - 6.4	5.6 ± 0.4	5.6 ± 0.4	4.1 - 6.5	5.2 ± 0.6	5.3 ± 0.6
creatinine (mg/dl)	0.250 - 0.339	0.295 ± 0.022	0.295 ± 0.02	0.248 - 0.430	0.307 ± 0.04 [†]	0.339 ± 0.05 [†]
urea (mg/dl)	34.3 - 95.6	65.0 ± 15.3	60.8 ± 8.3	33.5 - 87.2	67.2 ± 18.5	60.3 ± 13.4
uric acid (mg/dl)	0.0 - 0.8	0.3 ± 0.3	0.4 ± 0.3	0 - 1.6	0.6 ± 0.4	0.7 ± 0.5
cholesterol (mg/dl) [‡]	40.0 - 164.9	102.4 ± 31.2	107.1 ± 22.7	33.2 - 122.0	78.9 ± 15.8	77.6 ± 22.2
triglyceride (mg/dl)	30.5 - 92.3	61.4 ± 15.5 ^{***}	85.1 ± 23.2 ^{***}	12.9 - 119.1	55.2 ± 21.5	66.0 ± 26.6
creatine kinase (U/l) [‡]	0 - 162	57 ± 52	25 ± 9	0 - 152	99 ± 71	58 ± 47
alanine-amino-transferase (U/l) [‡]	0 - 18	9 ± 5	9 ± 3	0 - 38	18 ± 16	15 ± 12
aspartate-amino-transferase (U/l) [‡]	3 - 75	39 ± 18*	26 ± 5 *	19 - 46	56 ± 26	32 ± 7
alkaline phosphatase (U/l) [‡]	37 - 187	112 ± 37	118 ± 33	96 - 251	198 ± 32	174 ± 39
alpha amylase (U/l)	1750 - 5029	3389 ± 820	2874 ± 533	917 - 4974	3353 ± 1625	2946 ± 1014
glucose (mg/dl)	93 - 250	171 ± 39	192 ± 49.7	93 - 167	126 ± 25	130 ± 18.5
ferritin (ng/ml) [‡]	35.2 - 175.5	105.4 ± 35.1	74.4 ± 20.3	32.0 - 156.0	106.8 ± 52.3	94.0 ± 31.0
transferrin (mg/dl)	145.5 - 164.1	154.8 ± 4.7	165.2 ± 16.6	126.6 - 200.4	167.2 ± 16.4	163.5 ± 18.5

All data represent the mean ± SD, reference range: Mean of control group ± 2SD

Data from male and female animals were analyzed separately.

N = 12 male animals per genotype and N = 18 – 20 female animals per genotype were studied

[‡] only N = 13 – 16 female animals per genotype were studied due to haemolysis of samples

* significant difference between genotypes determined by Mann-Whitney U-test (* = p < 0.05, *** = p < 0.001)

[†] significant difference between genotypes determined by Student's t-test (p < 0.05)

Table 8: Free amino acids in plasma of male and female mice

amino acids (mmol/mol creatinine)	male		female	
	+/+	-/-	+/+	-/-
threonine n = 11-12	134.4 ± 18.6	126.4 ± 30.9	167.7 ± 39.4	171.7 ± 34.6
serine n = 8-11	86.7 ± 12.0	88.0 ± 6.9	103.6 ± 19.2	99.9 ± 10.4
glycine n = 11-12	248.3 ± 70.4	265.1 ± 61.1	222.0 ± 29.6	195.7 ± 36.8
alanine n = 10-12	248.4 ± 69.2	229.1 ± 58.2	245.8 ± 57.9**	182.6 ± 34.1**
valine n = 7-10	187.3 ± 33.1	233.8 ± 63.5	232.7 ± 48.0 [†]	290.5 ± 31.4 [†]
methionine n = 9-11	35.4 ± 6.0	41.5 ± 9.8	42.4 ± 9.8	39.9 ± 12.4
isoleucine n = 9-11	129.9 ± 40.3	142.7 ± 39.1	168.4 ± 40.0*	213.6 ± 38.5*
leucine n = 10-12	89.8 ± 31.9	95.1 ± 26.4	119.2 ± 26.7	126.2 ± 18.4
tyrosine n = 7-11	79.9 ± 33.4	93.1 ± 23.4	72.1 ± 23.2*	48.3 ± 8.4*

All values represent the mean ± SD. Data from male and female mice were analyzed separately.

* significant difference between genotypes determined by Student's t-test (* = p < 0.05, ** = p < 0.01)

[†] significant difference between genotypes determined by Mann-Whitney U-test (p < 0.05)

Reduced peptide reabsorption in the kidney and impaired peptide transport in further tissues that express PEPT2 might lead to altered plasma levels of amino acids in the transporter deficient animals. As for urine samples values for free amino acids in plasma are given for those that could be quantified reliably in Table 8. In male animals no significant differences in plasma levels for any of the determined amino acids was observed. Female transporter deficient animals displayed higher levels of valine and isoleucine and lower plasma levels of alanine and tyrosine. With regard to valine and isoleucine the same tendency is seen in male animals and leucine levels were slightly higher in knockout mice of both sexes as well indicating that possibly metabolism of branched chain amino acids might be affected in the transporter deficient animals.

1.7 Blood pressure

Little is known about the concentration of low molecular weight peptides circulating in plasma, but it has been suggested that 25-50% of all plasma amino acids might be present in the form of di- and tripeptides (194). Several studies have shown that selected dietary di- and tripeptides can lower the blood pressure in humans and animal models via inhibition of the angiotensin converting enzyme (ACE) (for review see (139)). ACE cleaves of a dipeptide by converting Angiotensin I into Angiotensin II and this dipeptide may be removed from plasma in kidney by PEPT2. As di- and tripeptides concentration in plasma might be altered in the *Pept2*^{-/-} animals we hypothesized that blood pressure may be altered in mice lacking the peptide transporter. However, no differences in mean arterial pressure between knockout and wild type animals neither for male (*Pept2*^{+/+} 90.4 ± 9.2 vs. *Pept2*^{-/-} 89.6 ± 10.4 mmHg) nor for female animals (*Pept2*^{+/+} 75.7 ± 8.7 vs. *Pept2*^{-/-} 76.8 ± 7.8 mmHg) could be observed (Fig. 10).

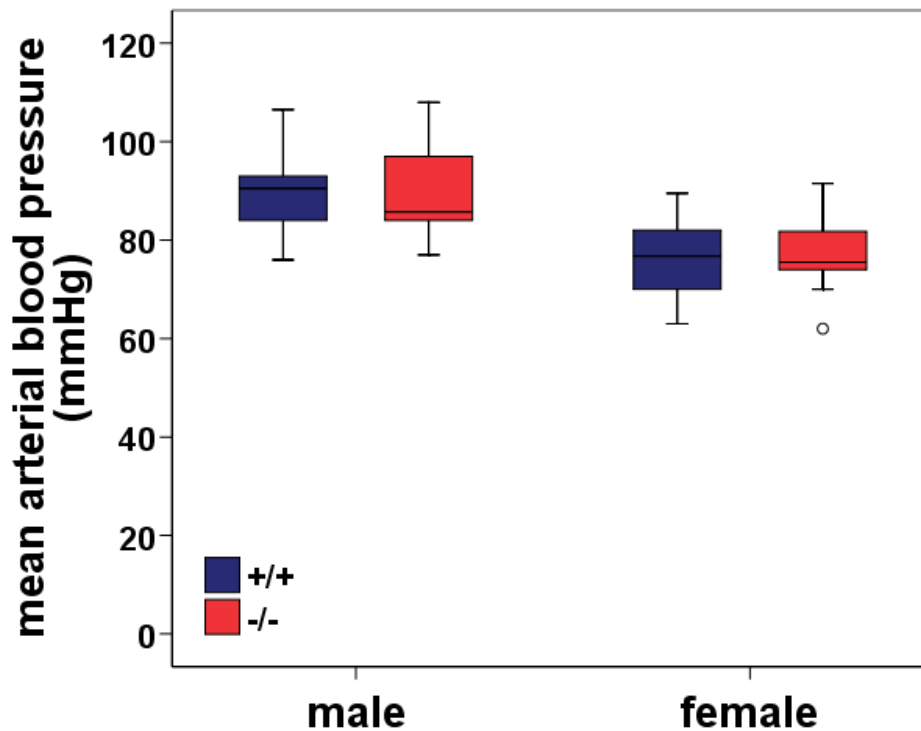


Fig. 10: Mean arterial blood pressure in male and female mice

The Boxplots represent the median, the quartiles and extreme values. N = 10 -11 animals per sex and genotype were analyzed. Data from male and female mice were analyzed separately. There is no significant difference between genotypes.

1.8 Glucagon

Expression of PEPT2 in the α -cells of the pancreatic islets of Langerhans has been shown in immunohistochemical studies previously and dipeptide uptake into isolated islet cells could be demonstrated with the fluorescently labelled dipeptide β -Ala-Lys-AMCA (150). α -Cells of the endocrine pancreas mediate the secretion of glucagon. Glucagon secretion is stimulated by a protein rich meal (123), by infusion of amino acids (179) and has also been shown to be induced by infusion of a dipeptide consisting of alanine and glutamine (132). We therefore assumed that peptide transport by PEPT2 might be one of the stimuli for glucagon secretion and that plasma glucagon levels might be affected in the transporter deficient animals, especially in the postprandial state. However, plasma glucagon levels did not differ significantly between *Pept2*^{+/+} and *Pept2*^{-/-} animals neither in the fasted (69.9 \pm 32.0 vs. 45.0 \pm 5.9 pg/ml in male and 97.8 \pm 46.2 vs. 70.5 \pm 13.9 pg/ml in female animals) nor in the postprandial state (69.4 \pm 18.7 vs. 82.8 \pm 24.1 pg/ml in male and 153.9 \pm 47.5 vs. 203.2 \pm 89.8 pg/ml in female animals) as shown in Fig. 11. We observed a striking gender difference in glucagon levels as has been described in the literature (111).

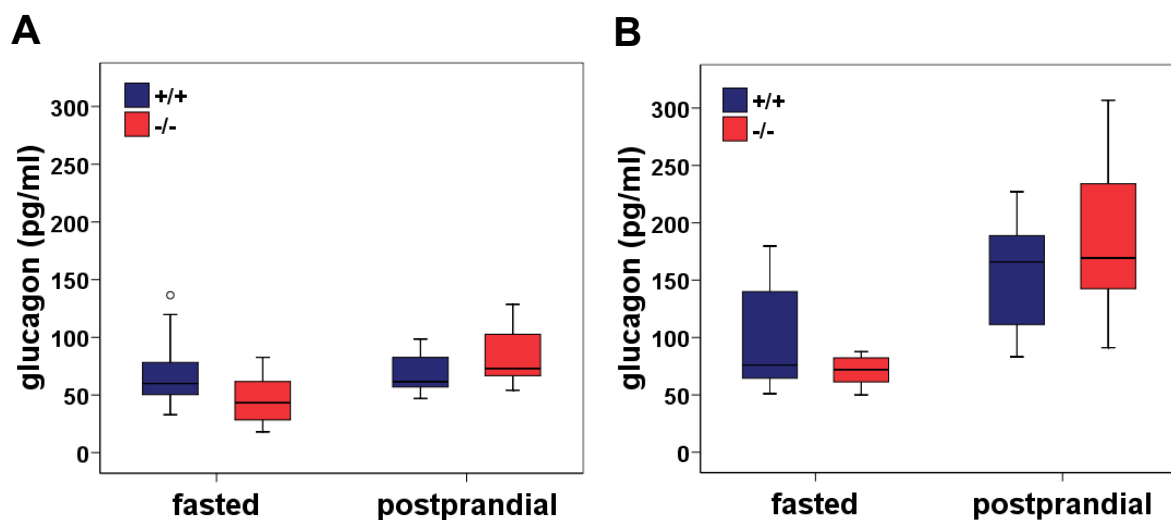


Fig. 11: Plasma glucagon levels in male and female mice

The Boxplots represent the median, the quartiles and extreme values. N = 11-12 animals per genotype and feeding state were studied in male (A) and female (B) animals. There is no significant difference between genotypes.

2. Response to different dietary protein contents

Tubular reabsorption of filtered di- and tripeptides by PEPT2 is supposed to contribute to systemic protein homeostasis. To analyze whether transporter-deficient animals respond to changes in protein supply with metabolic changes, we monitored body weight, food and water intake and determined plasma and urine parameters as well as expression of selected genes with functions in amino acid and dipeptide metabolism of animals that received either a low (10% protein), medium (20%) or high (30%) protein diet over 19 days.

2.1 Weight, food and water intake during the metabolic study

As shown in Table 9, mean food intake varied between genotypes and diets, but no significant differences in weight gain were observed. Wild type animals did not respond to the protein content of the diet with differences in food intake, whereas the transporter-deficient animals consumed significantly higher amounts of food on the low protein diet and significantly lower amounts on the high protein diet. Mean water consumption was significantly lower in null mice on the high protein diet. Water consumption increased as the protein content of the diet was increased most probably due to the higher demand of water for renal excretion of the larger quantities of urea produced from amino acid metabolism. Water intake rates in transporter deficient animals at the 30% protein level were significantly lower than in controls.

Table 9: Body weight and food and water intake in response to different protein content of the diet

	10% protein		20% protein		30% protein	
	+/+	-/-	+/+	-/-	+/+	-/-
weight day 1 (g)[†]	22.90 ± 1.89	24.31 ± 1.00	20.89 ± 1.30	23.40 ± 2.17	23.16 ± 2.02	24.07 ± 1.87
weight day 19 (g)[‡]	23.42 ± 1.18	25.97 ± 1.50	22.00 ± 1.20	23.61 ± 2.00	24.54 ± 1.66	25.81 ± 1.70
weight gain (g)[§]	1.11 ± 0.68	1.89 ± 0.95	1.43 ± 0.97	0.93 ± 0.85	1.85 ± 0.86	1.17 ± 0.85
food intake (g/24h)[*]	3.04 ± 0.10 ^a	3.44 ± 0.22 ^a	3.20 ± 0.15	3.30 ± 0.09	3.27 ± 0.21 ^b	2.90 ± 0.08 ^b
water intake (ml/24h)^{††}	1.95 ± 0.40	1.64 ± 0.23	2.85 ± 0.39	2.61 ± 0.43	3.58 ± 0.50 ^b	2.70 ± 0.26 ^b

All data represent the mean ± SD. N = 9–12 animals per genotype and diet were studied. All data were analyzed for differences in respect to genotype and protein content of the diet. Values in a row bearing identical superscripts (^a, ^b) indicate significant differences between groups (p < 0.05)

* Kruskal-Wallis and Mann-Whitney U-Test with Bonferroni correction

[†] univariate linear regression analysis: protein content of the diet p < 0.050, genotype p < 0.001, protein content of the diet x genotype n.s.

[‡] univariate linear regression analysis: protein content of the diet p < 0.001, genotype p < 0.001, protein content of the diet x genotype n.s.

[§] univariate linear regression analysis: protein content of the diet n.s., genotype n.s., protein content of the diet x genotype p < 0.05

^{††} univariate linear regression analysis: protein content of the diet p < 0.001, genotype p < 0.001, protein content of the diet x genotype p < 0.05

2.2 Clinical chemical plasma and urine parameters

Standard clinical chemistry performed in plasma and urine samples determined at the German Mouse Clinic (GSF, Neuherberg, Germany) revealed a number of significant differences in relation to genotype and / or protein content of the diet as shown in Table 10 and Table 11. Apart from an overall significant correlation between protein content of the diet and plasma urea levels, no consistent effect of either protein content of the diet or genotype could be observed. We furthermore calculated a reference range for each parameter by addition or subtraction of 2 standard deviations from the mean of these parameters with wildtype animals on the medium protein diet serving as the reference group.

Table 10: Clinical chemical parameters on diets with different protein content

	reference range	10% Protein		20% Protein		30% Protein	
		+/+	-/-	+/+	-/-	+/+	-/-
Sodium (mmol/l)* n = 10-17	147 - 160	155 ± 2.5 ^a	149 ± 4.8 ^a	154 ± 3.3	152 ± 3.5	155 ± 2.4	153 ± 2.5
Potassium (mmol/l) n = 7-11	3.6 - 6.0	4.8 ± 0.68	4.5 ± 0.30	4.8 ± 0.61	4.6 ± 0.41	4.5 ± 0.33	4.9 ± 0.57
Calcium (mmol/l) n = 9-14	1.0 - 2.4	1.8 ± 0.25	2.0 ± 0.13	1.7 ± 0.37	1.8 ± 0.23	1.8 ± 0.37	1.5 ± 0.14
Chloride (mmol/l)* n = 9-16	109.4 - 124.3	118.0 ± 2.04 ^a	112.7 ± 3.92 ^{a,b}	116.9 ± 3.74	115.5 ± 2.44	118.9 ± 3.05	118.0 ± 2.24
Phosphorus (mg/dl) n = 8-14	1.3 - 3.6	2.2 ± 0.39	1.9 ± 0.19	2.5 ± 0.59	2.0 ± 0.23	2.0 ± 0.37	2.2 ± 0.29
Total Protein (mg/dl) n = 10-17	4.3 - 5.5	4.8 ± 0.39	4.9 ± 0.32	4.9 ± 0.30	4.9 ± 0.32	5.0 ± 0.31	4.8 ± 0.30
Creatinine (mg/dl)* n = 10 - 17	0.194 - 0.313	0.271 ± 0.030 ^a	0.281 ± 0.020 ^b	0.253 ± 0.030	0.263 ± 0.026	0.232 ± 0.025 ^a	0.252 ± 0.017 ^b
Urea (mg/dl)[†] n = 10-17	28.7 - 48.8	37.2 ± 3.73	34.0 ± 3.55	38.7 ± 5.03	41.0 ± 5.61	47.6 ± 8.22	48.4 ± 5.75
Uric Acid (mg/dl)* n = 10 - 17	0.0 - 5.0	1.6 ± 0.97	0.8 ± 0.40	2.5 ± 1.23 ^{a,b}	0.9 ± 0.77 ^a	1.5 ± 1.35 ^b	1.4 ± 1.02
Cholesterol (mg/dl)[‡] n = 8-12	36.4 - 165.2	123.3 ± 16.68 ^a	163.3 ± 35.25 ^a	100.8 ± 32.22 ^b	147.1 ± 20.39 ^b	134.2 ± 29.06	133.0 ± 24.40
Triglyceride (mg/dl) n = 10-17	39.1 - 85.6	50.4 ± 12.01	58.7 ± 10.21	62.3 ± 11.60	65.5 ± 18.88	60.2 ± 17.27	62.1 ± 10.67
Creatine Kinase (U/l) n = 7-12	0 - 64	45 ± 20.0	38 ± 10.0	29 ± 17.6	40 ± 18.7	26 ± 16.2	50 ± 10.4
Alanine-Amino-Transferase (U/l) n = 8-12	0 - 18	7 ± 3.4	8 ± 3.6	8 ± 4.8	6 ± 1.9	7 ± 3.0	9 ± 3.7
Aspartate-Amino-Transferase (U/l)* n = 8-12	11 - 47	27 ± 6.7	23 ± 4.8 ^a	29 ± 9.0 ^b	27 ± 6.1	28 ± 9.4 ^c	45 ± 10.1 ^{a,b,c}
Alkaline Phosphatase (U/l) n = 7-12	53 - 214	86 ± 12.3	83 ± 11.2	133 ± 40.4	85 ± 23.9	95 ± 7.0	78 ± 8.1
Alpha Amylase (U/l) n = 9-15	956 - 3431	2586 ± 491.3	2582 ± 419.5	2193 ± 618.9	2420 ± 333.6	2328 ± 556.4	1953 ± 291.6
Ferritin (ng/ml)* n = 8-12	25.3 - 87.4	78.0 ± 9.92 ^{a,b}	71.3 ± 18.72	56.4 ± 15.52 ^a	52.0 ± 13.82	45.6 ± 14.75 ^{b,c}	76.5 ± 27.24 ^c
Transferrin (mg/dl)* n = 9-14	120.8 - 164.2	132.1 ± 6.74 ^a	131.1 ± 6.79	142.5 ± 10.84	136.5 ± 7.25	150.1 ± 14.30 ^{a,b}	129.8 ± 5.56 ^b

All data represent the mean \pm SD.

All data were analyzed for differences in respect to genotype and protein content of the diet.

Values in a row bearing identical superscripts (^{a, b}) indicate significant differences between groups ($p < 0.05$)

* Kruskal-Wallis and Mann-Whitney U-Test with Bonferroni correction

† univariate linear regression analysis: protein content of the diet $p < 0.001$, genotype n.s., protein content of the diet x genotype n.s.

‡ univariate linear regression analysis: protein content of the diet $p < 0.001$, genotype n.s., protein content of the diet x genotype $p < 0.05$

reference range: Mean of control group (wildtype on 20% Protein) \pm 2SD

None of the clinical-chemical parameters in any group of animals was outside of the corresponding reference range suggesting that the observed differences – although in some cases significant when compared between genotypes – are not representing a pronounced pathophysiological alteration.

Among the urine parameters (Table 11), transporter-deficient animals displayed a tendency towards lower urine volumes reflecting the reduced water intake with differences in urine volume reaching the level of significance in animals receiving the high protein diet. The differences in water consumption and the corresponding differences in urine volumes are also reflected in creatinine concentrations. Transporter-deficient animals had significantly higher urinary creatinine concentrations at low and medium protein diets. Urine osmolality and urea levels in urine were associated with water and protein intake with significantly lower levels on the low protein diet and highest levels on the high protein diet, but without any effect of the genotype. Total protein excretion was significantly lower in null mice on the low protein diet when compared to *Pept2*^{-/-} mice on the medium and high protein diet.

Table 11: Urine parameters in response to diets with different protein content

	reference range	10% protein		20% protein		30% protein	
		+/+	-/-	+/+	-/-	+/+	-/-
water consumption[†] (ml/24h) n = 10-13	1.9 – 4.1	1.8 ± 0.5 ^{a,b}	1.5 ± 0.2 ^{c,d}	3.0 ± 0.5 ^a	2.6 ± 0.7 ^c	3.3 ± 0.7 ^{b,e}	2.5 ± 0.4 ^{d,e}
urine volume (µl/12h) n = 8-13	119 - 503	169 ± 140	114 ± 75	311 ± 96	231 ± 150	290 ± 119	181 ± 68
creatinine (mmol/l)[†] n = 10-13	0.92 - 2.50	3.16 ± 1.66	4.45 ± 1.00 ^a	1.71 ± 0.40	2.37 ± 1.18 ^a	2.51 ± 1.12	2.59 ± 0.67 ^a
osmolality (mOsm/kg)[‡] n = 9-13	600 - 1378	989 ± 195	1272 ± 522	991 ± 418	1362 ± 260	1634 ± 348	2234 ± 273
urea[†] (g/mmol Creatinine) n = 10-12	14.1 - 39.1	12.5 ± 1.8 ^a	12.5 ± 0.5 ^{b,c}	26.6 ± 6.3 ^a	30.0 ± 4.8 ^b	35.8 ± 11.0 ^a	45.2 ± 10.6 ^c
total protein[†] (g/mmol Creatinine) n = 9-12	512.4 - 940.3	536.8 ± 192.5	325.4 ± 16.1 ^{a,b}	726.4 ± 107.0	541.3 ± 161.6 ^a	577.5 ± 210.2	524.5 ± 87.3 ^b
uric acid (mg/mmol Creatinine) n = 9-13	53.5 - 97.1	71.2 ± 11.6	76.8 ± 3.2	75.3 ± 10.9	64.5 ± 10.3	68.5 ± 15.7	61.5 ± 7.5

All values represent the mean ± SD. All data were analyzed for differences in respect to genotype and protein content of the diet.

Values in a row bearing identical superscripts (^{a, b}) indicate significant differences between groups (p < 0.05)

[†]Kruskal-Wallis and Mann-Whitney U-Test with Bonferroni correction;

[‡]univariate linear regression analysis: protein content of the diet p < 0.001, genotype p < 0.001, protein content x genotype n.s.

reference range: Mean of control group (wildtype on 20% Protein) ± 2SD

2.3 Amino acids and dipeptides in urine

Data for excretion of free amino acids on the different diets is given in Table 12 in the upper part. To what extent amino acids were excreted in the form of dipeptides was assessed indirectly by amino acid analysis after *in vitro* digestion of urine samples with a renal dipeptidase (Table 12, lower part). The data were analysed whether differences could be observed between genotypes, between levels of protein intake and whether amino acid concentration increased by dipeptidase digestion, indicating the presence of dipeptides in urine. A significantly higher excretion of free amino acids in the transporter deficient animals could only be observed for glycine when animals were fed the high protein diet. On the low protein diet knockout animals displayed a rather lower excretion of free amino acids that became significant in the case of threonine and alanine. Significant amounts of dipeptide bound amino acids could only be observed for glycine and cystine. For glycine the increase in amino acid concentration after dipeptidase hydrolysis was significant in knockout animals at all protein levels and for wildtype animals only on the high protein diet (Fig. 12). A significant fraction of dipeptide bound cystine was observed in urine samples of the transporter deficient animals on the medium protein diet and for both genotypes on the high protein diet. Yet, the dipeptide bound fraction of amino acids was again considerably larger in the transporter deficient animals. Thus, dipeptidase digestion led to significant differences between knockout and wildtype animals for amino acids after hydrolysis in the case of glycine, alanine, cystine and methionine on the high protein diet and in the case of glycine on the medium protein diet. Furthermore amino acid excretion, independent of analysis previous to or after digestion, was influenced by protein intake in the PEPT2 null mice but not in the wildtype animals. In transporter deficient animals excretion of all amino acids was significantly lower on the low protein diet in comparison to excretion on the medium protein diet. For the comparison between low and high protein diet, excretion was as well significantly lower at 10% protein intake for all amino acids apart from threonine and serine. The only case for influence of protein content of the diet on amino acid excretion in wildtype animals is glycine, with significantly higher excretion of glycine by animals on the medium protein diet in comparison to animals on the low protein diet.

Table 12: Free and dipeptide bound amino acids in urine

	10% Protein		20% Protein		30% Protein	
	+/+	-/-	+/+	-/-	+/+	-/-
free amino acids (mmol/mol creatinine)						
threonine n = 8-10	71.0 ± 24.3	54.5 ± 12.7 ^a	92.2 ± 24.6	90.8 ± 35.8 ^a	78.9 ± 26.0	77.2 ± 29.7
serine n = 7-10	37.7 ± 18.8 ^a	23.4 ± 8.8 ^{a,b}	43.5 ± 17.3	52.9 ± 51.7 ^b	32.6 ± 18.0	38.7 ± 13.4
glycine n = 9-12	146.0 ± 41.9 ^a	154.9 ± 53.0 ^{b,*}	207.9 ± 45.3 ^a	253.1 ± 151.9 [*]	152.6 ± 40.6 ^{c,*}	298.3 ± 69.6 ^{b,c,*}
alanine n = 9-10	94.4 ± 41.6 ^a	54.9 ± 15.2 ^{a,b,c}	88.8 ± 46.4	107.0 ± 75.0 ^b	72.9 ± 38.4	95.3 ± 32.6 ^c
cystine n = 8-12	67.4 ± 36.8	41.4 ± 10.7 ^a	73.1 ± 26.2	68.0 ± 23.9 ^{a,*}	107.9 ± 57.2 [*]	193.4 ± 58.2 ^{a,*}
methionine n = 5-11	31.4 ± 13.3	30.6 ± 12.2 ^a	62.0 ± 19.7	61.4 ± 22.7	51.2 ± 17.7	82.5 ± 12.5 ^a
isoleucine n = 5-10	33.4 ± 13.8	21.1 ± 3.9 ^{a,b}	47.6 ± 21.2	53.9 ± 41.6 ^a	46.7 ± 17.7	50.1 ± 14.5 ^b
leucine n = 6-11	62.6 ± 18.1	53.8 ± 15.4 ^{a,b}	76.6 ± 38.7	88.9 ± 49.8 ^a	59.9 ± 28.6	88.7 ± 22.9 ^b
amino acids after dipeptidase digestion (mmol/mol creatinine)						
threonine n = 6-12	72.9 ± 17.0	53.1 ± 10.7 ^a	92.8 ± 22.5	87.0 ± 21.4 ^a	63.6 ± 32.0	64.5 ± 31.8
serine n = 5-12	46.0 ± 19.4	21.9 ± 5.7 ^a	44.5 ± 18.1	47.6 ± 29.1 ^a	27.8 ± 17.5	32.4 ± 13.1
glycine n = 6-12	160.6 ± 44.6 ^a	227.5 ± 42.9 ^{b,*}	245.2 ± 49.7 ^{a,c}	462.1 ± 192.7 ^{b,c,*}	195.5 ± 62.3 ^{d,*}	451.1 ± 155.3 ^{b,d,*}
alanine n = 6-11	101.1 ± 44.7 ^a	57.2 ± 13.6 ^{a,b,c}	91.7 ± 42.6	96.9 ± 32.3 ^b	73.6 ± 36.0 ^d	105.8 ± 25.6 ^{c,d}
cystine n = 6-12	66.9 ± 20.2	63.9 ± 18.1 ^{a,b}	85.0 ± 29.3	161.0 ± 63.4 ^{b,*}	116.4 ± 59.8 ^{d,*}	240.8 ± 82.1 ^{c,d,*}
methionine n = 5-11	33.1 ± 9.4	26.9 ± 6.6 ^{a,b}	61.5 ± 19.0	56.0 ± 18.1 ^a	50.0 ± 17.9 ^c	81.5 ± 7.9 ^{b,c}
isoleucine n = 5-10	43.1 ± 14.2	20.7 ± 9.3 ^{a,b}	47.9 ± 18.3	50.2 ± 20.9 ^a	43.7 ± 17.6	52.2 ± 15.3 ^b
leucine n = 5-11	32.1 ± 1.8	49.3 ± 6.7 ^{a,b}	75.1 ± 36.0	85.5 ± 25.0 ^a	61.6 ± 29.1	93.6 ± 26.7 ^b

All values represent the mean ± SD

All data were analyzed by Kruskal-Wallis and Mann-Whitney U-Test with Bonferroni correction for differences in respect to genotype and protein content of the diet.

Values bearing identical superscripts (^{a, b, c}) indicate significant differences between groups (p < 0.05) Analysis for differences in amino acid concentration prior to and after dipeptidase hydrolysis was performed by Wilcoxon test for paired samples (* = p < 0.05).

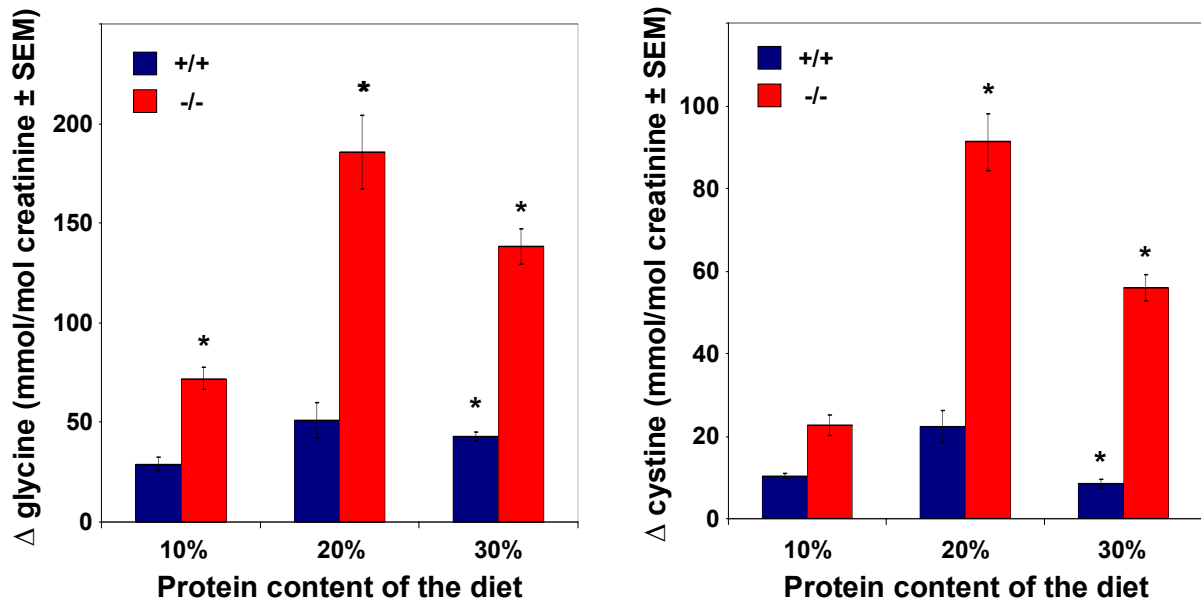


Fig. 12: Dipeptide bound glycine and cystine in urine

Dipeptide bound glycine and cystine were calculated as the difference between the amino acid concentration prior to and after dipeptidase digestion. N = 5-12 animals per genotype and diet were analyzed. Analysis for differences in amino acid concentration prior to and after dipeptidase digestion was performed by Wilcoxon test for paired samples (* = $p < 0.05$).

2.4 Additional ninhydrine positive metabolites in *Pept2*^{-/-} urine samples

In the amino acid analysis chromatograms of *Pept2*^{-/-} urine samples two additional peaks were detected with a retention time between 80 and 84 min. The metabolite that elutes shortly before tyrosine was termed X, and the metabolite that elutes with a retention time around 80 min was termed Y. However, peak X could often not be separated with the applied separation conditions from tyrosine. Sections of representative chromatograms of a *Pept2*^{-/-} and a *Pept2*^{+/+} urine sample together with the corresponding chromatogram section of a standard solution of physiologic amino acids are shown in Fig. 13.

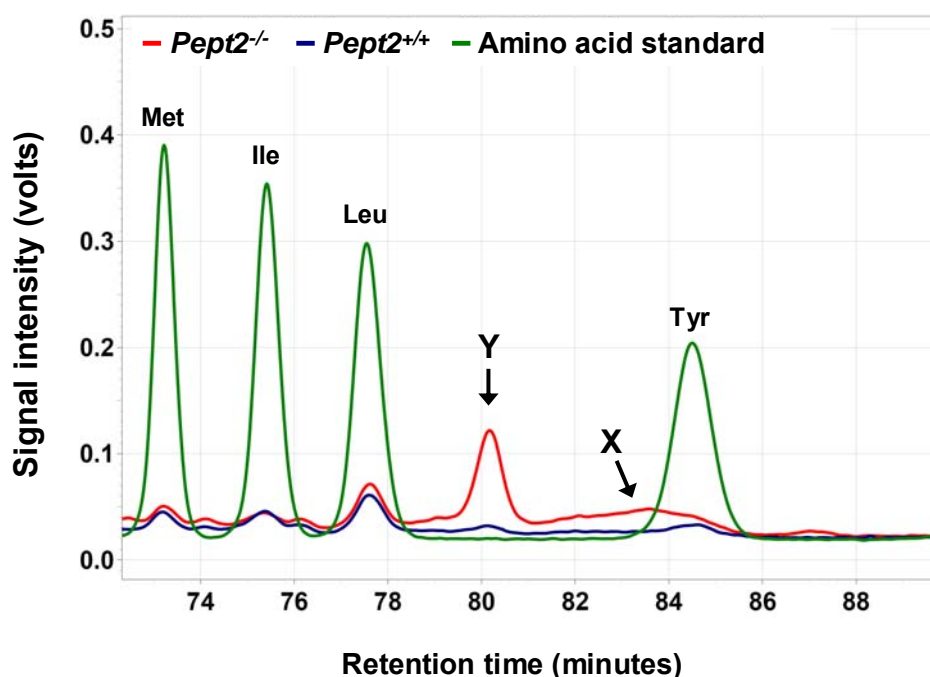


Fig. 13: Detection of additional ninhydrine positive metabolites in *Pept2*^{-/-} urine samples

Superimposed chromatogram sections from amino acid analysis of a representative *Pept2*^{-/-} urine sample, a representative *Pept2*^{+/+} urine sample and a standard solution of physiologic amino acids. Peaks at a retention time of 80 min and 83.5 min, that can be found in *Pept2*^{-/-} samples only, indicate the presence of additional ninhydrine positive compounds in the urine of transporter deficient animals

As in amino acid analysis the quantification is achieved by comparison of the peak area of the sample with the peak area of a standard solution with known concentration, the concentration of unidentified compounds cannot be determined. Therefore the peak area of the compound Y was normalized against urinary creatinine and was used for comparisons between genotypes, feeding conditions and analysis prior to and after dipeptidase hydrolysis (Fig. 14). Excretion of compound Y was significantly higher in the transporter deficient animals at all levels of dietary protein and irrespective of analysis prior to or after dipeptidase digestion.

Furthermore, urinary levels of compound Y increased with protein content of the diet in *Pept2*^{-/-} but not *Pept2*^{+/+} mice. Hydrolysis of the samples with purified membrane bound dipeptidase significantly reduced the peak area of compound Y in *Pept2*^{-/-} animals on the 20% and 30% protein diets.

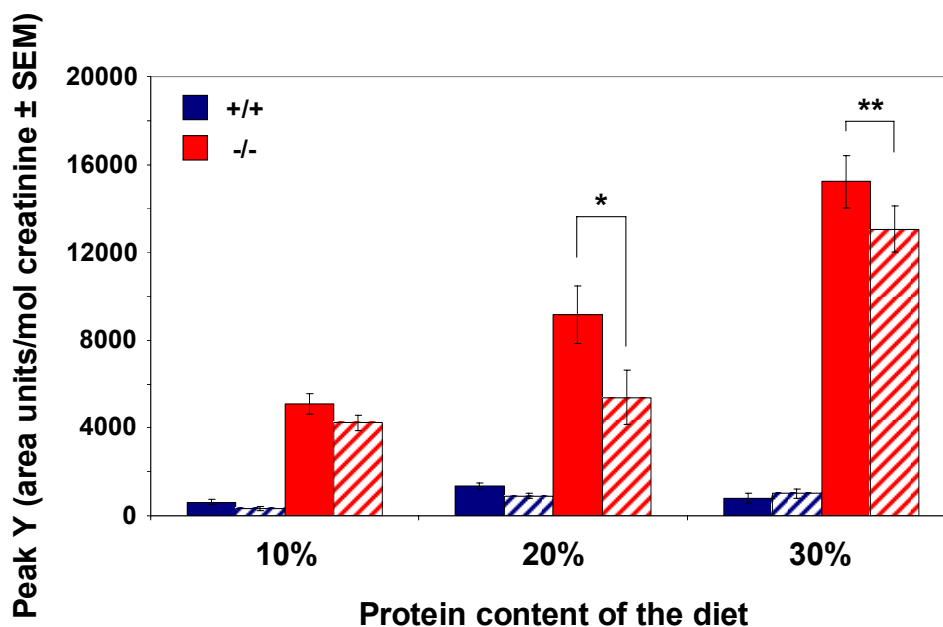


Fig. 14: Peak area of compound Y in relation to creatinine

Peak area of the unidentified compound Y in relation to creatinine in amino acid analysis chromatograms of urine samples prior to (indicated by solid bars) and after (indicated by striped bars) dipeptidase digestion. Samples from $n = 7-12$ animals per genotype and diet were studied. All data were analyzed by univariate linear regression analysis for differences in respect to genotype and protein content of the diet. Independent of analysis prior to or after dipeptidase digestion: protein content of the diet $p < 0.001$, genotype $p < 0.001$ and protein content of the diet \times genotype $p < 0.001$. Analysis for differences in peak area prior to or after dipeptidase hydrolysis of the samples was performed by Student's t-test for paired samples (* = $p < 0.05$, ** = $p < 0.01$).

Due to the presence or greatly enhanced concentration in *Pept2*^{-/-} urine samples, only, it can be assumed that Peak Y and X relate to substrates or breakdown products of substrates for PEPT2. Thus the loss of PEPT2 leads to their enhanced excretion. As the compounds were detected with ninhydrine post column derivatization they have to comprise a primary or secondary amino group and as the peak area increases with increasing protein intake it can be assumed that they are intermediates of protein metabolism. Compound Y seems to be a substrate of the renal dipeptidase as the peak area is decreased at least partially after dipeptidase digestion. Fractions containing the compounds Y or X were collected prior to ninhydrine derivatization for identification of the metabolites by mass spectrometry. Unfortunately the high salt content of the elution buffers applied in amino acid analysis prevented ionization of the compounds for mass spectrometry, and attempts

to desalt the fraction by HPLC on an unpolar C18 column or by solid phase extraction failed as well. Thus, the compounds still await identification.

2.5 Gene expression in kidney tissue

Gene expression of selected genes involved in amino acid and peptide transport and metabolism was determined in kidney samples by quantitative real-time RT-PCR (qPCR) to investigate whether compensatory regulation of gene expression occurs in the transporter deficient animals. These experiments were performed with the kind assistance of Daniela Sailer as part of her final year project. The lower excretion rates for serine and alanine in *Pept2*^{-/-} mice on the low protein diet e.g. might indicate that amino acids can be more efficiently reabsorbed due to higher expression of peptidases and / or amino acid transporters in the kidney. Mean normalized expression values of the studied genes are given in Table 13. Expression of the amino acid transporter *Slc6a19* (*B⁰AT1*) that is located in the apical membrane and of the subunit *Slc7a7* (*y⁺LAT1*) of the basolateral heterodimeric amino acid transport system y⁺L was significantly elevated in transporter deficient animals. No differential expression between genotypes was observed for the other subunit of system y⁺L *Slc3a2* and the amino acid transporter *Slc1a1* (apical membrane) displayed significantly lower expression in the transporter deficient animals. However, it was observed that the protein level of the diet had a pronounced effect on expression of some genes involved in amino acid metabolism. First of all *Pept2* expression was influenced by protein content of the diet with significantly higher expression in animals on the high protein diet in comparison to animals on the medium protein diet. Both subunits of system b^{0,+} (*Slc3a1*, *Slc7a9*) and *Slc9a3* showed significantly higher expression on the low protein diet. Expression of *Slc7a7* in relation to protein content of the diet was analyzed separately for wildtype and knockout animals due to the difference in expression between genotypes. Interestingly, expression of *Slc7a7* was influenced by protein content of the diet in the transporter deficient animals, with highest expression on the low protein diet, but not in the wildtype animals. Expression of *Slc6a19* was generally not influenced by protein content of the diet, but the increase in expression in the transporter deficient animals was more pronounced on the medium and low protein diet. Increasing expression with protein content of the diet with significant differences between every protein level of the diet was observed for *Slc15a1*.

Table 13: Expression of genes involved in peptide and amino acid metabolism

Gene (Accession No.)	10% protein			20% protein			30% protein		
	MNE +/+	MNE -/-	fold change -/- vs. +/+	MNE +/+	MNE -/-	fold change -/- vs. +/+	MNE +/+	MNE -/-	fold change -/- vs. +/+
SLC15A2[†] (<i>Pept2</i>) NM_021301	0.239 ± 0.083	n.d. ¹		0.156 ± 0.022	n.d.		0.263 ± 0.064	n.d.	
SLC15A1^{††} (<i>Pept1</i>) NM_053079	0.002 ± 0.001	0.002 ± 0.001	1.22	0.003 ± 0.001	0.004 ± 0.001	1.48	0.007 ± 0.001	0.005 ± 0.004	-1.32
Slc9a3[†] (<i>NHE3</i>) AF139194	0.304 ± 0.040	0.341 ± 0.123	1.12	0.184 ± 0.015	0.259 ± 0.058	1.41	0.187 ± 0.020	0.222 ± 0.055	1.19
Dpep1 NM_007876	0.225 ± 0.031	0.312 ± 0.074	1.38	0.281 ± 0.057	0.198 ± 0.043	-1.42	0.276 ± 0.074	0.238 ± 0.063	-1.16
SLC1A1^{***} (<i>EAAC1</i>) NM_009199	0.107 ± 0.028	0.076 ± 0.014	-1.42	0.109 ± 0.011	0.085 ± 0.014	-1.29	0.108 ± 0.013	0.078 ± 0.012	-1.39
SLC3A1^{††} (<i>rBAT</i>) BC013441	2.20 ± 0.55	2.06 ± 0.76	-1.07	1.23 ± 0.19	1.49 ± 0.55	1.21	1.59 ± 0.28	1.53 ± 0.29	-1.04
SLC7A9[†] (<i>b^{o+}AT</i>) NM_021291	1.10 ± 0.32	1.35 ± 0.29	1.22	0.736 ± 0.113	0.899 ± 0.140	1.22	0.856 ± 0.202	0.743 ± 0.256	-1.15
SLC3A2 (<i>4F2hc</i>) NM_008577	0.423 ± 0.107	0.402 ± 0.069	-1.05	0.298 ± 0.085	0.343 ± 0.045	1.15	0.506 ± 0.139	0.333 ± 0.040	-1.52
SLC7A7[*] (<i>y+LAT1</i>) NM_011405	0.219 ± 0.064	0.311 ± 0.076 ^{a,b}	1.42	0.189 ± 0.038	0.263 ± 0.056 ^{a,b}	1.39	0.166 ± 0.018	0.147 ± 0.059 ^b	-1.12
SLC6A19^{***} (<i>B^oAT1</i>) AC158359	0.050 ± 0.010	0.069 ± 0.006	1.37	0.046 ± 0.008	0.079 ± 0.015	1.71	0.047 ± 0.010	0.054 ± 0.019	1.15
SLC7A1 (<i>CAT1</i>) AC109498	0.002 ± 0.000	0.002 ± 0.000	1.22	0.002 ± 0.000	0.002 ± 0.000	1.28	0.002 ± 0.001	0.001 ± 0.001	-1.22
SLC38A2 (<i>SNAT2</i>) BC041108	0.029 ± 0.006	0.031 ± 0.006	1.10	0.024 ± 0.036	0.035 ± 0.015	1.48	0.038 ± 0.007	0.030 ± 0.005	-1.29

mRNA expression was analyzed by quantitative realtime RT-PCR (qPCR) in $n = 5$ kidney RNA samples per genotype and diet. Mean normalized expression (MNE) values were calculated with Q-Gen. The geometric mean of crossing point values of three housekeeping genes was calculated and this Bestkeeper index was applied for normalization. All MNE values were tested by Kruskal-Wallis- and Mann-Whithney-U-test for differences between genotypes and protein levels of the diet.

¹ n.d. = not determined

* Significant difference between genotypes (* $p < 0.05$, *** $p < 0.001$)

‡ significant difference between expression on the medium and on the high protein diet ($p < 0.05$)

‡‡ significant difference in expression between all levels of protein content of the diet ($p < 0.05$)

† significant difference between expression on the low protein diet in comparison to medium and high protein diet ($p < 0.05$)

†† significant difference between expression on the low and on the medium protein diet ($p < 0.01$)

MNE values bearing identical superscripts (^{a,b}) indicate significant differences between protein levels of the diet in the knockout animals ($p < 0.05$) only

3. Characterization of kidney tissue by profiling techniques

Phenotypic characterization *Pept2*^{-/-} mice so far has shown that transporter deficient animals have a markedly reduced capacity to reabsorb dipeptides in the kidney (186), and that PEPT2 accounts for 86% of overall peptide reabsorption in the proximal tubule (155). Yet under normal housing and feeding conditions as well as on diets with high or low protein supply they do not show marked phenotypic alterations. To assess to which extent this lack of a prominent phenotype is caused by biological redundancy we undertook a comprehensive analysis of mRNA, protein and metabolite levels in the same kidney tissue samples of transporter-deficient and control animals.

3.1 Transcriptome analysis by cDNA microarrays and qPCR

Differential gene expression in kidneys of *Pept2*^{-/-} and *Pept2*^{+/+} animals was assessed with 20k cDNA microarrays (197) by the group of Johannes Beckers (Institute of Experimental Genetics, GSF, Neuherberg, Germany). cDNA of each of the 5 *Pept2*^{-/-} mice was hybridized individually against an equimolar pool of the 5 *Pept2*^{+/+} animals (KO:WT). Additionally cDNA samples of four of the wildtype mice were hybridized individually against cDNA of the fifth wildtype mouse (WT:WT) to determine the biological variation within the control animals. The first statistical analysis of the microarray data was performed by Alexei Drobyshev in the group of Johannes Beckers with a newly developed ranking method termed PAM that allows for improved accounting of the biological variation assessed by the wildtype versus wildtype hybridization. The software for PAM analysis can be obtained at http://www.gsf.de/ieg/groups/expression/natural_variability.html. With this ranking method a gene is identified as differentially expressed if the degree of up or down regulation in all KO:WT hybridizations is larger than the up or down regulation in any of the WT:WT hybridizations, and if provided that the regulation in each KO:WT hybridization has the same direction i.e. either only up or only down regulation. Applying PAM analysis a list of 19 genes was identified to be differentially expressed (7 up and 12 down regulated) in the transporter deficient animals and can be found in Table 22 in the appendix. The very small number of differentially expressed genes detected is not surprising with regard to the very stringent terms applied in PAM. On the other hand, the advantage of PAM to select only genes with a very low risk of false positives is associated with decreased sensitivity to detect differentially

expressed genes, especially in the case of genes with an inherent high biological variability. We therefore analyzed the data set of KO:WT hybridizations with the kind assistance of Avner Bar Hen in a second approach with the *varmixt* package of R (56) which is based on variance modelling. In contrast to PAM, variability within the wildtype animals as observed by WT:WT hybridizations was not integrated in the analysis. According to the *varmixt* analysis 159 genes showed significantly altered mRNA levels in the transporter-deficient animals. As 12 of these genes were represented twice by two separate cDNA probes on the array the total number of unique regulated transcripts was 147 with higher mRNA abundance for 79 genes and lower mRNA levels for 68 genes in *Pept2*^{-/-} mice. The complete lists of altered mRNA species identified by *varmixt* analysis are provided in Table 20 and Table 21 in the appendix. 11 of the 19 genes identified as regulated by PAM analysis were also detected by *varmixt*. *Rnase4* and *Eaf2* which can be found among the most significantly regulated genes in both lists were chosen for validation of microarray results by qPCR. Differential expression of *Rnase4* and *Eaf2* could be verified in the RNA samples that had been used for the microarray analysis as well as in kidney tissue of mice of the metabolic study. *Rnase4* was consistently found up-regulated (with a mean change in *Pept2*^{-/-} mice as determined by qPCR of 5.4-fold and 3.0-fold in samples used for the microarray analysis and samples from animals of the metabolic study, respectively). *Eaf2* was always found down-regulated (mean change in *Pept2*^{-/-} mice as determined by qPCR of -1.6-fold and -1.8-fold in samples used for the microarray analysis and from animals of the metabolic study, respectively). These consistent changes in expression level of the target genes even under different housing and feeding conditions confirm that regulation of *Rnase4* and *Eaf2* expression is indeed due to loss of the peptide transporter PEPT2. Differential expression of *Eaf2* deserved particular attention as it is the immediate neighbour of *Pept2* directly upstream on mouse chromosome 16. Kidney samples for analysis by cDNA microarray analysis were taken from littermates with a mixed genetic background of 129X1 (supply of embryonic stem cells) and C57BL/6 (supply of blastocysts) which means that mice may differ for any allele at loci where the parental strains differ. Usually this does not interfere with comparison between wildtype and knockout animals as long as littermates are studied, as the distribution will be independent from the null mutation. Yet, for genes in direct vicinity of the null mutation we will find a so called linkage disequilibrium as the null mutation will be flanked by two alleles derived from 129X1 whereas the wildtype locus will be flanked

by two C57BL/6 derived alleles (252). To rule out the possibility that *Eaf2* is found differentially expressed due to differential expression between mouse strains rather than in relation to loss of *Pept2* we compared the level of *Eaf2* mRNA by qPCR in kidney samples from mice with either a pure 129X1 or pure C57BL/6 background. As shown in Fig. 15A *Eaf2* mRNA levels are rather higher in 129X1 samples than in C57BL/6 samples. Thus, the lower mRNA levels in the *Pept2*^{-/-} animals are not a consequence of linkage disequilibrium. Interestingly expression of *Pept2* is strain dependent (Fig. 15B) with higher expression in 129X1 samples in comparison to C57BL/6 samples.

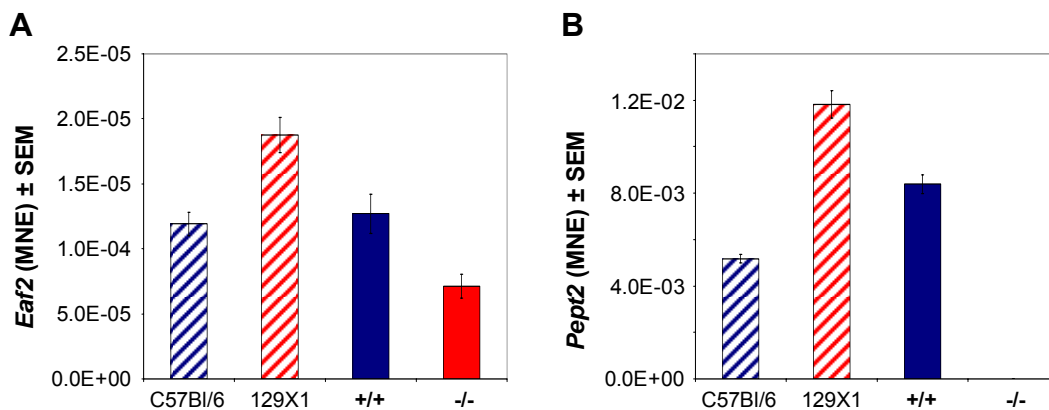


Fig. 15: Expression of *Eaf2* and *Pept2* in the parental strains 129X1 and C57BL/6

mRNA expression was analyzed by quantitative realtime RT-PCR (qPCR) in $n = 4$ kidney RNA samples per strain or genotype. Mean normalized expression (MNE) values were calculated with Q-Gene with GAPDH as reference gene for normalization. MNE values were tested by Kruskal-Wallis for differences between genotypes. Groups were significantly different at $p < 0.05$ for *Eaf2* and at $p < 0.01$ for *Pept2*

3.2 Proteome analysis by 2D-PAGE and MALDI-TOF-MS

Table 14 displays proteins with significantly altered levels in kidney tissues of transporter-deficient animals. On average, 350 proteins could be resolved on a gel by 2D-PAGE analysis of which 37 showed major changes. 18 of these proteins could be identified by MALDI-TOF-MS. A representative 2D-PAGE gel of a wildtype kidney protein extract and corresponding sections of a representative gel of a knockout kidney protein extract are shown in Fig. 16. 12 of the identified proteins with altered abundance in transporter-deficient animals were represented by a probe on the cDNA microarray. Yet, only glutathione transferase mu1 (*Gstm1*) showed a parallel increase in mRNA-abundance and protein. For none of the other identified proteins a regulation at transcript level was observed by cDNA microarray analysis.

Table 14: Changes in protein level in kidney tissue of PEPT2 deficient animals

a. Proteins with higher steady-state levels in kidneys of *Pept2*^{-/-} mice

Protein	Gene symbol	Function	Measured pI /MW	Theoretical pI /MW	% Sequence coverage	Ratio <i>Pept2</i> ^{-/-} / <i>Pept2</i> ^{+/+}	p (t-test)	ID ¹	mRNA Δ -fold change in <i>Pept2</i> ^{-/-}
Albumin	Alb1	plasmatic transport	6.51/52.1	5.62/68.7	36	2.83	0.024	MG-8-118e21	-
Sepiapterin reductase	Spr	metabolism	5.81/31.1	5.78/27.9	33	2.63	0.039	MG-15-219m12	-
Epoxide hydrolase	Ephx2	detoxification	6.10/61.3	5.86/52.6	34	2.22	0.016	MG-15-146f14	-
isocitrate dehydrogenase 3 (NAD ⁺) beta	Idh3b	metabolism	8.56/45.7	8.76/42.2	48	2.14	0.026		
Glycine amidinotransferase	Gatm	amino acid metabolism	6.91/ 51.8	8.00/48.3	29	2.13	0.004		
3-hydroxyantranilate 3.4-dioxygenase	Haa0	metabolism	6.70/ 36.7	6.09/32.8	46	2.11	0.001	MG-12-248l12	-
methionine sulfoxide reductase A	Msra	protein metabolism	7.32/ 28.8	8.60/26.0	53	2.07	0.023	MG-6-46m3	-
Glutathione transferase mu1	Gstm1	detoxification	9.03/30.0	7.92/25.8	33	2.07	0.036	MG-3-22g11	1.16
Pyruvate kinase M2 isozyme	Pkm2	metabolism	8.00/60.8	7.38/57.8	25	1.87	0.022	MG-6-48g14	-
phosphotriesterase related	Pter	metabolism	6.61/44.4	5.97/39.2	24	1.66	0.002		
3-oxoacid CoA transferase	Oxct1	lipid metabolism	8.22/58.6	8.86/56.0	30	1.65	0.029	MG-15-75h11	-
Nit protein 2	Nit2	metabolism	6.66/34.6	6.78/30.5	61	1.54	0.006	MG-12-178b2	-
Dihydrolipoamide transacylase precursor	Dbt	metabolism	6.56/55.5	8.79/53.2	29	1.51	0.007		
Quinolate phosphoribosyltransferase	Qprt	nucleotide biosynthesis	6.53/41.1	6.24/27.8	24	1.51	0.011		

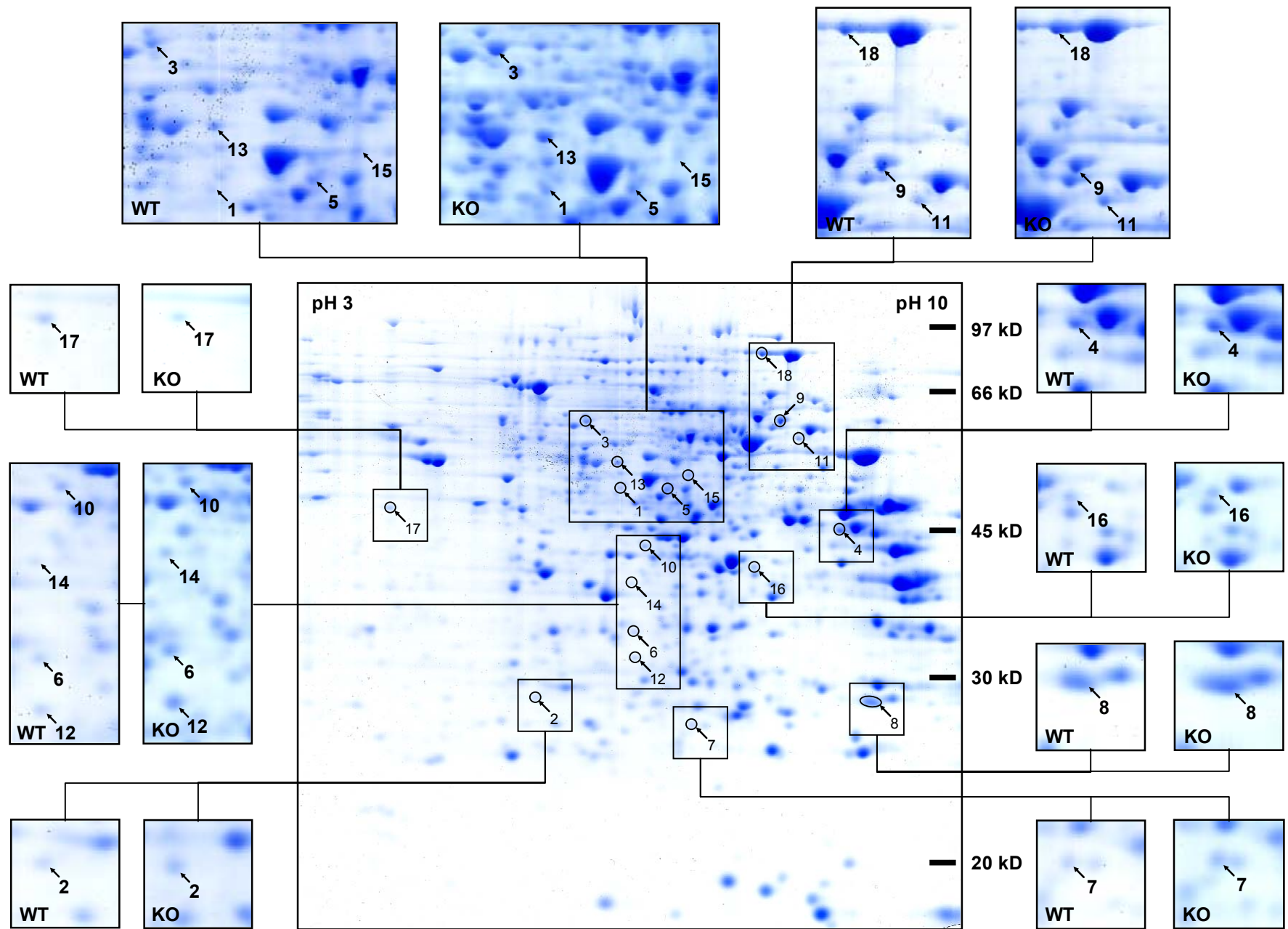
b. Proteins with lower steady-state levels in kidneys of *Pept2*^{-/-} mice

Protein	Gene symbol	Function	Measured pI /MW	Theoretical pI /MW	% Sequence coverage	Ratio <i>Pept2</i> ^{-/-} / <i>Pept2</i> ^{+/+}	p (t-test)	ID ¹	mRNA Δ -fold change in <i>Pept2</i> ^{-/-}
Homogentisate dioxigenase	Hgd	amino acid metabolism	7.06/53.6	6.86/50.0	31	0.49	0.008	MG-12-23i12	-
Coproporphyrinogen oxidase	Cpox	cellular biosynthesis	7.95/ 42.4	8.00/49.7	55	0.57	0.031		
Laminin receptor 1	Lamr1	cytoskeletal protein	4.12/43.1	4.77/32.6	35	0.60	0.027	MG-12-147c15	-
Aconitate hydratase	Aco1	metabolism	7.89/97.0	7.10/98.2	22	0.65	0.019	MG-12-136j1	-

1, Lion Biosciences Probe ID for proteins that are represented by a cDNA probe on the cDNA microarray

Fig. 16: 2D-PAGE analysis of proteins from kidney tissue samples (see next page)

Protein extracts from kidney tissue samples (n = 5 per genotype) were analyzed individually by 2D-PAGE. In the first dimension proteins were separated according to their isoelectric point on pH 3-10 IPG-strips. In the second dimension separation according to protein mass was performed by electrophoresis on 12.5% SDS-polyacrylamide gels. A representative Coomassie stained gel of a wildtype protein extract is shown in the middle and enlarged sections of a representative knockout gel in comparison to the wildtype gel are shown for areas that contain protein spots differing significantly in intensity between the genotypes. Protein spots which could be identified by MALDI-TOF MS are indicated by arrows and numbered as in Table 11.



3.3 Metabolite analysis by GC-TOF-MS

Metabolite analysis of kidney tissue extracts was performed in the group of Oliver Fiehn at the Max Planck Institute for Molecular Plant Physiology (Golm, Germany). On average, 746 metabolite peaks could be detected in kidney tissue extracts of which 139 could be assigned to known compounds. Multivariate data analysis was applied to the dataset to analyse whether a characteristic metabolic fingerprint differentiates between samples of knockout and wildtype animals. Principal component analysis (PCA) revealed that 29 % of the total variance of the data set was accounted for by the first principal component and that an additional 18 % of the overall variance was explained by the second principal component. Yet, only partial separation between samples of different genotypes could be observed Fig. 17 A. Analysis for metabolites that contribute most to discrimination between genotypes by partial least squares discriminant analysis (PLS-DA) with a two component model provided a clear separation between genotypes Fig. 17 B.

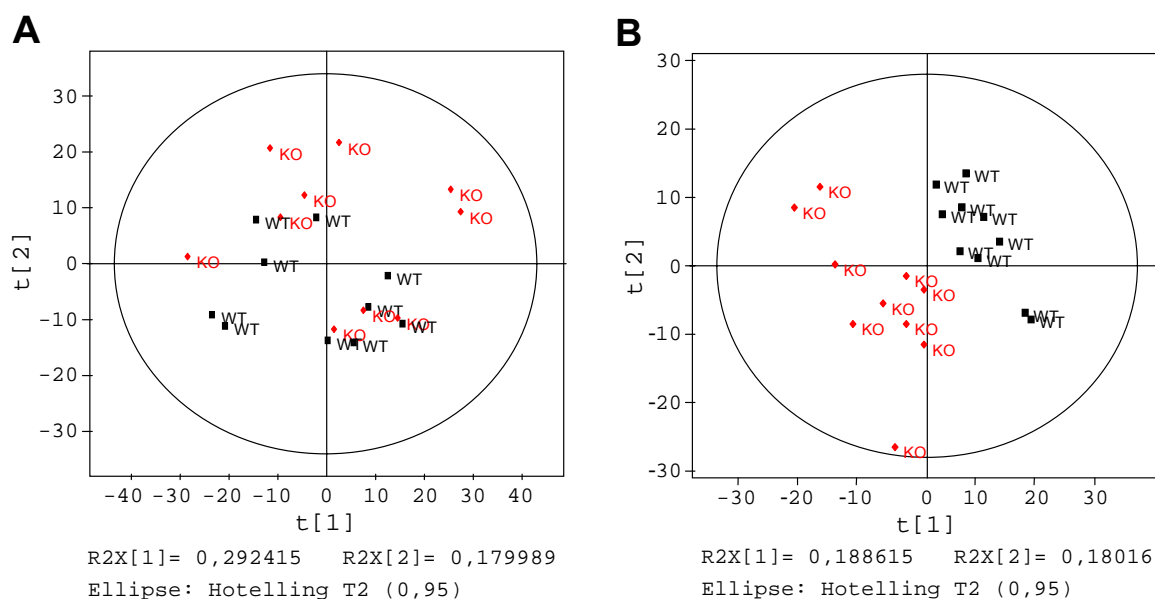


Fig. 17: Multivariate data analysis of metabolites

Identified and unidentified compounds determined by GC-TOF-MS were analyzed by PCA and PLS-DA. The PCA scores plot (A) displays the grouping of the samples according to the main variance in the data set. The PLS-DA scores plot (B) displays the grouping of the samples when the model is optimized for maximum separation between the genotypes. R2X[1] and R2X[2] denote the two first principal components and the fraction of the total variance they explain. The Hotelling T2 ellipse defines the normal area for 95% confidence. Samples outside the ellipse would classify as strong outliers that have high leverage on the model.

PLS-DA was cross-validated by leaving out 20% of the samples, calculating a new model on the remaining samples and predicting the class membership (knockout or wildtype) of the left out samples. This process was repeated five times. Class membership was predicted correctly by these training models for 9 out of 10 samples. Identified metabolites that contributed most to discrimination between genotypes can be derived from the PLS loadings and are listed in Table 15. They revealed primarily lower levels of amino acids and amino acid derivatives in kidney samples of transporter-deficient animals. The lower levels of amino acids in *Pept2*^{-/-} could be confirmed by amino acid analysis of an additional set of kidney samples (data not shown).

Table 15: Metabolites in kidney tissue that contribute most to differentiation between genotypes

Variable importance list ¹	Ratio KO / WT ²
oxoproline	0.6
putrescine	0.5
cysteine	0.8
tryptophane	0.7
threonine	0.8
pipecolic acid	0.8
glycolic acid	0.7
hydroxyproline	0.8
glutamate	1.1
pyruvate	0.5
azelaic acid	0.7
galactonic acid	0.7
proline	0.8
phosphoethanolamine	1.3
lysine	0.8
glycine	0.9
alanine	0.7
threonic acid	0.9
tyrosine	0.8
serine	0.9

Identified and unidentified compounds analyzed by GC-TOF-MS were examined by partial least squares discriminant analysis (PLS-DA) to identify compounds that contribute most to differentiation between knockout and wildtype kidney tissue

¹ Identified metabolites that contributed most to class prediction (*Pept2*^{-/-} / *Pept2*^{+/+})

² Ratio of mean concentration levels n = 5 per group

3.4 Classification of processes and pathway analysis

A classification of regulated gene products at mRNA and protein levels according to the GO classification for biological processes (Fig. 18) revealed that predominantly gene products involved in metabolism were altered in the transporter deficient animals. Underrepresented were processes like regulation of transcription, signal transduction and cell communication.

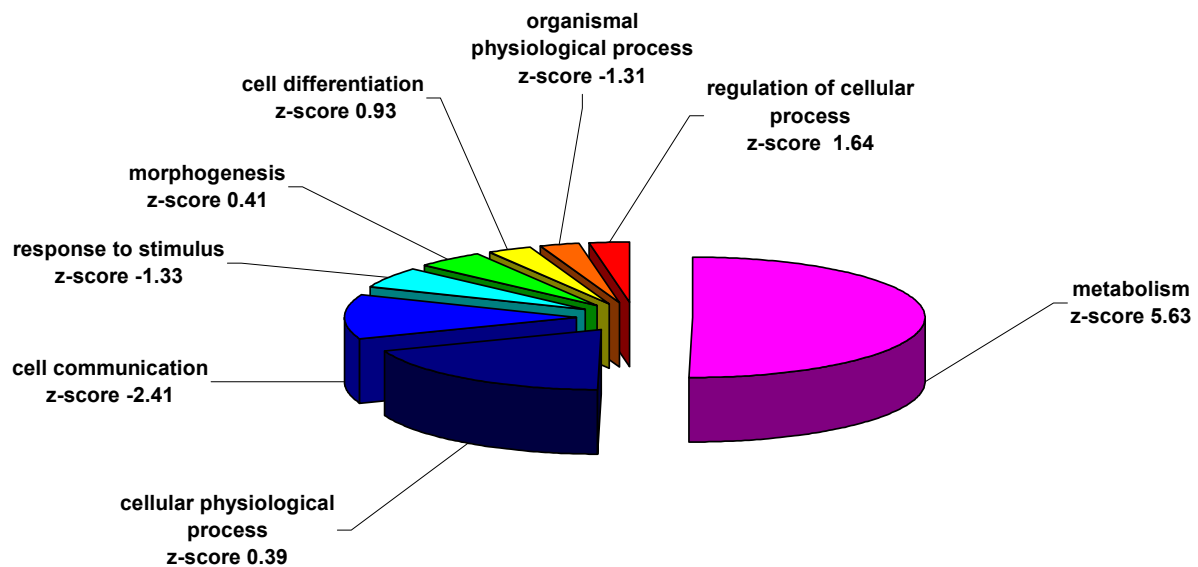


Fig. 18: Biological processes (GO) affected by loss of PEPT2

Differentially expressed gene products were analyzed with the software bibliosphere, which Gene Ontology (GO) categories of biological processes can be found in our data set and whether certain categories were over- or underrepresented. A z-score of > 2 indicates significant overrepresentation and a z-score < -2 indicates significant underrepresentation of a category.

Particularly enzymes of amino acid and derivative metabolism were over-represented within the groups of differentially expressed mRNAs and proteins (Table 16) as well as enzymes of lipid and fatty acid metabolism (Table 17). Although the changes observed for the latter enzymes suggested an increase in fatty acid beta oxidation in *Pept2^{-/-}* kidney tissues, no corresponding changes in metabolite levels (i.e. fatty acids) could be observed. Far more consistent, however, were alterations in amino acid metabolism in which not only mRNA and protein entities changed but also metabolites – in particular various amino acids and their derivatives as shown in Table 15.

Table 16: Differentially expressed genes involved in amino acid metabolism

ID ¹	Gene Symbol	Description	Fold change	eFDR/ p (t-test)
Gene products with increased expression in <i>Pept2</i>^{-/-} mice				
MG-16-7d5	Slc7a7	cationic amino acid transporter, y+ L system	1.22	2.28E-06
MG-6-80p15/ MG-8-58b6	Glud1	glutamate dehydrogenase 1	1.26/1.13	4.92E-04 7.97E-03
MG-12-1g3	Napsa	napsin A aspartic peptidase	1.24	3.32E-02
MG-6-82j16	Abhd4	abhydrolase domain containing 4	1.14	3.81E-02
MG-3-25c6	Xpnpep	X-prolyl aminopeptidase (aminopeptidase P) 1, soluble	1.10	4.22E-02
MG-8-55h19	Gluc	glycine decarboxylase	1.20	6.92E-03
	Gatm	glycine amidinotransferase (L-arginine:glycine amidinotransferase)	2.13	4.00E-03
	Msra	methionine sulfoxid reductase A	2.07	2.31E-02
	Qprt	mus musculus quinolinate phosphoribosyltransferase	1.51	1.10E-02
	Dbt	dihydrolipoamide transacylase precursor - mouse	1.51	7.00E-02
Gene products with decreased expression in <i>Pept2</i>^{-/-} mice				
MG-68-104c23/ MG-3-16p4	Odc	mouse ornithine decarboxylase gene	-1.18	5.37E-06 5.78E-03
MG-3-27116	Cndp2	CNDP dipeptidase 2 (metallopeptidase M20 family)	-1.20	2.71E-03
MG-12-277g11	Sardh	sarcosine dehydrogenase	-1.08	2.25E-02
MG-3-55c24	Galnt1	UDP-N-acetyl-alpha-D-galactosamine:polypeptide N-acetylgalactosaminyltransferase 1	-1.13	4.91E-02
	Hgd	homogentisate 1,2-dioxygenase	-2.05	8.00E-03

1, Lion Biosciences cDNA probe ID, if no ID is given the gene product was found to be regulated at protein level.

2, for mRNA: eFDR = estimated false discovery rate, FDR cut-off set at 0.05
for protein: p-Value of student's t-test

Table 17: Differentially expressed genes involved in fatty acid metabolism








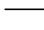

ID ¹	Gene Symbol	Description	Fold change	eFDR/ p (t-test) ²
Gene products with increased expression in <i>Pept2</i>^{-/-} mice				
MG-15-135k15	Acsl1	acyl-CoA synthetase long-chain family member 1	1.24	2.46E-04
MG-12-171j2	Acot3	acyl-CoA thioesterase 3	1.23	2.48E-04
MG-3-88110	Acaa1b	3-ketoacyl-CoA thiolase B	1.18	1.41E-03
MG-8-70n14	Mgll	monoglyceride lipase	1.13	2.91E-03
MG-6-22h16	Acaa1a	acetyl-Coenzyme A acyltransferase 1A	1.12	3.02E-02
MG-6-54h14	Acly	ATP citrate lyase	1.09	3.98E-02
MG-14-3m20	Cpt2	carnitine palmitoyltransferase 2	1.11	3.19E-02
MG-78-2j16	Lyplal	lysophospholipase-like 1	1.10	4.02E-02
	Oxct1	3-oxoacid CoA transferase	1.65	2.90E-02
	Dbt	dihydrolipoamide transacylase precursor - mouse	1.51	7.00E-03
Gene products with decreased expression in <i>Pept2</i>^{-/-} mice				
MG-6-6716	Dhrs8	dehydrogenase/reductase (SDR family) member 8	-1.35	5.37E-06
MG-8-44o23	Agps	alkylglycerone phosphate synthase	-1.23	5.37E-06
MG-16-28m11	Hsd11b1	hydroxysteroid 11-beta dehydrogenase 1 (Hsd11b1)	-1.35	8.81E-05
MG-3-37f4	Idi1	isopentenyl-diphosphate delta isomerase	-1.22	5.94E-04
MG-12-140c23	Cyp7b1	cytochrome P450, family 7, subfamily b, polypeptide 1	-1.18	3.14E-03
MG-12-3e4	Cyp4b1	cytochrome P450, family 4, subfamily b, polypeptide 1	-1.18	1.58E-03
MG-12-20815	Ces2	carboxylesterase 2	-1.16	2.15E-03
MG-8-46f9	Hsd17b2	hydroxysteroid (17-beta) dehydrogenase 2	-1.10	4.09E-02
MG-12-258e15	Adh1	alcohol dehydrogenase 1 (class I)	-1.13	1.40E-02
MG-16-137h5	Scd2	stearoyl-Coenzyme A desaturase 2	-1.11	4.75E-02

1, Lion Biosciences cDNA probe ID, if no ID is given the gene product was found to be regulated at protein level

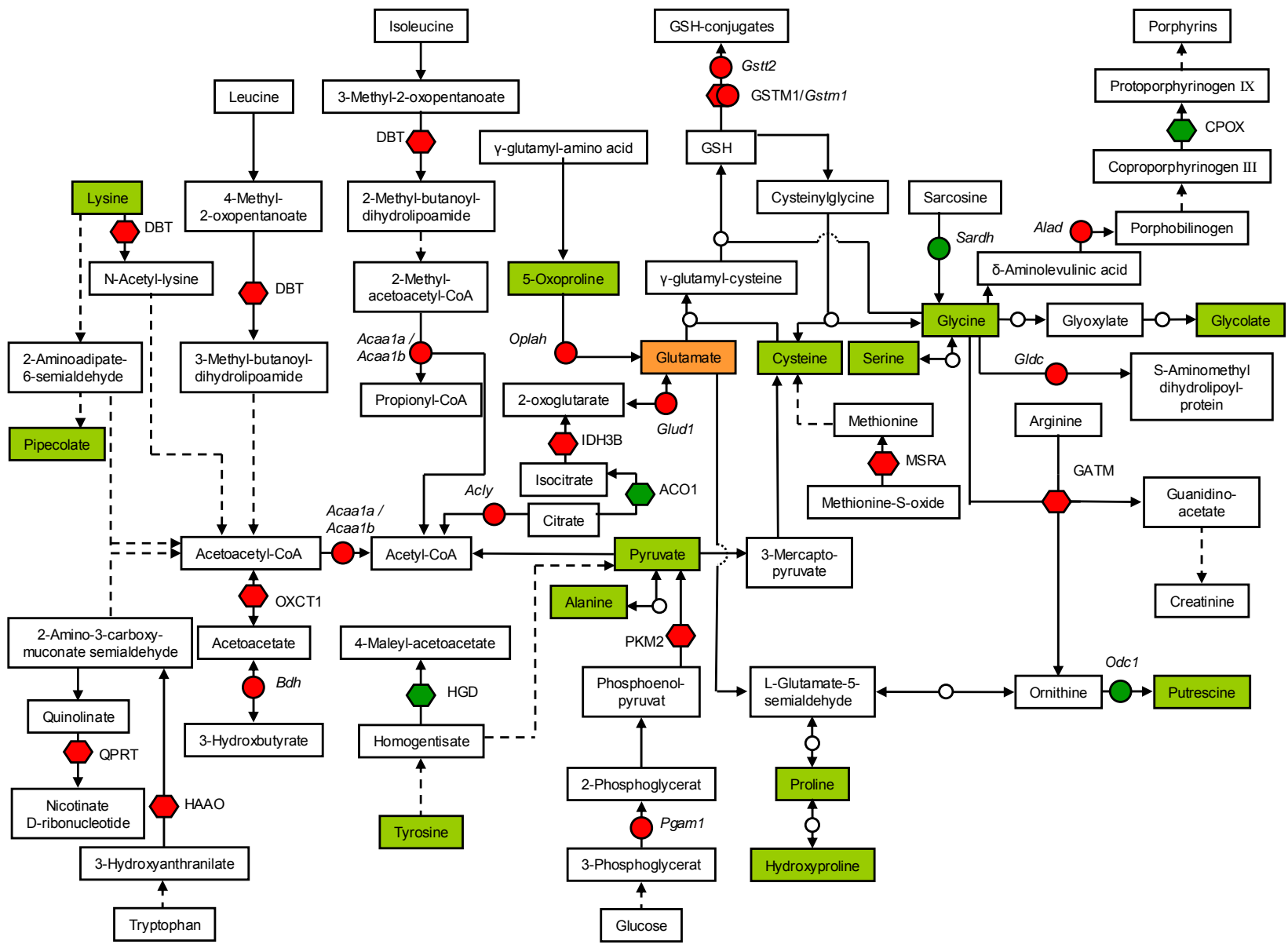
2, for mRNA: eFDR = estimated false discovery rate, for protein: p-Value of student's t-test

Pathway analysis tools such as KEGG (<http://www.genome.jp/kegg/>), Brenda (Cologne University Bioinformatics Centre, Germany, Release 5.2 [<http://www.brenda.uni-koeln.de/>]) and MetaCore™ (GeneGo, St. Joseph, Mi, USA [<http://www.genego.com/>]) were used to compile Fig. 19 that represents in a scheme metabolic pathways and their links for which corresponding changes in any of the biological entities could be identified in kidney tissues of transporter-deficient mice.

Fig. 19: Pathways affected by loss of PEPT2 (see next page)

-  Metabolites with increased concentration in *Pept2*^{-/-} mice
-  Metabolites with lower concentration in *Pept2*^{-/-} mice
-  Metabolites with no change in concentration between genotypes
-  Elevated mRNA level in *Pept2*^{-/-} mice
-  Decreased mRNA level in *Pept2*^{-/-} mice
-  Elevated protein concentration in *Pept2*^{-/-} mice
-  Decreased protein concentration in *Pept2*^{-/-} mice
-  Direct reaction within the pathway
-  Intermediary metabolites and reactions omitted

Changes at mRNA, protein and/or metabolite level that could be assigned to metabolic pathways are depicted. Differentially expressed gene products (mRNA or protein) are denoted with the gene symbol for Acaa1a, acetyl-Coenzyme A acyltransferase 1A; Acaa1b, 3-ketoacyl-CoA thiolase B; Acly, ATP citrate lyase; Aco1, Aconitate hydratase; Alad, delta-aminolevulinatase dehydratase; Bdh, 3-hydroxybutyrate dehydrogenase; Cpox, Coproporphyrinogen oxidase; Dbt, dihydrolipoamide transacylase precursor; Gatm, Glycine amidinotransferase; Gldc, glycine decarboxylase; Glud1, glutamate dehydrogenase 1; Gstm1, glutathione S-transferase mu 1; Gstm2, glutathione S-transferase theta 2; Hhao, 3-hydroxyanthranilate 3,4-dioxygenase; Hgd, homogentisate dioxygenase; Idh3b, isocitrate dehydrogenase 3 (NAD⁺) beta; Msra, methionine sulfoxide reductase A; Odc1, mouse ornithine decarboxylase gene; Oplah, 5-oxoprolinase; Oxct1, 3-oxoacid CoA transferase; Pgam1, phosphoglycerate mutase 1; Pkm2, pyruvate kinase M2 isozyme; Qprt, Quinolinatase; Sardh, sarcosine dehydrogenase



4. Analysis of constituents of glutathione metabolism

On close examination of the profiling data it became obvious that the amino acids glutamate, cysteine and glycine as well as 5-oxo-proline are in prominent position and both, transcripts and proteins associated with their metabolism, were found regulated in the transporter deficient animals. These amino acids are all constituents of glutathione (GSH) respectively break-down products thereof, indicating that renal tubular handling of GSH might be impaired in *Pept2*^{-/-} mice. We therefore analyzed GSH and intermediates of GSH metabolism in urine, plasma and kidney tissue samples as well as mRNA levels of enzymes involved in GSH metabolism in the proximal tubulus.

4.1 Urinary excretion of Cys-Gly

GSH is cleaved in the proximal tubule lumen by the γ -glutamyl-transferase into the dipeptide cysteinyl-glycine (cys-gly) and a γ -glutamyl-amino acid. As amino acid analysis had shown that predominantly glycine and cystine can be found in dipeptide bound form in urine samples of *Pept2*^{-/-} mice, we hypothesized that the reabsorption of cys-gly might be a major function of PEPT2, thus that we would expect elevated cys-gly excretion in the transporter deficient animals. We therefore analyzed spot urine samples for cys-gly by HPLC with a thiol-specific derivatization procedure.

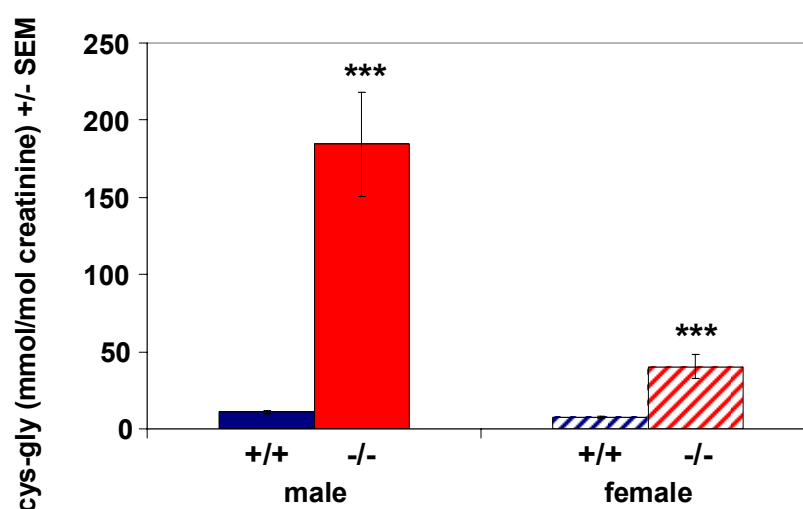


Fig. 20: Urinary cysteinyl-glycine in male and female mice

Urinary concentration of cys-gly in spontaneous urine samples of male and female animals. N = 10 animals per sex and genotype were studied. All data was analyzed by Student's t-test for differences between genotypes (***) = $p < 0.001$.

As shown in Fig. 20, excretion of the dipeptide cys-gly was increased 18-fold in male *Pept2^{-/-}* animals and 5-fold in female *Pept2^{-/-}* mice.

To rule out the possibility that increased excretion of cys-gly in the transporter deficient animals is due to differences in plasma levels, plasma levels of cys-gly were determined. Concentration of cys-gly in plasma was around 15 $\mu\text{mol/l}$ with no differences between sexes or genotypes.

4.2 GSH in urine, plasma and kidney tissue

We hypothesized that the drastically increased loss of cys-gly in the urine of the transporter deficient animals might lead to a decreased supply of substrates for resynthesis of GSH in the kidney. Metabolite analysis had indeed shown that glycine and cysteine levels are reduced in *Pept2^{-/-}* kidneys. We therefore determined GSH levels in kidney tissue samples, urine and plasma (Table 18). For none of the studied sample materials a significant difference in GSH concentration between genotypes was observed. Analyses of thiols in urine and plasma samples were performed with kind assistance of Anne Sailer as part of her final year project.

Table 18: GSH in kidney tissue, urine and plasma

	male		female	
	+/+	-/-	+/+	-/-
GSH in kidney tissue ($\mu\text{mol/g}$) n = 8-11	4.19 \pm 0.63	3.87 \pm 0.35	n.d. ¹	n.d. ¹
urinary GSH (mmol/mol creatinine) n = 8-10	5.1 \pm 1.0	7.2 \pm 2.8	4.8 \pm 1.2	5.1 \pm 2.0
plasma GSH				
free GSH ($\mu\text{mol/l}$)	37.9 \pm 10.0	39.4 \pm 7.5	30.8 \pm 4.8	33.7 \pm 7.8
total GSH² ($\mu\text{mol/l}$) n = 9-10	53.7 \pm 14.7	50.4 \pm 11.0	38.8 \pm 5.1	38.5 \pm 8.3

All data represent the mean \pm SD. Data from male and female animals were analyzed separately. There is no significant difference between genotypes as determined by Students t-test

¹ n.d. = not determined ² total GSH represents free and protein bound GSH

4.3 Analysis of changes at mRNA level of genes involved in GSH-metabolism

Unaltered GSH concentrations in kidney tissue despite lower substrate levels for GSH synthesis might be achieved by compensatory regulation of genes involved in GSH synthesis and metabolism. Gene expression of selected genes involved in GSH metabolism was determined by qPCR with kind assistance of Daniela Sailer and MNE values are given in Table 19. No differences in expression level between genotypes were observed. On the other hand, gene expression was again significantly influenced by protein content of the diet. Glutathione synthetase (*Gss*) displayed the most consistent relation between protein content of the diet and gene expression, with highest expression in samples from animals on the low protein diet and lowest expression in samples from animals on the high protein diet.

Table 19: Expression of genes involved in GSH metabolism

Gene Accession No.	10% protein			20% protein			30% protein		
	MNE +/+	MNE -/-	fold change -/- vs. +/+	MNE +/+	MNE -/-	fold change -/- vs. +/+	MNE +/+	MNE -/-	fold change -/- vs. +/+
<i>Gclm</i> [*] NM_145953	1.40 ± 0.50	1.48 ± 0.43	1.06	0.583 ± 0.067	0.817 ± 0.133	1.40	1.45 ± 0.28	1.26 ± 0.35	-1.15
<i>Gclc</i> NM_010295	0.624 ± 0.325	0.792 ± 0.340	1.27	0.634 ± 0.101	0.650 ± 0.110	1.03	1.21 ± 0.46	0.722 ± 0.226	-1.68
<i>Gss</i> [†] NM_008180	1.49 ± 0.58	1.70 ± 0.34	1.14	1.16 ± 0.10	1.07 ± 0.10	-1.09	1.03 ± 0.31	0.833 ± 0.159	-1.24
<i>Ggt1</i> [‡] NM_008116	12.1 ± 4.7	14.2 ± 2.3	1.17	11.3 ± 1.8	9.45 ± 1.02	-1.20	18.3 ± 4.3	17.9 ± 6.5	-1.02
<i>Gsr</i> [†] NM_010344	0.993 ± 0.329	1.189 ± 0.236	1.20	0.449 ± 0.092	0.739 ± 0.092	1.65	0.734 ± 0.154	0.654 ± 0.154	-1.12
<i>Cth</i> NM_145953	1.02 ± 0.41	1.26 ± 0.44	1.24	0.585 ± 0.106	0.922 ± 0.161	1.58	1.05 ± 0.30	0.769 ± 0.452	-1.36

mRNA expression was analyzed by quantitative realtime RT-PCR (qPCR) in n = 5 kidney RNA samples per genotype and diet. Mean normalized expression (MNE) values were calculated with Q-Gene. The geometric mean of crossing point values of three housekeeping genes was calculated and this Bestkeeper index was applied for normalization. All MNE values were tested by Kruskal-Wallis- and Mann-Whitney-U-test for differences between genotypes and protein levels of the diet.

* significant difference between expression on the medium protein diet in comparison to low and high protein diet (p < 0.01)

† significant difference between expression on the low protein diet in comparison to medium and high protein diet (p < 0.05)

‡ significant difference between expression on the medium protein and high protein diet (p < 0.01)

Discussion

At present only limited knowledge exists about the physiological function and relevance of the mammalian peptide transporter PEPT2. To get further insight into its role in the mammalian organism, a *Pept2*^{-/-} mouse model that is lacking a functional PEPT2 protein has been created by targeted disruption of the *Pept2* gene in embryonic stem cells (186). The present work describes the phenotypic characterization of the *Pept2*^{-/-} mouse line.

1. Basal phenotypic characterization

Visual observation of the *Pept2*^{-/-} animals did not reveal any obvious phenotypic abnormalities, also fertility and life span were not affected. Although the body weight of male PEPT2 null mice – monitored over 25 weeks - displayed a tendency towards lower weights, significant differences were observed for animals of a certain age, only. In female *Pept2*^{-/-} mice kidney weights relative to body weight were significantly reduced. However, inspection of tissue morphology did not reveal any obvious changes (personal communication S. Bachmann). In male animals heart weights in the transporter-deficient line were significantly lower. Although a recent study claimed identification of PEPT2 in rat cardiomyocytes (128), we and others (204) could not detect PEPT2 transcripts in mouse heart by RT-PCR. Thus the lower heart weight cannot be explained as a consequence of altered expression of PEPT2 in this organ. The slightly lower number of surviving pups in *Pept2*^{-/-} litters is probably not due to altered milk composition in *Pept2*^{-/-} dams as the weight development of the pups was normal. To definitely show that milk composition is not the factor impairing *Pept2*^{-/-} pups survival, *Pept2*^{-/-} litters should be transferred to *Pept2*^{+/+} dams or the survival rate of the different genotypes in mixed litters from heterozygous matings should be monitored. As very little is known about the developmental expression of PEPT2, it can only be speculated what might affect the survival rate of *Pept2*^{-/-} pups.

Screening for plasma clinical chemical parameters revealed some statistically significant differences between knockout and wildtype animals. Yet, the values lay well within the reference range that was established on the basis of the wildtype animals, and thus do not represent a pronounced pathophysiological alteration. Similarly no alterations in plasma chemistry values were observed in another *Pept2*^{-/-}

mouse model that was generated independently by the group of D. Smith (202).

As the highest expression of PEPT2 is found in the kidney, the first step in our hypothesis driven phenotyping approach was to confirm that peptide reabsorption is indeed impaired in the transporter deficient animals. We previously demonstrated that the accumulation of the fluorescently labeled dipeptide D-Ala-Lys-AMCA after intravenous administration and that of the radioactively labeled dipeptide D-Phe-Ala after intraperitoneal administration displayed markedly reduced levels in kidney tissue of *Pept2*^{-/-} animals (186). Therefore, we studied next urine parameters to assess whether impaired reabsorption of di- and tripeptides has an effect on overall kidney function, which was not the case, neither in male nor in female animals. If peptides cannot be reabsorbed in the proximal tubule of the kidney due to loss of PEPT2 it could be anticipated that higher amounts of di- and tripeptides should be present in urine samples of the transporter deficient animals. Surprisingly, the indirect determination of dipeptides by analysis of urinary amino acid concentration prior to and after dipeptidase digestion revealed that the only amino acid with significantly elevated amounts in dipeptide-bound form is glycine. As di- and tripeptides that are not reabsorbed in the proximal tubule might get hydrolyzed along the nephron we also analyzed the free urinary amino acids. There was a tendency towards higher excretion in *Pept2*^{-/-} animals for all the amino acids studied which was most pronounced for glycine, yet these slight differences did not reach significance. These findings indicate that the contribution of PEPT2 to overall protein homeostasis via reabsorption of peptide bound amino acids is rather small and does not seem to have a major impact at least under conditions of normal protein supply. It is also unlikely that peptide reabsorption was concealed by a compensatory increase in PEPT1 and PHT1 mediated peptide transport as expression of these two transporters was not elevated in the *Pept2*^{-/-} animals.

Since essentially nothing is known about interorgan metabolism and fate of di- and tripeptides, it is difficult to search for specific effects as a consequence of the lack of function of PEPT2, and very little is known about the di- and tripeptide fraction of plasma. Studies in experimental animals suggested that a considerable fraction of amino acids in plasma is peptide bound and that up to 25% thereof may consist of di- and tripeptides (194). The composition of this di- and tripeptide fraction has not been studied in detail, yet. Of the possible 400 different dipeptides and 8000 tripeptides derived from the L- α -amino acids only a few have been identified in plasma with

concentrations in the range of 0.1 nM to 50 μ M (135, 164, 258). On the other hand certain di- and tripeptides have been shown to be potent inhibitors of ACE (65, 125, 135, 185). Moreover, synthetic ACE-inhibiting drugs such as Captopril and Fosinopril display structural elements of dipeptides and are known substrates of PEPT2 (185). We therefore assumed that the reduced renal peptide reabsorption in *Pept2*^{-/-} mice could secondarily via alterations in plasma peptide levels affect ACE and in turn impair blood pressure regulation (47). Yet, no difference in arterial blood pressure could be observed between the genotypes even in gender-matched animals. However, Blood pressure was investigated only under basal conditions in anesthetized mice, but not in free-moving mice or challenged animals. Thus, blood pressure seems not to be related to the renal reabsorption of di- and tripeptides, at least under the conditions tested here.

PEPT2 expression in the glucagon-producing α -cells of the endocrine pancreas does not seem to be involved in nutrient sensing as a signal for secretion as glucagon levels were unaltered in the fasted as well as in the postprandial state in transporter deficient animals. Although the secretion of glucagon by α -cells of the endocrine pancreas can be stimulated by a protein rich meal (123), by infusion of amino acids (179) and also by infusion of a dipeptide consisting of alanine and glutamine (132), our finding that glucagon levels were unaltered suggest that it is unlikely that PEPT2 is part of the sensing mechanism. Final evidence whether peptide transport has an effect on glucagon secretion could be obtained by studying the glucagon secretion of isolated pancreatic islets from *Pept2*^{+/+} and *Pept2*^{-/-} animals during exposure to dipeptides.

2. Response to different dietary protein contents

Analyzing the transporter deficient animals for their response to diets with increasing protein content was based on the assumption that PEPT2 contributes to protein homeostasis of the body and that a diet with limited protein supply should aggravate phenotypic alterations in the transporter deficient animals. When normal mice were fed a 10% protein diet, the feed efficiency ratio as calculated by the weight gain obtained by food intake (g) was slightly impaired (232) but overall food intake was not affected and animals usually reached the same mature body weight. 30% protein in the diet reflects a protein intake with a maximum feed efficiency (231). When mice

were offered a low and a high protein diet, they chose from both diets to reach a mean protein intake of around 25% (39). Rats were shown to choose a high protein diet when kept on diets with 5 – 20% protein content, whereas no clear preference was observed when they were fed diets with more than 30% protein (250). Based on these reports we offered the *Pept2*^{-/-} mice diets with 10%, 20% or 30% protein content representing a marginally deficient, normal and optimal protein supply. Unexpectedly, we observed that the *Pept2*^{-/-} animals responded with alterations in food intake to the different diets when compared to control animals. *Pept2* deficient animals kept on the low protein diet displayed significantly higher food consumption rates than controls, whereas on the high protein diet, food consumption was significantly lower as compared to controls. Whereas wild type animals consumed equal quantities of food over all protein levels, transporter deficient animals adapted food intake obviously to the protein content of the diet with higher food intakes on the low and reduced food intake on the high protein diets. Yet, changes in food intake did not compensate for different protein intake rates that secondarily affect for example renal urea and water excretion. Our data suggest that the transporter deficient animals have an altered sensing mechanism for the protein or carbohydrate content of the diet that translates into corresponding changes in food intake. Presently, it is not clear at which level the absence of PEPT2 could alter protein sensing, i.e. gustation or via central nervous system. To provide isocaloric diets, the different protein contents were balanced by carbohydrates. Carbohydrate content of the diets is therefore inversely related to the protein content, and as sugar accounts for 15% of carbohydrate fraction, the sweetness of the diet is also inversely related to its protein content. For assessing of what causes the differences in food intake with diets of different protein content in the PEPT2 null mice further studies are needed. As for the animals studied under conventional housing and feeding conditions we did observe some significant differences between knockout and wild type mice among the tested plasma clinical-chemical parameters, but no consistent changes in response to the dietary protein supply could be found. As expected, plasma urea levels increased with increased protein intake (177, 215) but independent of genotype. In spite of the significant differences as shown in Table 10, mean values for all parameters and all groups were found to lie within the reference ranges as calculated for control mice on the 20% protein diet.

The rise in plasma urea values with increasing protein intake determines a higher

osmotic load that is reflected in higher urine volumes and increased water consumption. Still, urea levels in urine were significantly different when animals were fed the diets with increasing protein content. In addition to the overall effect of protein intake on water consumption, transporter-deficient animals displayed a tendency towards lower water intake that became significant on the high protein diet. *Pept2*^{-/-} mice showed also a trend towards lower urine volumes. It was not determined if either drinking behavior or renal function was primarily disturbed. Virtually all of the significant differences observed for urine parameters as indicated in table Table 11 can be related either to different protein or water intake rates and are therefore likely secondary to the changes in dietary intake.

Analysis of free and dipeptide bound amino acids in urine samples provided two major findings: Amino acid excretion was influenced by protein content of the diet in the transporter deficient animals, only, and glycine and cystine were the only amino acids of which a significant dipeptide bound fraction could be detected in urine samples. Excretion of further amino acids (alanine, methionine) in dipeptide bound form was observed only on the high protein diet. The dipeptide bound fraction of these amino acids was also rather small as the increase in amino acid concentration in response to dipeptidase hydrolysis was not significant by itself, but the concentration of alanine and methionine was higher in urine samples of *Pept2*^{-/-} mice after dipeptidase hydrolysis. The fact that amino acid excretion is selectively influenced by dietary protein content in the transporter deficient animals, suggests that indeed compensatory mechanisms set in, when protein supply to the organism is limited. As dipeptides can be cleaved by membrane-bound dipeptidases along the proximal tubule, cleavage of dipeptides and reabsorption of free amino acids by amino acid transporters is one possible mechanism, how the *Pept2*^{-/-} mice might compensate for the loss of PEPT2. To study adaptive changes in gene expression in the knockout animals we analysed expression of *Pept1* that transports the identical substrates as *Pept2* but with lower affinity, of *Dpep1* encoding for the renal brush border membrane dipeptidase and of selected amino acid transporters located in the apical and basolateral membrane of proximal tubule epithelial cells by quantitative RT-PCR. Compensatory upregulation in kidneys of transporter deficient animals was observed for *Slc6a19* and *Slc7a7* and was more pronounced in animals that had been kept on the medium and low protein diet. *Slc6a19* mediates the reabsorption of a wide range of neutral amino acids in the apical membrane of epithelial cells of the

proximal tubule (29). It is therefore a very suitable candidate for compensatory amino acid reabsorption in comparison to other amino acid transporters with narrower substrate specificity. *Slc7a7* mediates uptake of neutral amino acids in exchange against cationic intracellular amino acids at the basolateral membrane and thereby participates in the transcellular transport of cationic amino acids in the proximal tubule (230). However, its increase in expression may rather reflect a compensatory mechanism for the lower amino acid levels observed in kidneys of transporter deficient animals (see metabolite data) instead of contribution to reabsorption of amino acids from urine as there was no indication for disturbed apical transport of cationic amino acids. The finding that dipeptide bound glycine and cystine were observed in increased levels in *Pept2*^{-/-} urine samples will be discussed in conjunction with the findings derived from application of profiling techniques.

Amino acid analysis further revealed that urine samples contained two compounds that occur exclusively or with drastically enhanced concentration in urine samples from transporter deficient animals. These data indicate that the unknown compounds are most likely high affinity substrates of PEPT2 reabsorbed very efficiently by PEPT2 in the wildtype animals. Detection with ninhydrin derivatization indicates that the compounds contain a primary or secondary amino group and the increase in urinary concentration in parallel to the increase in protein content of the diet suggests that they are protein metabolism intermediates. Our previous studies revealed that predominantly glycine and cystine in free and dipeptide bound form are elevated in urine of the transporter deficient animals. Urinary cystine can form mixed disulfides with other thiols. This principle is applied in the treatment of cystinuria patients who develop kidney stones, as cystine has low solubility in neutral or acidic solutions. Treatment with e.g. D-Penicillamine leads to formation of a mixed disulfide (cys-SS-D-Penicillamine) with higher solubility (181). Elevated cystine in urine samples of the transporter deficient animals might form mixed disulfides with the dipeptide cys-gly leading to cys-SS-cys-gly or with homocysteine leading to cys-SS-homocysteine. Cys-SS-cys-gly was prepared by in vitro oxidation of cysteine with the dipeptide cys-gly but appeared with a slightly later retention time in the amino acid chromatogram than peaks X or Y. Cys-SS-homocysteine was prepared by in vitro oxidation of cysteine with homocysteine and led to a peak that coeluted with peak X (data not shown). Further evidence that peak X might indeed be related to elevated urinary cystine levels comes from amino acid determination in urine samples from a

cystinuria mouse model (76) that also displayed presence of an unidentified compound that eluted with the same retention time as peak X (unpublished observations). Unfortunately no unequivocal identification of peak X and peak Y is possible, unless fractions containing compound X or Y collected before ninhydrin derivatization can be analyzed by mass spectrometry. Probably due to the high salt content of the amino acid analysis running buffer in the fractions that prevents ion formation of the compounds, identification of peak X and peak Y could not be achieved up to date. A variety of methods (reverse phase HPLC, solid phase extraction) for desalting of the collected fractions were tested, but resulted in loss of the compounds.

3. Characterization of kidney tissue by profiling techniques

Our data show that despite its expression in a variety of tissues, a loss of the peptide transporter PEPT2 leads to rather subtle phenotypic changes in *Pept2*^{-/-} mice on a standard diet as well as when animals are fed a low or high protein diet. To assess to which extent this lack of a prominent phenotype in *Pept2*^{-/-} mice is caused by biological redundancy and/or to assess phenotypic alterations that could not be identified with the methods applied, we performed a comprehensive analysis of mRNA, protein and metabolite levels in kidney tissue samples of transporter deficient and control animals.

3.1 Methodological aspects of the applied profiling techniques

Transcriptome analysis by cDNA or oligonucleotide microarray technology has become a well established methodology over the past decade. Yet, the various sources of technical variability (62, 145) as well as biological variation (171, 197) necessitate highly standardized procedures and careful experimental design to obtain meaningful results in a microarray experiment. An introduction to experimental designs for dual colour microarrays can be found in (42). Our collaborative study with Johannes Beckers allowed us to hybridize samples of five *Pept2*^{-/-} animals individually against a pool of five *Pept2*^{+/+} animals with four technical replicates per sample including two dye swaps. Biological variation within the control group was determined by hybridizing the *Pept2*^{+/+} animals 1 - 4 individually against the fifth wildtype animal. Our approach represents a combination of a replicated dye swap design with a reference design. Pooling of the wildtype animals generating a reference sample simplified the data analysis and the use of five animals for the pool

should suffice to avoid a bias in the pool in case of contribution of one animal with extreme values. The microarrays were spotted in the laboratory of Johannes Beckers with cDNAs from a 20 K nonredundant clone set from Lion Biosciences that covered more than two thirds of the mouse genome. Our design contained ample technical replicates that should minimize the technical variation that is sometimes observed to be increased for inhouse produced microarrays in comparison to commercially available microarrays.

After hybridization and scanning of the microarrays, data analysis methods are applied to identify differentially expressed genes. The requirements for these methods are quite demanding. They have to cope with the various sources of variation, should reliably identify differentially expressed genes (low type 2 error rate), should strongly control the false positive rate (low type 1 error rate) and have to handle the multiplicity of test that is associated with the parallel testing of thousands of genes taking into account that regulation of individual transcripts is not independent. Data analysis methods have therefore been identified as a key issue in microarray experiments and various methods have been developed in the past few years (12). At present there is little consensus or evidence that a certain category of data analysis is superior but rather all are associated with individual strengths in addressing one issue and flaws in addressing another.

Therefore we applied different analysis methods to identify differentially expressed genes in our data set. The data set was first analyzed by a novel ranking method named pattern analysis of microarrays (PAM) developed by Aleksey Drobyshchev. The central feature of PAM is that the normal biologic variation of a certain gene within the group of control animals is taken into account. In PAM a gene is identified as differentially expressed when it shows a high degree of up- or downregulation in the KO:WT hybridizations in combination with a low degree of regulation within the WT:WT hybridizations. In our analysis a gene was identified as differentially expressed when it had a uniform expression pattern in all KO:WT hybridizations (either only up- or only downregulation) and when the lowest absolute value of regulation in all knockout versus wildtype hybridizations was higher than the highest absolute value of regulation in all WT:WT hybridizations. Permutations were used to estimate the number of false significant genes within a list of differentially expressed genes and based on these values the false discovery rate (FDR) at a certain rank was determined. This very stringent ranking procedure in combination with several

technical replicates of individual animals identifies genes that are very reliably differentially expressed. Yet, inherent with the low probability of falsely identifying a gene as differentially expressed is a low sensitivity to detect all differentially expressed genes. On the other hand, this method is very sensitive to outliers e.g. a gene with slight downregulation in one knockout animal but upregulation in all other knockout animals would not be identified as differentially expressed. Using the difference between the mean degree of regulation in the KO:WT hybridizations and the mean degree of regulation in the WT:WT hybridizations for the ranking instead of ranking according to the difference between the minimum in KO:WT and the maximum in WT:WT or allowing for one sample with opposite sense of regulation would decrease the influence of extreme values and might therefore be more appropriate. Yet, the risk of identifying false positive genes would certainly rise. In our data set, PAM identified predominantly genes with a very low fold change in expression. It appears that larger fold changes are associated with a greater risk of increased variation within the wildtype animals and/or extreme values. About the biological relevance of these low fold changes can only be speculated so far. Due to limited sample material the individual knockout samples were hybridized against a pool of all knockout samples whereas for the WT:WT hybridizations samples 1-4 were hybridized against the fifth wildtype sample. This approach systematically overestimates the wildtype variability and therefore further reduces the power to detect differentially expressed genes in the knockout samples. PAM was originally developed for the high throughput screening of gene expression in mouse models with ethylnitrosourea (ENU) induced mutations and in this case identification of the most reliably differentially expressed genes with a low risk of false positives is more profitable than screening with a higher sensitivity at the cost of a larger number of false positives as additional verification e.g. by qPCR is not feasible (197).

The second analysis was performed with the VarMixt procedure developed by Paul Delmar (56). This approach is based on a flexible variance modelling strategy that partially assigns genes to groups with similar variance. Differentially expressed genes are then detected by a two-sided, unpaired t-test computed for every gene. The FDR was estimated according to Benjamini & Hochberg (22), applying a sequential Bonferroni type procedure. VarMixt has been shown to perform well in a comparison with other data analysis procedures on real and simulated data sets (56). Applying VarMixt to our experimental design, the biological variation within the

control group assessed by WT:WT hybridizations could not be integrated into the detection of differentially expressed genes. We therefore applied the VarMixt procedure also to the WT:WT data and removed genes that were identified as differentially expressed between individual wildtype animals from the list of differentially expressed genes in the knockout animals. This approach obviously removes genes with high variability within the control group but the risk to falsely remove genes that are indeed differentially expressed in the knockout animals is difficult to estimate as due to the use of different reference samples (wildtype pool, the fifth wildtype mouse) the expression ratios cannot be compared directly. On the other hand this approach allows to identify and reanalyse these highly variable genes e.g. by qPCR.

Analysis of the dataset with PAM led to a much shorter list of differentially expressed genes than analysis with the VarMixt procedure, which is not surprising taking into account the very stringent approach of PAM that has probably not an optimal detection power. Whether the risk to identify false positives is different between the two methods is difficult to judge as the FDR was estimated with different procedures. Possibly the FDR has been overestimated in the analysis with PAM, as it has been shown that estimation of the FDR by permutations tends to overrate it (256), further shortening the list of differentially expressed genes when the FDR is the measure for the cut off. This becomes obvious when the two lists of differentially expressed gene are compared. Genes that were identified to be differentially expressed with both methods – that is a list of 13 genes out of the 20 identified with PAM – are presented with a considerably higher FDR in the PAM list than in the VarMixt list. That seven of the genes that were identified with PAM were not identified with the VarMixt procedure illustrates the diversity of both tests and the dilemma which test to choose from the wide number of methods that have emerged over the last years. That different methods lead to quite different lists of differentially expressed genes is a common observation. In a recent study 9 publicly available dual colour microarray data sets were analyzed with ten different methods. Although some subsets of similar methods produced similar lists of differentially expressed genes, in a comparison of the 100 top differentially expressed genes only 21.6% were identified by all methods (108). For a final decision which method is superior, qPCR analysis for all genes that were detected by only one method would be necessary. We decided to use the list obtained with the VarMixt procedure complemented with those genes identified by

PAM only to minimize the risk of not identifying truly differentially expressed genes. As our data set was generated with ample technical replicates we were able to detect significant differences in gene expression between knockout and wildtype animals with very low fold changes in expression. Only one gene - *Rnase4* – showed a greater than twofold increase in mRNA levels in the transporter deficient animals. For all other differentially expressed genes fold changes in the range between 1.08 and 1.43 were observed. These results are statistically significant, yet that does not mean necessarily that these low fold changes are of biological relevance. How much the mRNA level of a gene has to change to be meaningful for the organism e.g. to lead to a relevant change in protein level has not been studied systematically so far. A meta-analysis of published transcriptome data found that low fold changes predominate (254). Yet, in this study a two fold change in expression was defined as a low fold change, as the analysis goes back to times when fold change was used for identification of differentially expressed genes and a twofold change was the customary cut off. No information is given about the meaning of changes in the range of one- to twofold and again the mere observation that twofold changes are observed most frequently does not allow drawing conclusions about their biological relevance. Our transcriptome analysis provides therefore a relatively comprehensive analysis of the kidney transcriptome covering 20'000 of the ~23'000 genes of the mouse genome but the results have to be critically evaluated with respect to their biological meaning.

The proteome analysis of the *Pept2*^{-/-} kidney samples was performed by separation of the proteins with 2D-PAGE and by identification of proteins by peptide mass fingerprinting with MALDI-TOF-MS. In comparison to one or two dimensional LC-MS techniques this approach has the advantage that differences in protein expression between knockout and wildtype samples can be quantified directly by determination of the density or volume of the CBB stained protein spots in the 2D-gels. On the other hand, 2D-PAGE in combination with MALDI-TOF-MS has several limitations. First of all the concentrations of proteins in a tissue have a wide dynamic range that is estimated to reach from 100 protein copies per cell up to 10'000'000 copies per cell. 2D-PAGE cannot cover this wide dynamic range, as low abundant proteins cannot be detected especially with the rather insensitive Coomassie blue staining (131). This problem can be partially ameliorated by prefractionation of the samples,

but renders the analysis much more time consuming. Without prefractionation predominantly enzymes of the main metabolic pathways that constitute the highly abundant proteins of a tissue will be detectable (138). The optimal procedure of sample preparation has to be determined empirically for every sample type (131). In the case of kidney samples the high salt content led to streaky patterns of the 2D gels necessitating dialysis of the protein extracts. 2D-PAGE has clear limitations in detection of large, basic or hydrophobic proteins (84). Membrane proteins that have several hydrophobic transmembrane domains have been very rarely observed with 2D-PAGE as large hydrophobic proteins are difficult to fully extract from tissue and do not enter the IPG strip but tend to precipitate at the spot of their application (84). As reabsorption of all kinds of compounds from the glomerular filtrate is a major function of the kidney, transmembrane proteins constitute a major fraction of renal proteins. Yet, studies that analyzed kidney tissue, isolated proximal tubule or brush border membrane vesicles by 1D- or 2D-PAGE did not detect membrane proteins (45, 46, 133). In our experiment we were interested in changes of the proteome in kidney tissue of mice that lack a peptide transporter. We expected that the *Pept2*^{-/-} mice display either alterations in enzymes involved in protein and amino acid metabolism and/or enhanced expression of amino acid transport proteins to compensate for the loss of PEPT2. Analysis of the kidney proteome by 2D-PAGE and MALDI-TOF-MS is a valuable tool to detect changes in metabolic enzymes, but it has to be kept in mind that the approach cannot provide a comprehensive protein analysis and can only partly cover the anticipated alterations as the technique is not suitable for determination of membrane proteins. Nevertheless those changes that can be detected at the protein level are regarded as more meaningful in comparison to changes at the transcriptome level as proteins are the acting entities e.g. catalyzing metabolic reactions.

Changes in metabolite levels can be regarded as the final downstream product of regulatory processes (64), and it has therefore been proposed that changes in the metabolome might be amplified relative to changes at mRNA and protein level rendering metabolomics more sensitive in comparison to transcriptome and proteome analysis (102). Although some early approaches to measure all low molecular compounds in a biological sample have been reported (89, 148) metabolomics is the youngest of the presented profiling techniques, and the term was not coined before 1998 (160). Today a variety of different technologies is applied

and has been reviewed in (64). Due to the wide concentration range of metabolites that is estimated to span nine orders of magnitude and their very diverse chemical properties no single technology is capable of covering the complete metabolome (88). The three most frequently applied technologies are ^1H - or ^{13}C -nuclear magnetic resonance (NMR) spectroscopy, GC-MS and LC-MS. NMR provides high sample throughput with minimal sample preparation. NMR-spectra of urine have been shown to provide metabolic fingerprints that can reliably differentiate between mouse strains (86) or detect responses to toxic insults (44). If NMR is carried out with isotope labelling it has a high potential for unravelling the pathways of metabolic fluxes (245). Yet it is the most insensitive of the mentioned techniques, thus that only metabolites present at high concentrations can be detected. It has been suggested that these high concentration metabolites are mainly key players of metabolism that are altered by all kinds of stimuli making their changes usually not specific for a certain condition but rather represent a general stress response (44, 90). Although chemical shift, spin-spin coupling and relaxation provide structural information about the studied compound, most compounds result in several signals that are difficult to resolve in the complex mixture present in biological samples. The identification of a compound is therefore not possible without the respective reference substance (64, 245). A much higher sensitivity in comparison to NMR provides GC-MS. Gas chromatography results in very reproducible chromatograms that can be easily analyzed by the well developed software available. Yet, only volatile, thermally stable compounds can be analyzed which introduces a bias against certain compound classes and makes derivatization of metabolites necessary. LC-MS provides the most global approach in comparison to NMR and GC-MS combining excellent sensitivity with the ability to analyze metabolites without derivatization allowing for a wider mass range to be analyzed. Drawbacks of LC-MS are a lower peak resolution and reproducibility of the chromatograms in comparison to GC-MS and biases against some compound classes due to ion suppression by matrix effects (64, 245). Several new combinations e.g. multidimensional GC or LC techniques to obtain better chromatographic resolution or a coupling of LC with NMR and MS (LC-NMR-MS) have been developed in the past years (64). In general combinations that comprise mass spectrometry are superior in compound identification. Yet there is a large discrepancy between the amount of a metabolite necessary for its detection and for its structural elucidation thus that at the moment the lists of unidentified

compounds are growing rapidly (247).

In our study metabolite profiling was performed by GC-TOF-MS in the mass range 85-500 m/z leading to detection of 746 individual compounds of which 139 could be identified. Time-of-flight mass spectrometry is especially appropriate for metabolite analysis in complex samples as this technique allows high scan rates providing accurate peak deconvolution and high mass accuracy (64, 247) necessary for compound identification by database searches with the elemental composition. Databases of NMR or mass spectral data for compound identification are in their infancy in comparison to the databases available for genomic, transcriptomic and proteomic data (113, 247) and although metabolites are per se not species specific in contrast to genes and proteins, species specific databases that contain meta-information e.g. sample origin, tissue, experimental conditions would greatly enhance the interpretation of metabolome data. A first approach in this direction is the recently made available Human Metabolome Database (HMDB) that aims at listing all metabolites with a mass up to 1500 m/z and a concentration $\geq 1\mu\text{M}$. It contains at the moment >2180 endogenous metabolites, with 430 compounds listed for kidney tissue (251). Metabolite profiling generates data torrents requiring pattern recognition and data reduction tools for interpretation (88, 90). Among the chemometric approaches that have been developed for this purpose, multivariate statistical projection methods have been widely applied as they can handle many and correlated variables and provide transparent, interpretable results (110). Multivariate data analysis tools can be divided into unsupervised techniques where class membership (e.g. belonging to a certain genotype) of the samples is not used or supervised approaches where class membership of the samples is used to find variables that maximise the separation of the data into known sample classes. A frequently applied unsupervised technique is the principal component analysis (PCA). The principal components that set the axes of an usually two- or three dimensional scores plot represent dimensions describing the maximum variation within the data set. Thus the scores plot gives an overview about groupings and relationships in the data set. Yet it is often observed that the maximum variation within the data set is unrelated to the class membership of the samples and does not allow for maximum separation between the classes (86, 246). This was also the case in our data set, where PCA did not result in separation between *Pept2*^{-/-} and *Pept2*^{+/+} samples. When unsupervised methods do not lead to clear separation of the sample classes supervised approaches can be applied to

search for the variables that result in maximum class separation. We therefore analyzed our data set by partial least squares – discriminant analysis (PLS-DA). PLS-DA led to clear separation of the *Pept2^{-/-}* and *Pept2^{+/+}* samples in the scores plot, indicating that there is a metabolic fingerprint that can differentiate between the genotypes. The PLS loadings can then be analyzed for the contribution of individual variables to the class separation, i.e. the metabolites that contribute most to the class separation can be identified. Supervised approaches are susceptible to overfitting, meaning generation of a PLS model on the basis of too many components and therefore require cross-validation (90, 110). If a data set with many samples is available, cross validation is performed by splitting of the data set; one part is used as a training set to generate the PLS-DA model which is then applied to the other part of the data to test whether the model can reliably predict the class membership of new samples. In the case of a limited sample number, a “leave one out” crossvalidation can be performed, which we applied to our data set. To test whether samples can be classified correctly by PLS-DA models built from the available data, we left out one knockout and one wildtype sample, built the PLS-DA model on the remaining samples and tested whether the class membership of the left out samples was correctly predicted. This process was repeated five times to perform class prediction for every sample which resulted in correct class prediction for nine of the ten samples, indicating that our metabolite data provide indeed a metabolic fingerprint that differentiates between *Pept2^{-/-}* and *Pept2^{+/+}* tissue samples.

A major concern about metabolite data is that, as it is the most downstream result of genomic modifications, it is also the most distant from the genome. Changes in metabolite levels can result from numerous underlying changes at protein, mRNA and genomic level. It has been shown in yeast that less than 30% of metabolites are involved in only two reactions, whereas 12% participate in more than 10 reactions and 4% participate in more than 20 reactions (78). The various possibilities for one metabolite make it difficult if not impossible to deduce the mechanisms that lead to a certain metabolite pattern from the metabolite data alone.

The limitations of every of the profiling techniques – from a technical point of view as well as with regard to their explanatory power - make clear that they are complementary in the information they can provide, and that a combined approach encompassing analysis at all the different levels is advisable if the goal is to fully

understand the consequences of e.g. deleting a gene in a mouse model. An important point of such an analysis is how to integrate the data from different levels of analysis. Computational integration of transcriptomic, proteomic and metabolomic data for a holistic understanding of function has lately been termed systems biology (105). Its final goal is to generate mathematical models that can describe the structure of a system and its response to perturbations building the basis for in silico phenotype analysis. An introduction to the principles of network biology can be found in (19). The most advanced examples of biological network modelling can be found for single cell organisms like *E. coli* (13) and *S. cerevisiae* (69). When it comes to mammalian organisms the matter gets much more complicated as Jeremy Nicholson and Ian Wilson have stated: “How can we understand modulations in transcriptomic, proteomic or metabolomic data in relation to standardized metabolic pathways that have no compartmental constraints, when mammalian metabolic control functions are dispersed across many cell types in topographically distinct locations that are in different physiological states simultaneously?” (149) Software tools for the integrated analysis of data from all the different “omics” techniques in mammals are also scarce because there was little demand up to now. Apart from our study only two examples (43, 54, 192) are available currently, where analysis at transcript, protein and metabolite levels has been applied to a mammalian organism. In one of these studies – monitoring of valproic acid toxicity in mouse liver tissue – a comprehensive integrative data analysis was neither necessary nor possible as no changes in transcript levels and differential expression of only two proteins was observed (192). What are the currently available options for integrative data analysis in mammals? A widely used approach for interpretation of transcriptome and proteome data is analysis according to Gene Ontology (GO) categories and a number of software tools are available (116). This approach provides valuable information which processes or pathways are over- or underrepresented in a data set. Analysis of our transcript and protein data according to GO biological processes with the software BiblioSphere (195) identified overrepresentation of amino acid and derivative metabolism, which may be anticipated in a mouse model lacking a peptide transporter, but surprisingly also a variety of transcripts and proteins could be mapped to lipid metabolism. Yet, data interpretation according to GO terms suffers from various limitations: 1. only a subset of genes is functionally annotated. 2. Many genes are involved in several biological processes. According to the currently available tools they are weighted

equally for all processes, although the function is in most cases either one or the other depending on the context. 3. GO based sorting is uncoupled from the gene / protein expression data. The magnitude of regulation is not taken into account. 4. There is an annotation bias, as some processes e.g. apoptosis have been studied in more detail, thus, more data on functional annotation is available. 5. Metabolite data cannot be integrated in the analysis. Pathway analysis tools like GenMAPP (48), Metacore (66) and Pathway-Express (117) provide a more detailed analysis mapping the data to metabolic pathways as available from KEGG, BioCarta and other databases. GenMAPP allows users to modify existing pathways or to design new pathways. Metacore additionally offers biological network analysis. We used a combination of the pathway analysis tool Metacore and manual data mining using the metabolic maps of KEGG (<http://www.genome.jp/kegg/>), data from BRENDA (Cologne University Bioinformatics Centre, Germany, Release 5.2 [<http://www.brenda.uni-koeln.de/>]), and the text mining software Bibliosphere (195) to compile Fig. 19 that displays the pathways affected in the *Pept2*^{-/-} animals.

A different approach for integrative data analysis of transcriptome, proteome and metabolome data is application of pattern finding algorithms, like the dimensionality reduction methods we used for analysis of our metabolite data, to the complete data set or to calculate correlation networks. Alterations at mRNA, protein and metabolite level in liver tissue and plasma of the APOE*3-Leiden transgenic mouse, which is a humanized mouse model for studies of atherosclerosis, have been studied in the laboratory of Stephen Naylor (43, 54). By calculation of a correlation network of alterations in lipid metabolism they identified changes in triglyceride levels and corresponding mRNA and proteins as anticipated but also changes in lyso phosphatidyl cholines indicating a more complex perturbation of lipid metabolism. Multivariate data analysis methods or correlation networks are very useful to reveal unanticipated connectivity in a data set. Obviously there exist much more pathways than depicted by the metabolic maps available from KEGG and other databases, and correlation networks offer an unbiased alternative to generate hypotheses for new pathways. Yet, their impartiality is also their weakness, as they disregard the wealth of knowledge about the functions of a certain gene, protein or metabolite that has been accumulated in the past. When integrating data from different levels from genome to phenotype it has to be taken into account that changes at the different levels need not to happen simultaneously but rather take place along a timeline

(147). The timescales for different regulatory processes can be very diverse and are often simply not known. This might explain at least partly the finding that frequently weak correlations are observed between transcriptome and proteome data in the usual snapshot provided by analysis of samples from just one timepoint (15, 40, 98). In general, it cannot be overstated that integration and modelling of the data torrents generated by the different “omics” techniques is very challenging and software tools for mammalian models are clearly in their infancy. Integrative data analysis cannot, at least for the moment, provide firm conclusions about the precise functions or mechanisms involved e.g. in the response to a genetic alteration. It is a very valuable tool to develop new hypotheses but these have to be evaluated in the context of available knowledge and tested experimentally (173).

3.2 Integrated analysis of kidney tissue at mRNA, protein and metabolite level in combination with urine analysis reveals alterations in renal amino acid and glutathione metabolism

Profiling techniques employed to identify changes in kidney tissue at the mRNA, protein and metabolite levels revealed a number of significant but rather subtle changes. A classification of regulated gene products at mRNA and protein levels according to the GO classification for biological processes provided predominantly targets of kidney epithelial cell metabolism that changed by loss of PEPT2. Underrepresented were processes such as regulation of transcription, signal transduction and cell communication. As reported by others (15, 40, 98), we also found very little concordance between changes in mRNA and the corresponding protein levels. Glutathione-S-transferase mu 1 (*Gstm1*) was the only gene product with a similar regulation at mRNA and protein level. Yet, differentially expressed mRNAs and proteins all fell into the same categories of the GO classification. Particularly enzymes of amino acid metabolism were over-represented within the groups of differentially expressed mRNAs and proteins (Table 16). In addition a number of enzymes of lipid and fatty acid metabolism (Table 17) such as carnitine-palmitoyltransferase 2 (*Cpt2*), long chain acyl CoA synthetase (*Acs11*), acyl-CoA-thioesterase 3 (*Acot3*) and acetyl-CoA acyltransferase 1A and 1B (*Acaa1a*, *Acaa1b*) were found regulated. Although the changes observed for the latter enzymes suggested an increase in fatty acid beta oxidation in *Pept2*^{-/-} kidney tissues no

corresponding changes at the metabolite levels (i.e. fatty acids) could be observed. Far more consistent, however, were alterations in amino acid metabolism in which not only mRNA and protein entities changed but also metabolites – in particular various amino acids and their derivatives (Table 15) which were the predominant metabolites contributing to the class separation according to genotype in the metabolite PLS-DA analysis. Visualization of pathways affected in kidneys of *Pept2*^{-/-} animals was accomplished by a combination of the pathway analysis tool Metacore™ (GeneGo, St. Joseph, Mi, USA [<http://www.genego.com/>]) with manual integration of the metabolite data and data provided by KEGG (<http://www.genome.jp/kegg/>), Brenda (Cologne University Bioinformatics Centre, Germany, Release 5.2 [<http://www.brenda.uni-koeln.de/>]) and the text mining software Bibliosphere (195). Fig. 19 represents a scheme of metabolic pathways and their links for which corresponding changes in any of the biological entities could be identified in kidney tissues of transporter-deficient mice. Changes in metabolic pathways of amino acids suggest that for example less ornithine is used for polyamine synthesis involving the identified *Odc1* enzyme that could lead to the decreased levels of putrescine found. Identified transcripts for enzymes involved in metabolism of glutamate, alanine and pyruvate suggest that nitrogen-shuttling may also be altered. Two regulated enzymes of the pathway that leads from glycine via δ-aminolevulinic acid to porphyrins (*Alad* and *CPOX*) suggest impairments in this metabolic route and in this context it is interesting to note that δ-aminolevulinic acid has been shown to be a good substrate of the peptide transporter PEPT2. Whether its renal uptake and metabolism is affected in *Pept2*^{-/-} mice, needs further studies. The amino acids glutamate, cysteine and glycine as well as 5-oxo-proline are among the metabolites that contributed most to PLS-DA class separation and both, transcripts and proteins associated with their metabolism were found regulated. These amino acids are all constituents of GSH, respectively, break-down products thereof, and this suggested that tubular GSH handling might be altered in *Pept2*^{-/-} mice. Glycine and cystine had already attracted our attention in the urine analysis for free and dipeptide bound amino acids as they were the only amino acids for which a significant fraction of the dipeptide bound form could be found in urine. With regard to the indication that PEPT2 might be involved in GSH metabolism we hypothesized that glycine and cystine come from the dipeptide cysteinyl-glycine. Urinary cysteinyl-glycine is most likely a product of the break-down of GSH as extracellular degradation of GSH by γ-glutamyl-transferase (*Ggt1*) leads

to cysteinyl-glycine and γ -glutamyl-amino acids (45). GSH is found in plasma with mean concentrations of 10 μ M and reaches after glomerular filtration the tubular system in which also a GSH secretion takes place (122). In the tubule, GSH is then cleaved by *Ggt1* into cysteinyl-glycine and a γ -glutamyl-amino acid. It can be anticipated that a fraction of cysteinyl-glycine is normally cleaved further by membrane-bound dipeptidases and that the free amino acids are then reabsorbed for resynthesis of GSH in tubular cells.

How the γ -glutamyl-amino acids are taken up into epithelial cells is not understood as yet, but γ -glutamyl-amino acids can be metabolized within the cell by γ -glutamyl-cyclotransferase (*Ggc*) to oxoproline, which can be converted to glutamate by oxoprolinase (*Oplah*). Although γ -glutamyl-amino acids are not transported by PEPT2 (personal communication G. Kottra), we observed lower levels of oxoproline and increased mRNA levels of oxoprolinase in the transporter-deficient animals.

An alternative and most likely more important route for reabsorption of the GSH break-down products is the uptake of cysteinyl-glycine via PEPT2 followed by intracellular hydrolysis to yield glycine and cysteine. Cys-gly has been shown to be a good substrate for PEPT2, and can be used efficiently for GSH synthesis (61). We therefore assumed that reabsorption of urinary cys-gly is one of the main functions of PEPT2 in the kidney. In this case deletion of PEPT2 should lead to increased excretion of cys-gly. We followed this hypothesis by analyzing urinary cys-gly by HPLC with thiol specific derivatization and found indeed a massive increase of cys-gly excretion in the transporter deficient animals. The increased excretion of cysteinyl-glycine by the *Pept2* deficient animals did not result from increased plasma levels and a higher tubular load since plasma levels of cysteinyl-glycine did not differ between *Pept2*^{+/+} and *Pept2*^{-/-} animals.

The drastically increased excretion of cys-gly in the transporter deficient animals suggests that the uptake of the intact dipeptide is important for renal scavenging of the GSH constituents. It is interesting to note that two intracellular peptidases (*Napsa*, *Xpnpep*) and a cytosolic dipeptidase (*Cndp2*) were identified as regulated in expression level in *Pept2*^{-/-} mice which suggests that they could be involved in hydrolysis of cys-gly after its uptake into tubular cells or intracellular protein hydrolysis if cellular free amino acid levels are low. GSH is resynthesized in renal tubular cells from glutamate, cysteine and glycine via γ -glutamyl-cysteine by glutamylcysteine synthetase (consisting of the subunits *Gclm* and *Gclc*) and

glutathione synthetase (Gss). Fig. 21 gives a schematic view of renal GSH metabolism and the proposed involvement of PEPT2.

For assessing whether the enzymes needed for GSH re-synthesis showed any changes in expression levels in kidney tissues, qPCR amplifications of mRNA were performed but did not reveal any significant adaptations in transcript levels. Surprisingly, GSH levels in kidney tissue determined by HPLC with thiol-specific derivatization also revealed no differences between control animals and transporter-deficient animals despite lower cellular concentrations of the precursor amino acids. These unchanged GSH-levels, however, may be explained best by an increased uptake of GSH from the blood across the basolateral membrane of tubular cells. It is supposed that basolateral GSH uptake from plasma provides a major fraction of GSH in epithelial cells of the proximal tubule and it has been suggested that the sodium-dicarboxylate transporter 2 (Sdct-2, Slc13a3) and the organic anion transporters 1 (Oat1, Slc22a6) and 3 (Oat3, Slc22a8) mediate basolateral GSH uptake (122). Our cDNA microarray analysis revealed indeed increased mRNA levels for Oat3 as a putative GSH import system. Despite the lack of changes in tissue GSH levels, an up-regulation of the glutathione-transferases *Gstt2* at the mRNA level and an up-regulation of *Gstm1* at mRNA and protein level suggests that the GSH turnover of renal cells may not only be affected by the identified lower levels of the precursor amino acids in *Pept2*^{-/-} mice but also by its use for conjugation and detoxification employing the glutathione transferases.

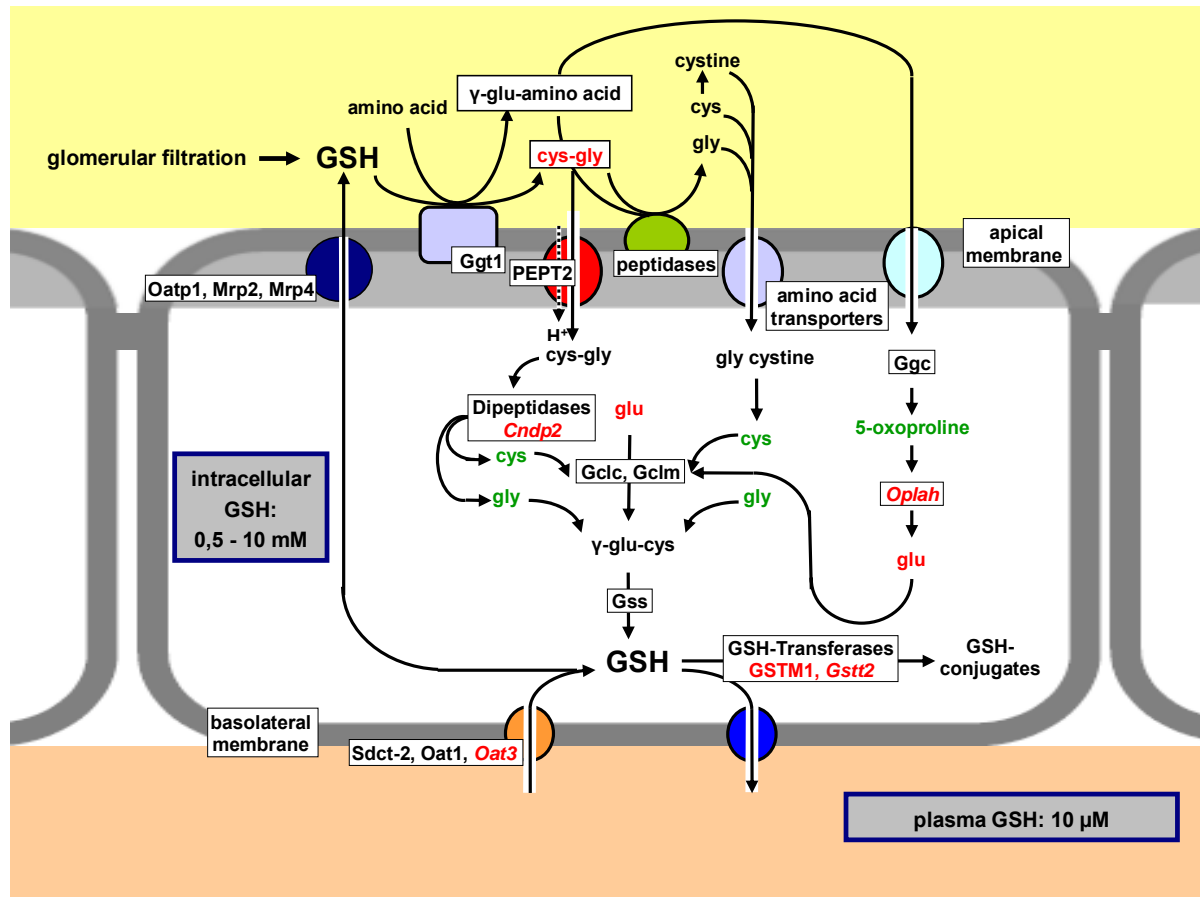


Fig. 21: Schema of GSH metabolism in epithelial cells of the proximal tubule

GSH is degraded and resynthesized in proximal tubular cells via the γ -glutamyl-cycle. By reabsorption of cys-gly, PEPT2 could deliver substrates for resynthesis of GSH. Enzymes, transporters and metabolites with increased expression or concentration in the transporter deficient animals are labeled in red and entities with decreased expression or concentration are labeled in green.

Gclc, glutamylcysteine ligase catalytic subunit; Gclm, glutamylcysteine ligase modifier subunit; Ggc, γ -glutamyl-cyclotransferase; Ggt1, γ -glutamyl-transferase; Gss, glutathione synthetase; Gstm1, glutathione S-transferase mu1; Gstt2, glutathione S-transferase theta 2; Mrp2, multidrug resistance-associated protein 2; Mrp4, multidrug resistance-associated protein 4; Oat1, organic anion transporter 1; Oat3, organic anion transporter 3; Oatp1, organic anion transporting polypeptide 1; Oplah, 5-oxoprolinase; Sdct-2, sodium-dicarboxylate transporter 2

Application of profiling techniques identified a number of rather subtle alterations at mRNA, protein and metabolite level. Although every of the applied profiling techniques has its limitations either in terms of sensitivity, coverage and identification (proteomics and metabolomics) or in terms of interpretation of biological relevance (transcriptomics), their combination provided evidence for a previously unanticipated function of PEPT2 in epithelial cells of the proximal tubule. Even though only selected enzymes involved in GSH metabolism were altered in the transporter deficient animals, the consistent changes in enzymes and metabolites across the different biological levels studied allow to hypothesize that PEPT2 might be involved in renal GSH metabolism. Together with our findings that excretion of cys-gly is drastically

increased in the transporter deficient animals it seems justified to propose that a prime function of PEPT2 in epithelial cells of the proximal tubule is the reabsorption of the GSH breakdown product cys-gly. Cys-gly is found in plasma in concentrations of 15 - 70 μM and is filtered in the glomerulum to reach tubular cells (17, 85, 215). Cys-gly concentrations in human urine are $< 10 \mu\text{M}$ (129, 165) indicating an efficient reabsorption in renal tubules. Filtered plasma GSH and GSH secreted into the tubule are hydrolysed by membrane-bound *Ggt1* to yield cys-gly which we propose is then taken up together with the filtered cys-gly into renal tubular cells via PEPT2. Reabsorption of cys-gly by PEPT2 might play an important role for provision of substrates for intracellular GSH resynthesis. Although the markedly reduced tubular uptake capacity for cys-gly in *Pept2*^{-/-} mice is obviously compensated without functional impairments in kidney - probably via an increased basolateral GSH uptake mediated by Oat 3 - it can be anticipated that conditions with a higher demand for GSH such as increased load of reactive oxygen species may cause a pathophysiology in these mice.

4. Future perspectives

General phenotypic characterization, studies with different protein supply to the organism and application of profiling techniques for determination of mRNA, protein and metabolite levels revealed on the one hand compensatory mechanisms realized by rather subtle alterations in gene or protein expression. For all studies addressing the function of PEPT2 in the proximal tubule of the kidney, whole kidney tissue was used as the object of study. Yet, PEPT2 is only expressed in epithelial cells of the S2 and S3 segment of the proximal tubule. As these cells constitute only a fraction of kidney tissue our results are “diluted” with mRNA, protein and metabolite levels of other compartments of the kidney. Studying isolated proximal tubule might provide a much clearer and more detailed insight into the alterations associated with the loss of PEPT2.

Studying the mechanisms that elicit the observed alterations in gene and protein expression were out of scope of the current analysis. The metabolic consequences of the lack of peptide reabsorption have to be sensed and translated into changes in gene and protein expression. One possibility is transcriptional activation or repression of gene expression. Regulation by the transcription factor peroxisome

proliferator-activated receptor α (Ppar- α) has a prominent role in fatty acid metabolism but also influences amino acid metabolism and GSH dependent detoxification (115, 134, 199). In our data set of differentially expressed genes and proteins in *Pept2*^{-/-} kidney tissue we find 12 genes with a confirmed Ppar- α response element and additionally the same number of genes for which Ppar- α mediated regulation has been proposed as they were found to be regulated by application of Ppar- α agonists. So far, only little is known about Ppar- α mediated regulation in kidney tissue (217) and to study its function might provide further insights into the mechanisms behind adaptive gene regulation in the PEPT2 deficient animals and in general into the regulation of amino acid and fatty acid metabolism in kidney.

On the other hand, the drastically increased excretion of cys-gly in *Pept2*^{-/-} animals demonstrates that the loss of PEPT2 is not compensated completely. Although the cyclic metabolism of GSH in epithelial cells of the proximal tubule that comprises intracellular GSH synthesis, GSH secretion into the tubule lumen, breakdown of GSH and reabsorption of the substrates for GSH resynthesis has been described as the γ -glutamyl-cycle more than 30 years ago (196), only little information is available on the transport processes involved (122). GSH in epithelial cells is derived from intracellular GSH synthesis and from basolateral GSH uptake from plasma, but the available evidence is ambiguous with regard to which processes are more important for maintaining epithelial GSH levels. In our PEPT2 deficient animals total renal GSH concentration did not show alterations. Whether increased basolateral GSH uptake is indeed responsible for the compensation could either be studied by application of inhibitors (e.g. probenecid) for the presumptive basolateral GSH transporters or by generation of a double knockout mouse model deficient for PEPT2 and Oat3 with the Oat3 knockout mouse model available in the group of J. Pritchard (216). The relevance of PEPT2 mediated reabsorption of cys-gly for epithelial GSH synthesis could further be studied by application of a nephrotoxic substance (e.g. acetaminophen) that requires GSH conjugation for detoxification. The level of nephrotoxicity in *Pept2*^{-/-} animals in comparison to wild type animals should allow evaluating the relevance of PEPT2 mediated cys-gly reabsorption and intracellular GSH synthesis to provide the elevated GSH levels required for detoxification. We recently performed a pilot study on acetaminophen toxicity. Based on the preliminary data of three animals per group plasma urea and creatinine levels together with urinary glucose levels show a more pronounced elevation in the transporter deficient

animals indicating more severe nephrotoxicity in response to acetaminophen. Correspondingly, tissue morphology displayed a higher degree of damage in the *Pept2*^{-/-} animals.

PEPT2 is localized in a wide variety of tissues. Although the *Pept2*^{-/-} animals do not show obvious phenotypic alterations, it is not justified to assume that PEPT2 is of minor relevance. Our findings in kidney tissue demonstrate that by application of profiling techniques a previously unanticipated function of PEPT2 which can be compensated for under normal conditions could be identified. Most likely that would also be possible in the various other tissues expressing PEPT2. Studying these tissues for the consequences of the loss of PEPT2 at the various biological levels should eventually provide a more complete picture of the physiological function of PEPT2 mediated peptide transport and allow for identification of conditions in which PEPT2 is indispensable.

Appendix

1. Complete lists of differentially expressed genes

Table 20: Genes with elevated mRNA levels in *Pept2^{-/-}* animals as identified by VarMixt

ID ¹	Gene Symbol	Description	Δ -fold change in <i>Pept2^{-/-}</i>	estimated FDR ²
MG-11-1o21	Rnase4	ribonuclease, RNase A family 4	2.39	0.00E+00
MG-12-28a11		cis-retinol/3alpha hydroxysterol short-chain dehydrogenase-like protein isoform mRNA	1.43	1.35E-05
MG-12-279c15	Slc22a8	carrier family 22 (organic anion transporter), member 8	1.41	1.43E-05
MG-12-142f22	Cyp4a14	Cytochrome P450, family 4, subfamily a, polypeptide 14, mRNA	1.39	5.06E-03
MG-12-212j24		RIKEN cDNA 4121402D02 gene (4121402D02Rik), transcript variant 1	1.29	4.85E-02
MG-3-27f11	Apoe	Mus musculus apolipoprotein E	1.26	2.20E-04
MG-6-80p15	Glud1	glutamate dehydrogenase 1	1.26	4.92E-04
MG-15-135k15	Acs11	acyl-CoA synthetase long-chain family member 1	1.24	2.46E-04
MG-12-1g3	Napsa	napsin A aspartic peptidase	1.24	3.32E-02
MG-6-32a17	Mdk	midkine (Mdk), transcript variant 1,2,3	1.24	2.24E-03
MG-12-171j2	Acot3	acyl-CoA thioesterase 3	1.23	2.48E-04
MG-12-128l8	Rdh16	retinol dehydrogenase 16	1.23	2.53E-04
MG-16-7d5	Slc7a7	cationic amino acid transporter, y+ system	1.22	2.28E-06
MG-3-134i15	Tst	thiosulfate sulfurtransferase, mitochondrial	1.22	6.29E-04
MG-12-213j4		BAC clone RP23-77K23 from chromosome 14	1.22	4.27E-02
MG-8-11b5	Akp2	alkaline phosphatase 2, liver	1.21	6.30E-04
MG-68-180f14	Bdh1	3-hydroxybutyrate dehydrogenase (heart, mitochondrial)	1.20	6.11E-04
MG-12-42l4		coactosin-like 1 (Dictyostelium)	1.20	1.85E-04
MG-12-213b19		DNA sequence from clone RP23-402l8 on chromosome 4	1.20	3.81E-02
MG-8-55h19	Gldc	glycine decarboxylase	1.20	6.92E-03
MG-3-88l10	Acaa1b	clone RP23-129C12, complete sequence, 3-ketoacyl-CoA thiolase B	1.18	1.41E-03
MG-15-3k1	Igfbp4	insulin-like growth factor binding protein 4	1.18	6.88E-04

ID ¹	Gene Symbol	Description	Δ -fold change in <i>Pept2</i> ^{-/-}	estimated FDR ²
MG-3-111c24		sequence from clone RP23-399H3 on chromosome 4	1.18	2.57E-03
MG-6-22n21	Cirbp	cold inducible RNA binding protein	1.18	2.66E-02
MG-6-86k24		chromosome 7, clone RP24-69E5, complete sequence	1.17	1.16E-02
MG-6-48o4	Acp6	acid phosphatase 6, lysophosphatidic (Acp6)	1.17	5.83E-03
MG-12-234j10		TIB-55 BB88 cDNA, RIKEN full-length enriched library, clone:l730035A10	1.17	5.47E-03
MG-6-35g19	Hgs	HGF-regulated tyrosine kinase substrate	1.17	3.60E-02
MG-3-24c22	Alad	aminolevulinate, delta-, dehydratase	1.16	2.74E-04
MG-8-42i11	C1qtnf6	C1q and tumor necrosis factor related protein 6	1.16	5.54E-03
MG-3-22g11	Gstm1	glutathione S-transferase, mu 1	1.16	4.04E-02
MG-6-2d10		clone RP23-188A12 on chromosome 4	1.15	1.99E-02
MG-3-64c10	Dcxr	dicarbonyl L-xylulose reductase (AK161732)	1.15	5.78E-03
MG-3-68i14	Ucp2	uncoupling protein 2 (mitochondrial, proton carrier)	1.15	3.56E-02
MG-3-45k11	H3f3b	H3 histone, family 3B	1.15	3.19E-02
MG-15-108n8	Cish2	suppressor of cytokine signalling-2	1.15	5.73E-03
MG-8-46e22	Apoe	apolipoprotein E	1.15	1.43E-02
MG-3-40e12		macrophage migration inhibitory factor	1.15	1.39E-02
MG-26-267m8		BAC clone RP23-11i13 from 18	1.15	4.43E-02
MG-12-211k1		cDNA clone IMAGE:6766474	1.14	6.92E-03
MG-6-82j16	Abhd4	abhydrolase domain containing 4	1.14	3.81E-02
MG-12-164j1	Miox	myo-inositol oxygenase	1.14	4.38E-02
MG-8-70n14	Mgll	monoglyceride lipase	1.13	2.91E-03
MG-3-5m6	Oplah	chromosome 15, clone RP24-127H11, complete sequence, 5-oxoprolinase (ATP-hydrolysing)	1.13	5.91E-03
MG-3-32f3	Supt16h	suppressor of Ty 16 homolog	1.13	4.32E-02
MG-4-2o4		BAC clone RP23-106G24 from chromosome 3	1.13	2.25E-02
MG-8-58b6	Glud1	glutamate dehydrogenase 1	1.13	7.97E-03
MG-3-244j20		chromosome 5, clone RP23-170E15	1.13	1.49E-02
MG-14-31e12	Erb3	v-erb-b2 erythroblastic signalling viral oncogene homolog 3 (avian)	1.13	7.90E-03

ID ¹	Gene Symbol	Description	Δ -fold change in <i>Pept2</i> ^{-/-}	estimated FDR ²
MG-6-65d4	Hlf	hepatic signallin factor	1.12	5.91E-03
MG-68-178m17	Socs2	suppressor of cytokine signalling 2	1.12	3.98E-02
MG-6-22h16	Acaa1a	acetyl-Coenzyme A acyltransferase 1A	1.12	3.02E-02
MG-6-68h16	Car14	carbonic anhydrase 14	1.12	1.70E-02
MG-6-51k15	Lphn1	latrophilin 1	1.12	4.91E-02
MG-12-166a24		catechol-O-methyltransferase, mRNA (cDNA clone MGC:13804 IMAGE:4210097)	1.12	2.73E-02
MG-3-15a14	Mnat1	menage a trois 1	1.12	3.81E-02
MG-8-47n3	Zfp503	zinc finger protein 503	1.12	3.19E-02
MG-3-113j5		heterogeneous nuclear ribonucleoprotein K	1.11	2.65E-02
MG-3-96i6	Gst2	glutathione S-transferase, theta 2	1.11	2.71E-02
MG-8-19i4		DNA sequence from clone RP23-362B9 on chromosome 2	1.11	2.99E-02
MG-3-110p22	Supt16h	suppressor of Ty 16 homolog	1.11	2.66E-02
MG-6-46f24		BAC clone RP23-199B2 from 3	1.11	2.89E-02
MG-6-13h17	Lmo4	LIM domain only 4	1.11	3.19E-02
MG-13-55o4	Cda	cytidine deaminase	1.11	3.93E-02
MG-14-3m20	Cpt2	carnitine palmitoyltransferase 2	1.11	3.19E-02
MG-12-256i19	Ipmk	inositol polyphosphate multikinase	1.11	2.73E-02
MG-3-49d6	Lzf	leucine zipper domain protein	1.11	3.46E-02
MG-15-100p1	Rpl26	ribosomal protein L26	1.11	4.91E-02
MG-12-218d4		adult male olfactory brain cDNA	1.11	2.56E-02
MG-6-70e2		RIKEN cDNA 3110006E14 gene	1.11	4.73E-02
MG-3-46k8		RIKEN cDNA 1810015C04 gene (1810015C04Rik), transcript variant 1	1.11	4.27E-02
MG-68-101p16		histone protein Hist1h2bf gene	1.11	4.02E-02
MG-6-34d23	Hpcal1	hippocalcin-like	1.11	4.31E-02
MG-3-49i24	Oplah	5-oxoprolinase (ATP-hydrolysing)	1.10	1.01E-02
MG-3-116i15		Mus musculus hypothetical protein LOC622422	1.10	3.67E-02
MG-3-25c6	Xpnpep1	X-prolyl aminopeptidase (aminopeptidase P) 1, soluble	1.10	4.22E-02

ID ¹	Gene Symbol	Description	Δ -fold change in <i>Pept2</i> ^{-/-}	estimated FDR ²
MG-15-241c15	Pgam1	phosphoglycerate mutase 1	1.10	4.44E-02
MG-78-2j16	Lyplal1	lysophospholipase-like 1	1.10	4.02E-02
MG-3-7g5		Mus musculus similar to hypothetical protein LOC75438	1.10	4.38E-02
MG-3-121n1	Slc16a6	solute carrier family 16 (monocarboxylic acid transporters), member 6 (Slc16a6), transcript variant 2	1.09	4.05E-02
MG-26-209a15		chromosome 7, clone RP24-180J10	1.09	4.27E-02
MG-6-24f21		RIKEN full-length enriched library, clone:9430078C22	1.09	3.56E-02
MG-6-54h14	Acly	ATP citrate lyase	1.09	3.98E-02

1, Lion Biosciences Probe ID

2, FDR = False Discovery Rate, FDR cut-off set at 0.05

Table 21: Genes with decreased mRNA levels in *Pept2*^{-/-} animals as identified by VarMixt

ID ¹	Gene Symbol	Description	Δ -fold change in <i>Pept2</i> ^{-/-}	estimated FDR ²
MG-12-194e2	Slc15a2	solute carrier family 15 (H+/peptide transporter),	-2.63	0.00E+00
MG-11-1e9	Ttr	transthyretin	-1.41	1.84E-05
MG-6-67i6	Dhrs8	dehydrogenase/reductase (SDR family) member 8	-1.35	5.37E-06
MG-6-43b23		clone:1810043H04 product:unclassifiable	-1.35	5.37E-06
MG-16-28m11	Hsd11b1	hydroxysteroid 11-beta dehydrogenase 1 (Hsd11b1)	-1.35	8.81E-05
MG-6-60f22		clone:C630010C08 product:unclassifiable	-1.29	3.15E-04
MG-3-16p4	Odc	gene for ornithine decarboxylase	-1.29	5.78E-03
MG-68-104c23	Odc	Mouse ornithine decarboxylase gene	-1.28	5.37E-06
MG-12-200k12	Eaf2	ELL associated factor 2	-1.26	6.45E-05
MG-3-263a17		BAC clone RP24-458F14 from chromosome 19	-1.25	6.32E-04
MG-6-13o7		clone RP23-105M23 on chromosome 2	-1.24	2.16E-06
MG-12-256p6	Slco1a6	solute carrier organic anion transporter family, member 1a6	-1.24	2.36E-05
MG-8-44o23	Agps	alkylglycerone phosphate synthase	-1.23	5.37E-06
MG-6-15i10	Rps6ka4	ribosomal protein S6 kinase, polypeptide 4	-1.23	2.15E-03
MG-16-186g23	Sepp1	plasma selenoprotein P (SELP) gene	-1.23	1.85E-02
MG-6-75i11	GNB2	GNB2 gene for guanine nucleotide binding protein beta2 subunit, complete cds.	-1.23	1.40E-02

ID ¹	Gene Symbol	Description	Δ -fold change in <i>Pept2</i> ^{-/-}	estimated FDR ²
MG-15-127h14	Pcnp	PEST containing nuclear protein RIKEN cDNA 1110018D06 gene	-1.22	6.29E-04
MG-12-3n11		RIKEN full-length enriched library, clone:F520013M09 product:weakly similar to Ornithine decarboxylase 1	-1.22	2.24E-03
MG-3-37f4	Idi1	isopentenyl-diphosphate delta isomerase	-1.22	5.94E-04
MG-6-26i9		clone:C730029E02 product:hydroxysteroid 11-beta dehydrogenase 1	-1.21	2.36E-05
MG-12-164i12		RIKEN full-length enriched library, clone:F430114C21 product:unclassifiable	-1.21	6.29E-04
MG-12-238a23	Cndp2	CNDP dipeptidase 2 (metallopeptidase M20 family)	-1.20	6.29E-04
MG-8-93b10	Sfpq	splicing factor proline/glutamine rich (polypyrimidine tract binding protein associated)	-1.20	8.21E-03
MG-8-16c13		ATPase, class VI, type 11A	-1.19	3.09E-03
MG-8-42a18	Tra1	tumor rejection antigen gp96	-1.19	6.09E-03
MG-3-66n23	Slc35a5	solute carrier family 35, member A5 (Slc35a5)	-1.19	2.91E-03
MG-3-17d1		DNA sequence from clone RP23-56I20 on chromosome 11 Contains the 5' end of the gene for a novel protein similar to dynein, the Efnb3 gene for ephrin B3, a novel gene, the Trp53 gene for transformation related protein 53, the Atp1b2 gene for Na ⁺ /K ⁺ transporting ATPase beta 2 polypeptide, the Shbg gene for sex hormone binding globulin, the 5' end of the Sat2 gene for spermidine/spermine N1-acetyl transferase 2 and two CpG islands	-1.19	2.02E-02
MG-12-140c23	Cyp7b1	cytochrome P450, family 7, subfamily b, polypeptide 1	-1.18	3.14E-03
MG-3-27I16	Cndp2	CNDP dipeptidase 2 (metallopeptidase M20 family)	-1.18	2.71E-03
MG-12-1k1	Mrpl48	mitochondrial ribosomal protein L48	-1.18	2.15E-03
MG-12-3e4	Cyp4b1	cytochrome P450, family 4, subfamily b, polypeptide 1	-1.18	1.58E-03
MG-12-277g11	Sardh	sarcosine dehydrogenase	-1.18	2.25E-02
MG-6-91m19		DNA sequence from clone RP23-442G9 on chromosome 2	-1.17	2.69E-02
MG-6-31i2	Dynll1	dynein light chain LC8-type 1	-1.16	2.40E-02
MG-3-23p15	Hspa5	heat shock 70kD protein 5 (glucose- regulated protein)	-1.16	5.81E-03
MG-12-208I5	Ces2	RIKEN cDNA 0610012H03 gene (0610012H03Rik), product: carboxylesterase 2	-1.16	2.15E-03
MG-12-206c6	Galnt1	UDP-N-acetyl-alpha-D- galactosamine:polypeptide N- acetylgalactosaminyltransferase 1	-1.16	4.91E-02

ID ¹	Gene Symbol	Description	Δ -fold change in <i>Pept2</i> ^{-/-}	estimated FDR ²
MG-8-47b24		RIKEN cDNA 2210023G05 gene	-1.15	6.90E-03
MG-4-86g10		RIKEN full-length enriched library, clone:B830031F14, product: sarcosine dehydrogenase	-1.15	2.15E-03
MG-6-64d16	Eif1	eukaryotic translation initiation factor 1	-1.15	2.15E-03
MG-8-60f17	Nola2	nucleolar protein family A, member 2	-1.15	1.43E-02
MG-12-24f21	Smarca2	SWI/SNF related, matrix associated, actin dependent regulator of chromatin, subfamily a, member 2 (Smarca2), transcript variant 1	-1.15	4.91E-02
MG-15-171p17		RIKEN full-length enriched library, clone:I420008H14 product:PEST-containing nuclear protein homolog [Homo sapiens]	-1.14	3.19E-02
MG-12-274k12		PREDICTED: Mus musculus similar to Alstrom syndrome 1	-1.14	7.90E-03
MG-15-3m11	serum IgG2a	immunoglobulin heavy chain 1a	-1.14	4.44E-02
MG-3-46c14		BAC clone RP24-90L20 from chromosome 8	-1.14	3.34E-02
MG-3-8p18	Atp11a	ATPase, class VI, type 11A	-1.14	3.05E-02
MG-14-2n11	Atrnl1	attractin like 1	-1.13	9.13E-04
MG-12-150p12	Anxa13	annexin A13	-1.13	2.24E-03
MG-12-258e15	Adh1	alcohol dehydrogenase 1 (class I)	-1.13	1.40E-02
MG-16-142p11	Tspan13	tetraspanin 13	-1.13	1.28E-02
MG-3-55c24		BAC clone RP23-379C1 from 14	-1.13	3.12E-02
MG-12-155p10	Gas2	growth arrest specific 2	-1.13	4.20E-02
MG-3-44m2		RIKEN cDNA 5730592L21 gene (5730592L21Rik)	-1.12	1.11E-02
MG-8-66g20	Armet	arginine-rich, mutated in early stage tumors	-1.12	1.52E-02
MG-15-115h10		RIKEN full-length enriched library, clone:3732404F06 product:glutamate-cysteine ligase, catalytic subunit	-1.12	1.66E-02
MG-15-236p4	Tm4sf1	transmembrane 4 superfamily member 1	-1.12	4.91E-02
MG-26-279p9	Mylk	myosin, light polypeptide kinase	-1.11	1.46E-02
MG-15-190c11	Scpep1	serine carboxypeptidase 1	-1.11	4.02E-02
MG-16-137h5	Scd2	stearoyl-Coenzyme A desaturase 2	-1.11	4.75E-02
MG-3-247k18	Smarca2	SWI/SNF related, matrix associated, actin dependent regulator of chromatin, subfamily a, member 2 (Smarca2), transcript variant 1	-1.11	3.32E-02

ID ¹	Gene Symbol	Description	Δ -fold change in <i>Pept2</i> ^{-/-}	estimated FDR ²
MG-15-192i7		transducin-like enhancer of split 3, homolog of <i>Drosophila</i> E(spl)	-1.11	4.14E-02
MG-15-155o4		RIKEN cDNA 1500006O09 gene	-1.11	3.98E-02
MG-3-228p10	Rai14	retinoic acid induced 14	-1.11	4.20E-02
MG-12-165m10	Fcmd	Fukuyama type congenital muscular dystrophy homolog	-1.10	3.57E-02
MG-12-206k20	Gatad1	GATA zinc finger domain containing 1	-1.10	2.02E-02
MG-8-46f9	Hsd17b2	hydroxysteroid (17-beta) dehydrogenase 2	-1.10	4.09E-02
MG-16-262e2	Epc1	enhancer of polycomb homolog 1	-1.10	4.91E-02
MG-12-155n21	Gimap4	IMAP family member 4	-1.09	3.98E-02
MG-3-137c3		RIKEN cDNA 1110017F19 gene	-1.09	4.91E-02
MG-14-119n19	Ttr	transthyretin	-1.08	4.52E-02

1, Lion Biosciences Probe ID

2, FDR = False Discovery Rate, FDR cut-off set at 0.05

Table 22: Differentially expressed genes in *Pept2*^{-/-} animals as identified by PAM

Rank	ID ¹	Gene Symbol	Description	Δ -fold change in <i>Pept2</i> ^{-/-}	FDR
1	MG-12-194e2	Slc15a2	solute carrier family 15 (H+/peptide transporter)	-2.63	0.00
2	MG-11-1o21	Rnase4	ribonuclease, RNase A family 4	2.39	0.00
3	MG-12-200k12	Eaf2	ELL associated factor 2	-1.26	0.01
4	MG-12-164i12		RIKEN full-length enriched library, clone:F430114C21 product:unclassifiable	-1.21	0.01
5	MG-3-37f4	Idi1	isopentenyl-diphosphate delta isomerase	-1.22	0.01
6	MG-15-127h14	Pcnp	PEST containing nuclear protein RIKEN cDNA 1110018D06 gene	-1.22	0.02
7	MG-8-16c13	Atp11a	ATPase, class VI, type 11A	-1.14	0.02
8	MG-12-279c15	Slc22a8	carrier family 22 (organic anion transporter), member 8	1.41	0.02
9	MG-15-158l12	Rab11a		-1.16	0.02
10	MG-3-32f3	Supt16h	suppressor of Ty 16 homolog	1.13	0.04
11	MG-12-42l4	Cot1	coactosin-like 1 (Dictyostelium)	1.20	0.06
12	MG-3-263a17	Malat1	BAC clone RP24-458F14 from chromosome 19	-1.25	0.06
13	MG-16-217i22	Oxa1		1.14	0.06
14	MG-6-67i6	Dhrs8	dehydrogenase/reductase (SDR family) member 8	-1.35	0.06
15	MG-3-134i15	Tst	thiosulfate sulfurtransferase, mitochondrial	1.22	0.08
16	MG-4-148l18	Rpl24		-1.15	0.08
17	MG-3-37d1		1200009B18Rik	-1.11	0.09
18	MG-26-267a23	Rnpc2		-1.08	0.12
19	MG-12-24a23	Calml4		-1.12	0.12
20	MG-14-114d20		D330022H12Rik	1.08	0.12

The false discovery rate (FDR) was calculated from the mean number of nonsignificant genes for a certain rank which was estimated by permutations.

1, Lion Biosciences Probe ID

2. Oligonucleotide primers for qPCR

Table 23: Primers for housekeeping genes

Acc. no.	gene	forward (FP) and reverse (RP) primer	amplicon	T _m
NM_008084	<i>Gapdh</i>	FP: 5'-ATCCCAGAGCTGAACG-3' RP: 5'-GAAGTCGCAGGAGACA-3'	198 bp	87.70
NM_013556	<i>Hprt1</i> ¹	FP: 5'-CCTAAGATGAGCGCAAGTTGAA-3' RP: 5'-CCACAGGACTAGAACACCTGCTAA-3'	86 bp	80.68
NM_023281.1	<i>Sdha</i> ²	FP: 5'-TCCTGCCTCTGTGGTTGAG-3' RP: 5'-AGCAACACCGATGAGCCTG-3'	134 bp	84.31

1, ID 45 aus RTPrimerDB

2, PrimerBank ID15030102a3

Table 24: Primers for genes involved in peptide and amino acid transport and metabolism

Acc. no.	gene	forward (FP) and reverse (RP) primer	amplicon	T _m
NM_021301	<i>Slc15a2</i> (<i>Pept2</i>)	FP: 5'-TTCAGCAGCCTCTGCTATTTTC-3' RP: 5'-GCTGCCACACAGGGTTTG-3'	215	84,3
NM_053079	<i>Slc15a1</i> (<i>Pept1</i>)	FP: 5'-TGATCCGAAGGGCGAG-3' RP: 5'-GGCGAATATCACGCAG-3'	308 bp	88.00
AF139194	<i>Slc9a3</i> (<i>NHE3</i>)	FP: 5'-TCATTCGCTCCCCAAG-3' RP: 5'-GTTAGCTCGTGCCGAC-3'	250 bp	87.55
NM_007876	<i>Dpep1</i>	FP: 5'-GCACAACGACTTGCCTTGG-3' RP: 5'-ATGCGGTGTATCACATCCATC-3'	230 bp	87.08
NM_009199	<i>Slc1a1</i> (<i>EAAC1</i>)	FP: 5'- TGTTGACTGGCTCCTGGACC-3' RP: 5'- GCTCCAGCTCCTTCTTCGAGA-3'	101bp	86.92
BC013441	<i>Slc3a1</i> (<i>rBAT</i>)	FP: 5'-CAAGTCACCGATGCAG-3' RP: 5'-CGTTATCTATGCCGTCCA-3'	260 bp	87.84
NM_021291	<i>Slc7a9</i> (<i>b⁰+AT</i>)	FP: 5'-TCAGCGGACTGGTCTT-3' RP: 5'-CCATTAGCAGCACCGAT-3'	379 bp	86.15
NM_008577	<i>Slc3a2</i> (<i>4F2hc</i>)	FP: 5'-CAGACTTTATACCGGACCA-3' RP: 5'-GTCACCGTGCAACAGA-3'	293 bp	88.43
NM_011405	<i>Slc7a7</i> (<i>y+LAT1</i>)	FP: 5'-TCGGGGGATTCCTTGC-3' RP: 5'-CCTTAGCGTAGGTGAAAATATCT-3'	243 bp	91.02
AC158359	<i>Slc6a19</i> (<i>B0AT1</i>)	FP: 5'- CAATGGGTTTCGACCTG-3' RP: 5'- CCTGAAGGGGTACGAC-3'	299 bp	87.40
AC109498	<i>Slc7a1</i> (<i>CAT1</i>)	FP: 5'- GGAGTGCGACTTTTGACGAG-3' RP: 5'- ACCAGGACATTGATACAGGTGA-3'	205 bp	87.40
BC041108	<i>Slc38a2</i> (<i>SNAT2</i>)	FP: 5'- CCAATGAGATCCGTGCAAAA-3' RP: 5'- TGGACCCAATCCAGCACAAT-3'	101 bp	83.82
AF159856	<i>Slc38a3</i> (<i>SNAT3</i>)	FP: 5'- CGAATCATGCCCACTGACAA-3' RP: 5'- AACCGCAGCGAAACAAAGG-3'	72 bp	83.77

Table 25: Primers for validation of microarray results

Acc. no.	gene	forward (FP) and reverse (RP) primer	amplicon	T _m
NM_021472	<i>Rnase4</i>	FP: 5'-CTTTCTCCCCTTGGATGGGATG-3' RP: 5'-TAGGCGAGTTGTCATTGCCTG-3'	200 bp	86.09
NM_134111	<i>Eaf2</i>	FP: 5'-CGGAGCACCTAGCATGTC-3' RP: 5'-CTGTGCTTTCTGACTC-3'	142 bp	85.6

Table 26: Primers for genes involved in GSH metabolism

Acc. no.	gene	forward (FP) and reverse (RP) primer	amplicon	T _m
NM_145953	<i>Gclm</i> *	FP: 5'-GGTACTCGGTCATCGTG-3' RP: 5'-GCTTCTTGTAAGGCGG-3'	198 bp	85.11
NM_010295	<i>Gclc</i>	FP: 5'-AGGATCAGTAAGTCTCGG-3' RP: 5'-GTGAGCAGTACCACGAATA-3'	380 bp	84.25
NM_008180	<i>Gss</i> [†]	FP: 5'-ACGACTATACTGCCCCG-3' RP: 5'-GTAGCACCACCGCATT-3'	333 bp	88.33
NM_008116	<i>Ggt1</i> [†]	FP: 5'-AGGAGAGACGGTGACT-3' RP: 5'-GGCATAGGCAAACCGA-3'	364 bp	89.14
NM_010344	<i>Gsr</i>	FP: 5'-TTCGACGGGACCCAAA-3' RP: 5'-ACATCGGGGTAAAGGC-3'	354 bp	86.13
NM_145953	<i>Cth</i>	FP: 5'-TTGCTAGAGGCAGCGA-3' RP: 5'-AAGCCGACTATTGAGGT-3'	285 bp	84.14

3. List of abbreviations

2D	two-dimensional
3D-QSAR	three dimensional quantitative structure affinity relationship
aa	amino acid(s)
ala	alanine
ALA	δ -aminolevulinic acid
arg	arginine
asn	asparagine
asp	aspartate
ATP	adenosine triphosphate
bp	base pair(s)
BRENDA	Braunschweiger Enzymdatenbank (Brunswick enzyme database)
bw	body weight
cAMP	cyclic adenosine monophosphate
CBB	coomassie brilliant blue
cDNA	complementary deoxyribonucleic acid
CHAPS	3-[(3-cholamidopropyl)dimethyl-ammonio]-1-propanesulfonate
CoMSIA	comparative molecular similarity indices analysis
C-terminus	carboxy-terminus
Cy3	fluorescence dye, emission 570
Cy5	fluorescence dye, emission 670
cys-gly	cysteinyl-glycine
D-Ala-Lys-AMCA	D-alanyl-lysyl-N- ϵ -7-amino-4-methylcoumarin-3-acetic acid
dATP	deoxyadenosine triphosphate
DMSO	dimethyl sulfoxide
D-Phe-Ala	D-phenylalanyl-alanine
DTT	dithiothreitol
EDTA	ethylenediaminetetraacetic acid
ENU	N-nitroso-N-ethylurea
ES cells	embryonic stem cells

FDR	false discovery rate
Fig.	figure
g	acceleration of gravity
GC	gas chromatography
GEO	gene expression omnibus
gln	glutamine
glu	glutamate
gly-sar	glycyl-sarcosine
GO	gene ontology
GSH	glutathione
h	hour(s)
his	histidine
HMDB	human metabolome database
HPLC	high performance liquid chromatography
IEF	isoelectric focusing
ile	isoleucine
IPG	immobilized pH gradient
kD	kilo dalton
KEGG	Kyoto encyclopedia of genes and genomes
KO	knockout
LC	liquid chromatography
leu	leucine
lys	lysine
M	molar (mol/l)
met	methionine
MIAME	minimum information about a microarray experiment
min	minute(s)
M-MLV-RT	moloney murine leukaemia virus reverse transcriptase
MNE	mean normalized expression
mRNA	messenger deoxyribonucleic acid
MS	mass spectrometry
MWCO	molecular weight cut off
n	number of samples
NMR	nuclear magnetic resonance

N-terminus	amino-terminus
PAGE	polyacrylamide gel electrophoresis
PAM	pattern analysis of microarrays
PCA	principal component analysis
PCR	polymerase chain reaction
pH	logarithm of the reciprocal of hydrogen-ion concentration
PKA	protein kinase A
PKC	protein kinase C
PLS-DA	partial least squares discriminant analysis
POT	proton coupled oligopeptide transporter superfamily
PTR	peptide transporter family
qPCR	quantitative real-time reverse transcription polymerase chain reaction
RT-PCR	reverse transcription polymerase chain reaction
SD	standard deviation
SDS	sodium dodecyl sulphate
SEM	standard error of the mean
SNP	single nucleotide polymorphism
SSC	sodium citrate sodium chloride buffer
TIGR	the institute for genomic research
TMD	transmembrane domain
TOF	time of flight
tyr	tyrosine
Val	valine
WT	wildtype
V_{\max}	maximum velocity

References

1. The HUGO solute carrier family series.
<http://www.bioparadigms.org/slc/menu.asp>, accessed 09.11.2006
2. **Adibi, S. A.** 1971. Intestinal transport of dipeptides in man: relative importance of hydrolysis and intact absorption. *J Clin Invest* **50**:2266-75.
3. **Adibi, S. A.** 1986. Presented at the Proc. Congr. Eur. Soc. Parenter. Enteral Nutr., 7th.
4. **Adibi, S. A.** 2003. Regulation of expression of the intestinal oligopeptide transporter (Pept-1) in health and disease. *Am J Physiol Gastrointest Liver Physiol* **285**:G779-88.
5. **Adibi, S. A.** 1997. Renal assimilation of oligopeptides: physiological mechanisms and metabolic importance. *Am J Physiol* **272**:E723-36.
6. **Adibi, S. A., B. A. Krzysik, and A. L. Drash.** 1977. Metabolism of intravenously administered dipeptides in rats: effects on amino acid pools, glucose concentration and insulin and glucagon secretion. *Clin Sci Mol Med* **52**:193-204.
7. **Adibi, S. A., and E. L. Morse.** 1977. The number of glycine residues which limits intact absorption of glycine oligopeptides in human jejunum. *J Clin Invest* **60**:1008-16.
8. **Adibi, S. A., E. L. Morse, S. S. Masilamani, and P. M. Amin.** 1975. Evidence for two different modes of tripeptide disappearance in human intestine. Uptake by peptide carrier systems and hydrolysis by peptide hydrolases. *J Clin Invest* **56**:1355-63.
9. **Adibi, S. A., and M. R. Soleimanpour.** 1974. Functional characterization of dipeptide transport system in human jejunum. *J Clin Invest* **53**:1368-74.
10. **Alberts, B., Johnson, A, Lewis, J, Raff, M, Robers, K, Walter, P.** 2002. *Molecular biology of the cell*, 4th ed. Garland Science, New York.
11. **Alcorn, J., X. Lu, J. A. Moscow, and P. J. McNamara.** 2002. Transporter gene expression in lactating and nonlactating human mammary epithelial cells using real-time reverse transcription-polymerase chain reaction. *J Pharmacol Exp Ther* **303**:487-96.
12. **Allison, D. B., X. Cui, G. P. Page, and M. Sabripour.** 2006. Microarray data analysis: from disarray to consolidation and consensus. *Nat Rev Genet* **7**:55-65.
13. **Almaas, E., B. Kovacs, T. Vicsek, Z. N. Oltvai, and A. L. Barabasi.** 2004. Global organization of metabolic fluxes in the bacterium *Escherichia coli*. *Nature* **427**:839-43.
14. **Amasheh, S., U. Wenzel, M. Boll, D. Dorn, W. Weber, W. Clauss, and H. Daniel.** 1997. Transport of charged dipeptides by the intestinal H⁺/peptide symporter PepT1 expressed in *Xenopus laevis* oocytes. *J Membr Biol* **155**:247-56.
15. **Anderson, L., and J. Seilhamer.** 1997. A comparison of selected mRNA and protein abundances in human liver. *Electrophoresis* **18**:533-7.
16. **Ashida, K., T. Katsura, H. Saito, and K. Inui.** 2004. Decreased activity and expression of intestinal oligopeptide transporter PEPT1 in rats with hyperthyroidism in vivo. *Pharm Res* **21**:969-75.
17. **Badiou, S., H. Bellet, S. Lehmann, J. P. Cristol, and S. Jaber.** 2005. Elevated plasma cysteinylglycine levels caused by cilastatin-associated antibiotic treatment. *Clin Chem Lab Med* **43**:332-4.

18. **Bahadduri, P. M., V. M. D'Souza, J. K. Pinsonneault, W. Sadee, S. Bao, D. L. Knoell, and P. W. Swaan.** 2005. Functional characterization of the peptide transporter PEPT2 in primary cultures of human upper airway epithelium. *Am J Respir Cell Mol Biol* **32**:319-25.
19. **Barabasi, A. L., and Z. N. Oltvai.** 2004. Network biology: understanding the cell's functional organization. *Nat Rev Genet* **5**:101-13.
20. **Basrai, M. A., M. A. Lubkowitz, J. R. Perry, D. Miller, E. Krainer, F. Naider, and J. M. Becker.** 1995. Cloning of a *Candida albicans* peptide transport gene. *Microbiology* **141 (Pt 5)**:1147-56.
21. **Beckers, J.** 2006. Molecular Phenotyping: Gene Expression Profiling, p. 15-34. *In* M. Hrabé de Angelis (ed.), *Standards of Mouse Model Phenotyping*, 1. ed. Wiley-VCH, Weinheim.
22. **Benjamini, Y., and Y. Hochberg.** 1995. Controlling the false discovery rate: a practical and powerful approach to multiple testing. *Journal of the Royal Statistical Society B (Statistical Methodology)* **57**:289-300.
23. **Berger, U. V., and M. A. Hediger.** 1999. Distribution of peptide transporter PEPT2 mRNA in the rat nervous system. *Anat Embryol (Berl)* **199**:439-49.
24. **Biegel, A., S. Gebauer, M. Brandsch, K. Neubert, and I. Thondorf.** 2006. Structural requirements for the substrates of the H⁺/peptide cotransporter PEPT2 determined by three-dimensional quantitative structure-activity relationship analysis. *J Med Chem* **49**:4286-96.
25. **Biegel, A., S. Gebauer, B. Hartrodt, M. Brandsch, K. Neubert, and I. Thondorf.** 2005. Three-dimensional quantitative structure-activity relationship analyses of beta-lactam antibiotics and tripeptides as substrates of the mammalian H⁺/peptide cotransporter PEPT1. *J Med Chem* **48**:4410-9.
26. **Biegel, A., I. Knutter, B. Hartrodt, S. Gebauer, S. Theis, P. Luckner, G. Kottra, M. Rastetter, K. Zebisch, I. Thondorf, H. Daniel, K. Neubert, and M. Brandsch.** 2006. The renal type H⁽⁺⁾/peptide symporter PEPT2: structure-affinity relationships. *Amino Acids* **31**:137-56.
27. **Bikhazi, A. B., M. M. Skoury, D. S. Zwainy, A. R. Jurjus, S. I. Kreydiyyeh, D. E. Smith, K. Audette, and D. Jacques.** 2004. Effect of diabetes mellitus and insulin on the regulation of the PepT 1 symporter in rat jejunum. *Mol Pharm* **1**:300-8.
28. **Bockamp, E., M. Maringer, C. Spangenberg, S. Fees, S. Fraser, L. Eshkind, F. Oesch, and B. Zabel.** 2002. Of mice and models: improved animal models for biomedical research. *Physiol Genomics* **11**:115-32.
29. **Bohmer, C., A. Broer, M. Munzinger, S. Kowalczyk, J. E. Rasko, F. Lang, and S. Broer.** 2005. Characterization of mouse amino acid transporter B0AT1 (slc6a19). *Biochem J* **389**:745-51.
30. **Boll, M., M. Herget, M. Wagener, W. M. Weber, D. Markovich, J. Biber, W. Clauss, H. Murer, and H. Daniel.** 1996. Expression cloning and functional characterization of the kidney cortex high-affinity proton-coupled peptide transporter. *Proc Natl Acad Sci U S A* **93**:284-9.
31. **Boll, M., D. Markovich, W. M. Weber, H. Korte, H. Daniel, and H. Murer.** 1994. Expression cloning of a cDNA from rabbit small intestine related to proton-coupled transport of peptides, beta-lactam antibiotics and ACE-inhibitors. *Pflugers Arch* **429**:146-9.
32. **Bolotin, A., P. Wincker, S. Mauger, O. Jaillon, K. Malarme, J. Weissenbach, S. D. Ehrlich, and A. Sorokin.** 2001. The complete genome sequence of the lactic acid bacterium *Lactococcus lactis* ssp. *lactis* IL1403. *Genome Res* **11**:731-53.

33. **Botka, C. W., T. W. Wittig, R. C. Graul, C. U. Nielsen, K. Higaka, G. L. Amidon, and W. Sadee.** 2000. Human proton/oligopeptide transporter (POT) genes: identification of putative human genes using bioinformatics. *AAPS PharmSci* **2**:E16.
34. **Bradford, M. M.** 1976. A rapid and sensitive method for the quantitation of microgram quantities of protein utilizing the principle of protein-dye binding. *Anal Biochem* **72**:248-54.
35. **Brandsch, M., I. Knutter, and F. H. Leibach.** 2004. The intestinal H⁺/peptide symporter PEPT1: structure-affinity relationships. *Eur J Pharm Sci* **21**:53-60.
36. **Brandsch, M., Y. Miyamoto, V. Ganapathy, and F. H. Leibach.** 1994. Expression and protein kinase C-dependent regulation of peptide/H⁺ co-transport system in the Caco-2 human colon carcinoma cell line. *Biochem J* **299 (Pt 1)**:253-60.
37. **Bravo, S. A., C. U. Nielsen, J. Amstrup, S. Frokjaer, and B. Brodin.** 2004. Epidermal growth factor decreases PEPT2 transport capacity and expression in the rat kidney proximal tubule cell line SKPT0193 cl.2. *Am J Physiol Renal Physiol* **286**:F385-93.
38. **Bretschneider, B., M. Brandsch, and R. Neubert.** 1999. Intestinal transport of beta-lactam antibiotics: analysis of the affinity at the H⁺/peptide symporter (PEPT1), the uptake into Caco-2 cell monolayers and the transepithelial flux. *Pharm Res* **16**:55-61.
39. **Chee, K. M., D. R. Romsos, W. G. Bergen, and G. A. Leveille.** 1981. Protein intake regulation and nitrogen retention in young obese and lean mice. *J Nutr* **111**:58-67.
40. **Chen, G., T. G. Gharib, C. C. Huang, J. M. Taylor, D. E. Misek, S. L. Kardia, T. J. Giordano, M. D. Iannettoni, M. B. Orringer, S. M. Hanash, and D. G. Beer.** 2002. Discordant protein and mRNA expression in lung adenocarcinomas. *Mol Cell Proteomics* **1**:304-13.
41. **Chen, X.-Z., T. Zhu, D. E. Smith, and M. A. Hediger.** 1999. Stoichiometry and Kinetics of the High-affinity H⁺-coupled Peptide Transporter PepT2. *J. Biol. Chem.* **274**:2773-2779.
42. **Churchill, G. A.** 2002. Fundamentals of experimental design for cDNA microarrays. *Nat Genet* **32 Suppl**:490-5.
43. **Clish, C. B., E. Davidov, M. Oresic, T. N. Plasterer, G. Lavine, T. Londo, M. Meys, P. Snell, W. Stochaj, A. Adourian, X. Zhang, N. Morel, E. Neumann, E. Verheij, J. T. Vogels, L. M. Havekes, N. Afeyan, F. Regnier, J. van der Greef, and S. Naylor.** 2004. Integrative biological analysis of the APOE*3-leiden transgenic mouse. *Omics* **8**:3-13.
44. **Connor, S. C., W. Wu, B. C. Sweatman, J. Manini, J. N. Haselden, D. J. Crowther, and C. J. Waterfield.** 2004. Effects of feeding and body weight loss on the 1H-NMR-based urine metabolic profiles of male Wistar Han rats: implications for biomarker discovery. *Biomarkers* **9**:156-79.
45. **Curthoys, N. P., L. Taylor, J. D. Hoffert, and M. A. Knepper.** 2007. Proteomic analysis of the adaptive response of rat renal proximal tubules to metabolic acidosis. *Am J Physiol Renal Physiol* **292**:F140-7.
46. **Cutillas, P. R., J. Biber, J. Marks, R. Jacob, B. Stieger, R. Cramer, M. Waterfield, A. L. Burlingame, and R. J. Unwin.** 2005. Proteomic analysis of plasma membrane vesicles isolated from the rat renal cortex. *Proteomics* **5**:101-12.

47. **Cvetkovic, B., and C. D. Sigmund.** 2000. Understanding hypertension through genetic manipulation in mice. *Kidney Int* **57**:863-74.
48. **Dahlquist, K. D., N. Salomonis, K. Vranizan, S. C. Lawlor, and B. R. Conklin.** 2002. GenMAPP, a new tool for viewing and analyzing microarray data on biological pathways. *Nat Genet* **31**:19-20.
49. **Daniel, H.** 2004. Molecular and integrative physiology of intestinal peptide transport. *Annu Rev Physiol* **66**:361-84.
50. **Daniel, H., and S. A. Adibi.** 1993. Transport of beta-lactam antibiotics in kidney brush border membrane. Determinants of their affinity for the oligopeptide/H⁺ symporter. *J Clin Invest* **92**:2215-23.
51. **Daniel, H., and G. Kottra.** 2004. The proton oligopeptide cotransporter family SLC15 in physiology and pharmacology. *Pflugers Arch* **447**:610-8.
52. **Daniel, H., E. L. Morse, and S. A. Adibi.** 1992. Determinants of substrate affinity for the oligopeptide/H⁺ symporter in the renal brush border membrane. *J Biol Chem* **267**:9565-73.
53. **Daniel, H., E. L. Morse, and S. A. Adibi.** 1991. The high and low affinity transport systems for dipeptides in kidney brush border membrane respond differently to alterations in pH gradient and membrane potential. *J Biol Chem* **266**:19917-24.
54. **Davidov, E., C. B. Clish, M. Oresic, M. Meys, W. Stochaj, P. Snell, G. Lavine, T. R. Londo, A. Adourian, X. Zhang, M. Johnston, N. Morel, E. W. Marple, T. N. Plasterer, E. Neumann, E. Verheij, J. T. Vogels, L. M. Havekes, J. van der Greef, and S. Naylor.** 2004. Methods for the differential integrative omic analysis of plasma from a transgenic disease animal model. *Omics* **8**:267-88.
55. **de Hoog, C. L., and M. Mann.** 2004. Proteomics. *Annu Rev Genomics Hum Genet* **5**:267-93.
56. **Delmar, P., S. Robin, and J. J. Daudin.** 2005. VarMixt: efficient variance modelling for the differential analysis of replicated gene expression data. *Bioinformatics* **21**:502-8.
57. **Dieck, S. T., H. Heuer, J. Ehrchen, C. Otto, and K. Bauer.** 1999. The peptide transporter PepT2 is expressed in rat brain and mediates the accumulation of the fluorescent dipeptide derivative beta-Ala-Lys-Nepsilon-AMCA in astrocytes. *Glia* **25**:10-20.
58. **Doring, F., D. Dorn, U. Bachfischer, S. Amasheh, M. Herget, and H. Daniel.** 1996. Functional analysis of a chimeric mammalian peptide transporter derived from the intestinal and renal isoforms. *J Physiol* **497 (Pt 3)**:773-9.
59. **Doring, F., R. Schmitt, W. M. Bernhardt, M. Klapper, S. Bachmann, H. Daniel, and D. A. Groneberg.** 2005. Hypothyroidism induces expression of the peptide transporter PEPT2. *Biol Chem* **386**:785-90.
60. **Doring, F., J. Will, S. Amasheh, W. Clauss, H. Ahlbrecht, and H. Daniel.** 1998. Minimal molecular determinants of substrates for recognition by the intestinal peptide transporter. *J Biol Chem* **273**:23211-8.
61. **Dringen, R., B. Hamprecht, and S. Broer.** 1998. The peptide transporter PepT2 mediates the uptake of the glutathione precursor CysGly in astroglia-rich primary cultures. *J Neurochem* **71**:388-93.
62. **Drobyshev, A. L., M. H. d. Angelis, and J. Beckers.** 2003. Artefacts and Reliability of DNA Microarray Expression Profiling Data. *Current Genomics* **4**:615-621.

-
63. **Dujon, B., D. Alexandraki, B. Andre, W. Ansorge, V. Baladron, J. P. Ballesta, A. Banrevi, P. A. Bolle, M. Bolotin-Fukuhara, P. Bossier, and et al.** 1994. Complete DNA sequence of yeast chromosome XI. *Nature* **369**:371-8.
 64. **Dunn, W. B., N. J. Bailey, and H. E. Johnson.** 2005. Measuring the metabolome: current analytical technologies. *Analyst* **130**:606-25.
 65. **Dziuba, J., P. Minkiewicz, D. Nalecz, and A. Iwaniak.** 1999. Database of biologically active peptide sequences. *Nahrung* **43**:190-5.
 66. **Ekins, S., Y. Nikolsky, A. Bugrim, E. Kirillov, and T. Nikolskaya.** 2007. Pathway mapping tools for analysis of high content data. *Methods Mol Biol* **356**:319-50.
 67. **Eppig, J. T., J. A. Blake, C. J. Bult, J. A. Kadin, and J. E. Richardson.** 2007. The mouse genome database (MGD): new features facilitating a model system. *Nucleic Acids Res* **35**:D630-7.
 68. **Erickson, R. H., J. R. Gum, Jr., M. M. Lindstrom, D. McKean, and Y. S. Kim.** 1995. Regional expression and dietary regulation of rat small intestinal peptide and amino acid transporter mRNAs. *Biochem Biophys Res Commun* **216**:249-57.
 69. **Famili, I., J. Forster, J. Nielsen, and B. O. Palsson.** 2003. *Saccharomyces cerevisiae* phenotypes can be predicted by using constraint-based analysis of a genome-scale reconstructed metabolic network. *Proc Natl Acad Sci U S A* **100**:13134-9.
 70. **Fei, Y. J., T. Fujita, D. F. Lapp, V. Ganapathy, and F. H. Leibach.** 1998. Two oligopeptide transporters from *Caenorhabditis elegans*: molecular cloning and functional expression. *Biochem J* **332 (Pt 2)**:565-72.
 71. **Fei, Y. J., Y. Kanai, S. Nussberger, V. Ganapathy, F. H. Leibach, M. F. Romero, S. K. Singh, W. F. Boron, and M. A. Hediger.** 1994. Expression cloning of a mammalian proton-coupled oligopeptide transporter. *Nature* **368**:563-6.
 72. **Fei, Y. J., J. C. Liu, T. Fujita, R. Liang, V. Ganapathy, and F. H. Leibach.** 1998. Identification of a potential substrate binding domain in the mammalian peptide transporters PEPT1 and PEPT2 using PEPT1-PEPT2 and PEPT2-PEPT1 chimeras. *Biochem Biophys Res Commun* **246**:39-44.
 73. **Fei, Y. J., W. Liu, P. D. Prasad, R. Kekuda, T. G. Oblak, V. Ganapathy, and F. H. Leibach.** 1997. Identification of the histidyl residue obligatory for the catalytic activity of the human H⁺/peptide cotransporters PEPT1 and PEPT2. *Biochemistry* **36**:452-60.
 74. **Fei, Y. J., E. Nara, J. C. Liu, C. A. Boyd, V. Ganapathy, and F. H. Leibach.** 1999. Preferential recognition of zwitterionic dipeptides as transportable substrates by the high-affinity peptide transporter PEPT2. *Biochim Biophys Acta* **1418**:344-51.
 75. **Fei, Y. J., M. Sugawara, J. C. Liu, H. W. Li, V. Ganapathy, M. E. Ganapathy, and F. H. Leibach.** 2000. cDNA structure, genomic organization, and promoter analysis of the mouse intestinal peptide transporter PEPT1. *Biochim Biophys Acta* **1492**:145-54.
 76. **Feliubadalo, L., M. L. Arbones, S. Manas, J. Chillaron, J. Visa, M. Rodes, F. Rousaud, A. Zorzano, M. Palacin, and V. Nunes.** 2003. Slc7a9-deficient mice develop cystinuria non-I and cystine urolithiasis. *Hum Mol Genet* **12**:2097-108.

77. **Ford, D., A. Howard, and B. H. Hirst.** 2003. Expression of the peptide transporter hPepT1 in human colon: a potential route for colonic protein nitrogen and drug absorption. *Histochem Cell Biol* **119**:37-43.
78. **Forster, J., I. Famili, P. Fu, B. O. Palsson, and J. Nielsen.** 2003. Genome-scale reconstruction of the *Saccharomyces cerevisiae* metabolic network. *Genome Res* **13**:244-53.
79. **Freeman, T. C., B. S. Bentsen, D. T. Thwaites, and N. L. Simmons.** 1995. H⁺/di-tripeptide transporter (PepT1) expression in the rabbit intestine. *Pflugers Arch* **430**:394-400.
80. **Fuchs, D., P. Erhard, G. Rimbach, H. Daniel, and U. Wenzel.** 2005. Genistein blocks homocysteine-induced alterations in the proteome of human endothelial cells. *Proteomics* **5**:2808-18.
81. **Gaildrat, P., M. Moller, S. Mukda, A. Humphries, D. A. Carter, V. Ganapathy, and D. C. Klein.** 2005. A novel pineal-specific product of the oligopeptide transporter PepT1 gene: circadian expression mediated by cAMP activation of an intronic promoter. *J Biol Chem* **280**:16851-60.
82. **Ganapathy, M. E., P. D. Prasad, B. Mackenzie, V. Ganapathy, and F. H. Leibach.** 1997. Interaction of anionic cephalosporins with the intestinal and renal peptide transporters PEPT 1 and PEPT 2. *Biochim Biophys Acta* **1324**:296-308.
83. **Ganapathy, V., G. Burckhardt, and F. H. Leibach.** 1984. Characteristics of glycylsarcosine transport in rabbit intestinal brush-border membrane vesicles. *J Biol Chem* **259**:8954-9.
84. **Garbis, S., G. Lubec, and M. Fountoulakis.** 2005. Limitations of current proteomics technologies. *J Chromatogr A* **1077**:1-18.
85. **Garibotto, G., A. Sofia, S. Saffioti, R. Russo, G. Deferrari, D. Rossi, D. Verzola, M. T. Gandolfo, and M. R. Sala.** 2003. Interorgan exchange of aminothiols in humans. *Am J Physiol Endocrinol Metab* **284**:E757-63.
86. **Gavaghan, C. L., E. Holmes, E. Lenz, I. D. Wilson, and J. K. Nicholson.** 2000. An NMR-based metabolomic approach to investigate the biochemical consequences of genetic strain differences: application to the C57BL10J and Alpk:ApfCD mouse. *FEBS Lett* **484**:169-74.
87. **Gershon, D.** 2005. DNA microarrays: more than gene expression. *Nature* **437**:1195-8.
88. **Goodacre, R., S. Vaidyanathan, W. B. Dunn, G. G. Harrigan, and D. B. Kell.** 2004. Metabolomics by numbers: acquiring and understanding global metabolite data. *Trends Biotechnol* **22**:245-52.
89. **Goodman, S. I.** 1980. An introduction to gas chromatography-mass spectrometry and the inherited organic acidemias. *Am J Hum Genet* **32**:781-92.
90. **Griffin, J. L.** 2006. Understanding mouse models of disease through metabolomics. *Curr Opin Chem Biol* **10**:309-15.
91. **Grimm, D.** 2006. Mouse genetics. A mouse for every gene. *Science* **312**:1862-6.
92. **Groneberg, D. A., F. Doring, P. R. Eynott, A. Fischer, and H. Daniel.** 2001. Intestinal peptide transport: ex vivo uptake studies and localization of peptide carrier PEPT1. *Am J Physiol Gastrointest Liver Physiol* **281**:G697-704.
93. **Groneberg, D. A., F. Doring, M. Nickolaus, H. Daniel, and A. Fischer.** 2001. Expression of PEPT2 peptide transporter mRNA and protein in glial cells of rat dorsal root ganglia. *Neurosci Lett* **304**:181-4.

94. **Groneberg, D. A., F. Doring, S. Theis, M. Nickolaus, A. Fischer, and H. Daniel.** 2002. Peptide transport in the mammary gland: expression and distribution of PEPT2 mRNA and protein. *Am J Physiol Endocrinol Metab* **282**:E1172-9.
95. **Groneberg, D. A., P. R. Eynott, F. Doring, Q. T. Dinh, T. Oates, P. J. Barnes, K. F. Chung, H. Daniel, and A. Fischer.** 2002. Distribution and function of the peptide transporter PEPT2 in normal and cystic fibrosis human lung. *Thorax* **57**:55-60.
96. **Groneberg, D. A., M. Nickolaus, J. Springer, F. Doring, H. Daniel, and A. Fischer.** 2001. Localization of the peptide transporter PEPT2 in the lung: implications for pulmonary oligopeptide uptake. *Am J Pathol* **158**:707-14.
97. **Groneberg, D. A., I. Rubio-Aliaga, M. Nickolaus, F. Doring, A. Fischer, and H. Daniel.** 2004. Direct visualization of peptide uptake activity in the central nervous system of the rat. *Neurosci Lett* **364**:32-6.
98. **Gygi, S. P., Y. Rochon, B. R. Franza, and R. Aebersold.** 1999. Correlation between protein and mRNA abundance in yeast. *Mol Cell Biol* **19**:1720-30.
99. **Hegde, P., R. Qi, K. Abernathy, C. Gay, S. Dharap, R. Gaspard, J. E. Hughes, E. Snestrud, N. Lee, and J. Quackenbush.** 2000. A concise guide to cDNA microarray analysis. *Biotechniques* **29**:548-50, 552-4, 556 passim.
100. **Helliwell, P. A., D. Meredith, C. A. Boyd, J. R. Bronk, N. Lister, and P. D. Bailey.** 1994. Tripeptide transport in rat lung. *Biochim Biophys Acta* **1190**:430-4.
101. **Herrera-Ruiz, D., Q. Wang, O. S. Gudmundsson, T. J. Cook, R. L. Smith, T. N. Faria, and G. T. Knipp.** 2001. Spatial expression patterns of peptide transporters in the human and rat gastrointestinal tracts, Caco-2 in vitro cell culture model, and multiple human tissues. *AAPS PharmSci* **3**:E9.
102. **Hollywood, K., D. R. Brison, and R. Goodacre.** 2006. Metabolomics: current technologies and future trends. *Proteomics* **6**:4716-23.
103. **Huang, N. C., C. S. Chiang, N. M. Crawford, and Y. F. Tsay.** 1996. CHL1 encodes a component of the low-affinity nitrate uptake system in Arabidopsis and shows cell type-specific expression in roots. *Plant Cell* **8**:2183-91.
104. **Hunt, M. C., P. J. Lindquist, J. M. Peters, F. J. Gonzalez, U. Diczfalusy, and S. E. Alexson.** 2000. Involvement of the peroxisome proliferator-activated receptor alpha in regulating long-chain acyl-CoA thioesterases. *J Lipid Res* **41**:814-23.
105. **Ideker, T., T. Galitski, and L. Hood.** 2001. A new approach to decoding life: systems biology. *Annu Rev Genomics Hum Genet* **2**:343-72.
106. **Irie, M., T. Terada, M. Okuda, and K. Inui.** 2004. Efflux properties of basolateral peptide transporter in human intestinal cell line Caco-2. *Pflugers Arch* **449**:186-94.
107. **Jaluria, P., K. Konstantopoulos, M. Betenbaugh, and J. Shiloach.** 2007. A perspective on microarrays: current applications, pitfalls, and potential uses. *Microb Cell Fact* **6**:4.
108. **Jeffery, I. B., D. G. Higgins, and A. C. Culhane.** 2006. Comparison and evaluation of methods for generating differentially expressed gene lists from microarray data. *BMC Bioinformatics* **7**:359.
109. **Jolly, R. A., K. M. Goldstein, T. Wei, H. Gao, P. Chen, S. Huang, J. M. Colet, T. P. Ryan, C. E. Thomas, and S. T. Estrem.** 2005. Pooling samples within microarray studies: a comparative analysis of rat liver transcription response to prototypical toxicants. *Physiol Genomics* **22**:346-55.

110. **Jonsson, P., S. J. Bruce, T. Moritz, J. Trygg, M. Sjostrom, R. Plumb, J. Granger, E. Maibaum, J. K. Nicholson, E. Holmes, and H. Antti.** 2005. Extraction, interpretation and validation of information for comparing samples in metabolic LC/MS data sets. *Analyst* **130**:701-7.
111. **Karlsson, S., A. J. Scheurink, and B. Ahren.** 2002. Gender difference in the glucagon response to glucopenic stress in mice. *Am J Physiol Regul Integr Comp Physiol* **282**:R281-8.
112. **Kato, Y., K. Yoshida, C. Watanabe, Y. Sai, and A. Tsuji.** 2004. Screening of the interaction between xenobiotic transporters and PDZ proteins. *Pharm Res* **21**:1886-94.
113. **Kell, D. B.** 2004. Metabolomics and systems biology: making sense of the soup. *Curr Opin Microbiol* **7**:296-307.
114. **Kennedy, D. J., F. H. Leibach, V. Ganapathy, and D. T. Thwaites.** 2002. Optimal absorptive transport of the dipeptide glycylsarcosine is dependent on functional Na⁺/H⁺ exchange activity. *Pflugers Arch* **445**:139-46.
115. **Kersten, S., S. Mandard, P. Escher, F. J. Gonzalez, S. Tafuri, B. Desvergne, and W. Wahli.** 2001. The peroxisome proliferator-activated receptor alpha regulates amino acid metabolism. *Faseb J* **15**:1971-8.
116. **Khatri, P., and S. Draghici.** 2005. Ontological analysis of gene expression data: current tools, limitations, and open problems. *Bioinformatics* **21**:3587-95.
117. **Khatri, P., S. Sellamuthu, P. Malhotra, K. Amin, A. Done, and S. Draghici.** 2005. Recent additions and improvements to the Onto-Tools. *Nucleic Acids Res* **33**:W762-5.
118. **Kihara, H., and E. E. Snell.** 1952. PEPTIDES AND BACTERIAL GROWTH. II. L-ALANINE PEPTIDES AND GROWTH OF LACTOBACILLUS CASEI. *J. Biol. Chem.* **197**:791-800.
119. **Kleta, R., E. Romeo, Z. Ristic, T. Ohura, C. Stuart, M. Arcos-Burgos, M. H. Dave, C. A. Wagner, S. R. Camargo, S. Inoue, N. Matsuura, A. Helip-Wooley, D. Bockenhauer, R. Warth, I. Bernardini, G. Visser, T. Eggermann, P. Lee, A. Chairoungdua, P. Jutabha, E. Babu, S. Nilwarangkoon, N. Anzai, Y. Kanai, F. Verrey, W. A. Gahl, and A. Koizumi.** 2004. Mutations in SLC6A19, encoding B0AT1, cause Hartnup disorder. *Nat Genet* **36**:999-1002.
120. **Knutter, I., I. Rubio-Aliaga, M. Boll, G. Hause, H. Daniel, K. Neubert, and M. Brandsch.** 2002. H⁺-peptide cotransport in the human bile duct epithelium cell line SK-ChA-1. *Am J Physiol Gastrointest Liver Physiol* **283**:G222-9.
121. **Knutter, I., S. Theis, B. Hartrodt, I. Born, M. Brandsch, H. Daniel, and K. Neubert.** 2001. A novel inhibitor of the mammalian peptide transporter PEPT1. *Biochemistry* **40**:4454-8.
122. **Lash, L. H.** 2005. Role of glutathione transport processes in kidney function. *Toxicol Appl Pharmacol* **204**:329-42.
123. **LeBlanc, J., J. Soucy, and A. Nadeau.** 1996. Early insulin and glucagon responses to different food items. *Horm Metab Res* **28**:276-9.
124. **Lewandoski, M.** 2001. Conditional control of gene expression in the mouse. *Nat Rev Genet* **2**:743-55.
125. **Li, G.-H. L. G.-W. S., Yong-Hui; Shrestha, Sundar.** 2004. Angiotensin I-converting enzyme inhibitory peptides derived from food proteins and their physiological and pharmacological effects. *Nutrition Research* **24**:469-486.

126. **Liang, R., Y. J. Fei, P. D. Prasad, S. Ramamoorthy, H. Han, T. L. Yang-Feng, M. A. Hediger, V. Ganapathy, and F. H. Leibach.** 1995. Human intestinal H⁺/peptide cotransporter. Cloning, functional expression, and chromosomal localization. *J Biol Chem* **270**:6456-63.
127. **Lin, C. J., and D. E. Smith.** 1999. Glycylsarcosine uptake in rabbit renal brush border membrane vesicles isolated from outer cortex or outer medulla: evidence for heterogeneous distribution of oligopeptide transporters. *AAPS PharmSci* **1**:E1.
128. **Lin, H., and N. King.** 2006. Demonstration of functional dipeptide transport with expression of PEPT2 in guinea pig cardiomyocytes. *Pflugers Arch*.
129. **Lochman, P., T. Adam, D. Friedecky, E. Hlidkova, and Z. Skopkova.** 2003. High-throughput capillary electrophoretic method for determination of total aminothiols in plasma and urine. *Electrophoresis* **24**:1200-7.
130. **Löffler, G., Petrides PE.** 1998. *Biochemie und Pathobiochemie*, 6. Auflage ed. Springer Verlag, Berlin, Heidelberg, New York.
131. **Lopez, J. L.** 2006. Two-dimensional electrophoresis in proteome expression analysis. *J Chromatogr B Analyt Technol Biomed Life Sci*.
132. **M'Bemba, J., L. Cynober, P. de Bandt, M. Taverna, A. Chevalier, C. Bardin, G. Slama, and J. L. Selam.** 2003. Effects of dipeptide administration on hypoglycaemic counterregulation in type 1 diabetes. *Diabetes Metab* **29**:412-7.
133. **Magni, F., C. Sarto, C. Valsecchi, S. Casellato, S. F. Bogetto, S. Bosari, A. Di Fonzo, R. A. Perego, M. Corizzato, G. Doro, C. Galbusera, F. Rocco, P. Mocarelli, and M. Galli Kienle.** 2005. Expanding the proteome two-dimensional gel electrophoresis reference map of human renal cortex by peptide mass fingerprinting. *Proteomics* **5**:816-25.
134. **Mandard, S., M. Muller, and S. Kersten.** 2004. Peroxisome proliferator-activated receptor alpha target genes. *Cell Mol Life Sci* **61**:393-416.
135. **Matsui, T., K. Tamaya, E. Seki, K. Osajima, K. Matsumoto, and T. Kawasaki.** 2002. Val-Tyr as a natural antihypertensive dipeptide can be absorbed into the human circulatory blood system. *Clin Exp Pharmacol Physiol* **29**:204-8.
136. **Meissner, B., M. Boll, H. Daniel, and R. Baumeister.** 2004. Deletion of the intestinal peptide transporter affects insulin and TOR signaling in *Caenorhabditis elegans*. *J Biol Chem* **279**:36739-45.
137. **Meredith, D., and C. A. Boyd.** 1995. Dipeptide transport characteristics of the apical membrane of rat lung type II pneumocytes. *Am J Physiol* **269**:L137-43.
138. **Mijalski, T., A. Harder, T. Halder, M. Kersten, M. Horsch, T. M. Strom, H. V. Liebscher, F. Lottspeich, M. H. de Angelis, and J. Beckers.** 2005. Identification of coexpressed gene clusters in a comparative analysis of transcriptome and proteome in mouse tissues. *Proc Natl Acad Sci U S A* **102**:8621-6.
139. **Mohr, M., M. Klempt, B. Rathkolb, M. H. de Angelis, E. Wolf, and B. Aigner.** 2004. Hypercholesterolemia in ENU-induced mouse mutants. *J Lipid Res* **45**:2132-7.
140. **Mori, K., Y. Ogawa, N. Tamura, K. Ebihara, T. Aoki, S. Muro, S. Ozaki, I. Tanaka, K. Tashiro, and K. Nakao.** 1997. Molecular cloning of a novel mouse aspartic protease-like protein that is expressed abundantly in the kidney. *FEBS Lett* **401**:218-22.

141. **Nakamura, N., S. Masuda, K. Takahashi, H. Saito, M. Okuda, and K. Inui.** 2004. Decreased expression of glucose and peptide transporters in rat remnant kidney. *Drug Metab Pharmacokinet* **19**:41-7.
142. **Nduati, V., Y. Yan, G. Dalmasso, A. Driss, S. Sitaraman, and D. Merlin.** 2007. Leptin transcriptionally enhances peptide transporter (hPepT1) expression and activity via the cAMP-response element-binding protein and Cdx2 transcription factors. *J Biol Chem* **282**:1359-73.
143. **Nduati, V., Y. Yan, G. Dalmasso, S. Sitaraman, and D. Merlin.** 2006. Leptin transcriptionally enhances peptide transporter (hPepT1) expression and activity via the CREB and Cdx2 transcription factors. *J Biol Chem*.
144. **Neumann, J., and M. Brandsch.** 2003. Delta-aminolevulinic acid transport in cancer cells of the human extrahepatic biliary duct. *J Pharmacol Exp Ther* **305**:219-24.
145. **Nguyen, D. V., A. B. Arpat, N. Wang, and R. J. Carroll.** 2002. DNA microarray experiments: biological and technological aspects. *Biometrics* **58**:701-17.
146. **Nicholson, B., C. K. Manner, J. Kleeman, and C. L. MacLeod.** 2001. Sustained nitric oxide production in macrophages requires the arginine transporter CAT2. *J Biol Chem* **276**:15881-5.
147. **Nicholson, J. K., E. Holmes, J. C. Lindon, and I. D. Wilson.** 2004. The challenges of modeling mammalian biocomplexity. *Nat Biotechnol* **22**:1268-74.
148. **Nicholson, J. K., J. A. Timbrell, J. R. Bales, and P. J. Sadler.** 1985. A high resolution proton nuclear magnetic resonance approach to the study of hepatocyte and drug metabolism. Application to acetaminophen. *Mol Pharmacol* **27**:634-43.
149. **Nicholson, J. K., and I. D. Wilson.** 2003. Opinion: understanding 'global' systems biology: metabonomics and the continuum of metabolism. *Nat Rev Drug Discov* **2**:668-76.
150. **Nickolaus, M.** 2001. Nachweis und zelluläre Lokalisation des Peptidtransporters (PepT2) in extrarenalen Geweben. Dissertation. Justus Liebig Universität, Gießen.
151. **Nielsen, C. U., J. Amstrup, R. Nielsen, B. Steffansen, S. Frokjaer, and B. Brodin.** 2003. Epidermal growth factor and insulin short-term increase hPepT1-mediated glycylsarcosine uptake in Caco-2 cells. *Acta Physiol Scand* **178**:139-48.
152. **Nielsen, C. U., J. Amstrup, B. Steffansen, S. Frokjaer, and B. Brodin.** 2001. Epidermal growth factor inhibits glycylsarcosine transport and hPepT1 expression in a human intestinal cell line. *Am J Physiol Gastrointest Liver Physiol* **281**:G191-9.
153. **Noshiro, R., N. Anzai, T. Sakata, H. Miyazaki, T. Terada, H. J. Shin, X. He, D. Miura, K. Inui, Y. Kanai, and H. Endou.** 2006. The PDZ domain protein PDZK1 interacts with human peptide transporter PEPT2 and enhances its transport activity. *Kidney Int* **70**:275-82.
154. **Ocheltree, S. M., R. F. Keep, H. Shen, D. Yang, B. A. Hughes, and D. E. Smith.** 2003. Preliminary investigation into the expression of proton-coupled oligopeptide transporters in neural retina and retinal pigment epithelium (RPE): lack of functional activity in RPE plasma membranes. *Pharm Res* **20**:1364-72.

155. **Ocheltree, S. M., H. Shen, Y. Hu, R. F. Keep, and D. E. Smith.** 2005. Role and relevance of peptide transporter 2 (PEPT2) in the kidney and choroid plexus: in vivo studies with glycylsarcosine in wild-type and PEPT2 knockout mice. *J Pharmacol Exp Ther* **315**:240-7.
156. **Ocheltree, S. M., H. Shen, Y. Hu, J. Xiang, R. F. Keep, and D. E. Smith.** 2004. Mechanisms of cefadroxil uptake in the choroid plexus: studies in wild-type and PEPT2 knockout mice. *J Pharmacol Exp Ther* **308**:462-7.
157. **Ocheltree, S. M., H. Shen, Y. Hu, J. Xiang, R. F. Keep, and D. E. Smith.** 2004. Role of PEPT2 in the choroid plexus uptake of glycylsarcosine and 5-aminolevulinic acid: studies in wild-type and null mice. *Pharm Res* **21**:1680-5.
158. **Ogihara, H., H. Saito, B. C. Shin, T. Terado, S. Takenoshita, Y. Nagamachi, K. Inui, and K. Takata.** 1996. Immuno-localization of H⁺/peptide cotransporter in rat digestive tract. *Biochem Biophys Res Commun* **220**:848-52.
159. **Ogihara, H., T. Suzuki, Y. Nagamachi, K. Inui, and K. Takata.** 1999. Peptide transporter in the rat small intestine: ultrastructural localization and the effect of starvation and administration of amino acids. *Histochem J* **31**:169-74.
160. **Oliver, S. G., M. K. Winson, D. B. Kell, and F. Baganz.** 1998. Systematic functional analysis of the yeast genome. *Trends Biotechnol* **16**:373-8.
161. **Palacin, M., G. Borsani, and G. Sebastio.** 2001. The molecular bases of cystinuria and lysinuric protein intolerance. *Curr Opin Genet Dev* **11**:328-35.
162. **Palacin, M., R. Estevez, J. Bertran, and A. Zorzano.** 1998. Molecular biology of mammalian plasma membrane amino acid transporters. *Physiol Rev* **78**:969-1054.
163. **Palmiter, R. D., R. L. Brinster, R. E. Hammer, M. E. Trumbauer, M. G. Rosenfeld, N. C. Birnberg, and R. M. Evans.** 1982. Dramatic growth of mice that develop from eggs microinjected with metallothionein-growth hormone fusion genes. *Nature* **300**:611-5.
164. **Pastore, A., R. Massoud, C. Motti, A. Lo Russo, G. Fucci, C. Cortese, and G. Federici.** 1998. Fully automated assay for total homocysteine, cysteine, cysteinylglycine, glutathione, cysteamine, and 2-mercaptopropionylglycine in plasma and urine. *Clin Chem* **44**:825-32.
165. **Pastore, A., F. Piemonte, M. Locatelli, A. Lo Russo, L. M. Gaeta, G. Tozzi, and G. Federici.** 2001. Determination of blood total, reduced, and oxidized glutathione in pediatric subjects. *Clin Chem* **47**:1467-9.
166. **Pattyn, F., F. Speleman, A. De Paepe, and J. Vandesompele.** 2003. RTPrimerDB: the real-time PCR primer and probe database. *Nucleic Acids Res* **31**:122-3.
167. **Paulsen, I. T., and R. A. Skurray.** 1994. The POT family of transport proteins. *Trends Biochem Sci* **19**:404.
168. **Peters, L. L., R. F. Robledo, C. J. Bult, G. A. Churchill, B. J. Paigen, and K. L. Svenson.** 2007. The mouse as a model for human biology: a resource guide for complex trait analysis. *Nat Rev Genet* **8**:58-69.
169. **Pfaffl, M. W., A. Tichopad, C. Prgomet, and T. P. Neuvians.** 2004. Determination of stable housekeeping genes, differentially regulated target genes and sample integrity: BestKeeper--Excel-based tool using pair-wise correlations. *Biotechnol Lett* **26**:509-15.
170. **Pinsonneault, J., C. U. Nielsen, and W. Sadee.** 2004. Genetic Variants of the Human H⁺/Dipeptide Transporter PEPT2: Analysis of Haplotype Functions. *J Pharmacol Exp Ther* **311**:1088-96.

171. **Pritchard, C. C., L. Hsu, J. Delrow, and P. S. Nelson.** 2001. Project normal: defining normal variance in mouse gene expression. *Proc Natl Acad Sci U S A* **98**:13266-71.
172. **Qiu, J.** 2006. Animal research: mighty mouse. *Nature* **444**:814-6.
173. **Quackenbush, J.** 2006. From 'omes to biology. *Anim Genet* **37 Suppl 1**:48-56.
174. **Quan, H., K. Athirakul, W. C. Wetsel, G. E. Torres, R. Stevens, Y. T. Chen, T. M. Coffman, and M. G. Caron.** 2004. Hypertension and impaired glycine handling in mice lacking the orphan transporter XT2. *Mol Cell Biol* **24**:4166-73.
175. **Reeves, P. G., F. H. Nielsen, and G. C. Fahey, Jr.** 1993. AIN-93 purified diets for laboratory rodents: final report of the American Institute of Nutrition ad hoc writing committee on the reformulation of the AIN-76A rodent diet. *J Nutr* **123**:1939-51.
176. **Reeves, P. G., K. L. Rossow, and J. Lindlauf.** 1993. Development and testing of the AIN-93 purified diets for rodents: results on growth, kidney calcification and bone mineralization in rats and mice. *J Nutr* **123**:1923-31.
177. **Remesy, C., C. Moundras, C. Morand, and C. Demigne.** 1997. Glutamine or glutamate release by the liver constitutes a major mechanism for nitrogen salvage. *Am J Physiol* **272**:G257-64.
178. **Roberts, P. R., J. D. Burney, K. W. Black, and G. P. Zaloga.** 1999. Effect of chain length on absorption of biologically active peptides from the gastrointestinal tract. *Digestion* **60**:332-7.
179. **Rocha, D. M., G. R. Faloona, and R. H. Unger.** 1972. Glucagon-stimulating activity of 20 amino acids in dogs. *J Clin Invest* **51**:2346-51.
180. **Rodriguez, L., A. Batlle, G. Di Venosa, A. J. MacRobert, S. Battah, H. Daniel, and A. Casas.** 2006. Study of the mechanisms of uptake of 5-aminolevulinic acid derivatives by PEPT1 and PEPT2 transporters as a tool to improve photodynamic therapy of tumours. *Int J Biochem Cell Biol* **38**:1530-9.
181. **Roessner-Tunali, U., E. Urbanczyk-Wochniak, T. Czechowski, A. Kolbe, L. Willmitzer, and A. R. Fernie.** 2003. De novo amino acid biosynthesis in potato tubers is regulated by sucrose levels. *Plant Physiol* **133**:683-92.
182. **Roman, G., V. Meller, K. H. Wu, and R. L. Davis.** 1998. The opt1 gene of *Drosophila melanogaster* encodes a proton-dependent dipeptide transporter. *Am J Physiol* **275**:C857-69.
183. **Romano, A., G. Kottra, A. Barca, N. Tiso, M. Maffia, F. Argenton, H. Daniel, C. Storelli, and T. Verri.** 2006. High-affinity peptide transporter PEPT2 (SLC15A2) of the zebrafish *Danio rerio*: functional properties, genomic organization, and expression analysis. *Physiol Genomics* **24**:207-17.
184. **Rubio-Aliaga, I., M. Boll, and H. Daniel.** 2000. Cloning and characterization of the gene encoding the mouse peptide transporter PEPT2. *Biochem Biophys Res Commun* **276**:734-41.
185. **Rubio-Aliaga, I., and H. Daniel.** 2002. Mammalian peptide transporters as targets for drug delivery. *Trends Pharmacol Sci* **23**:434-40.
186. **Rubio-Aliaga, I., I. Frey, M. Boll, D. A. Groneberg, H. M. Eichinger, R. Balling, and H. Daniel.** 2003. Targeted disruption of the peptide transporter Pept2 gene in mice defines its physiological role in the kidney. *Mol Cell Biol* **23**:3247-52.
187. **Ruhl, A., S. Hoppe, I. Frey, H. Daniel, and M. Schemann.** 2005. Functional expression of the peptide transporter PEPT2 in the mammalian enteric nervous system. *J Comp Neurol* **490**:1-11.

188. **Saito, H., H. Motohashi, M. Mukai, and K. Inui.** 1997. Cloning and characterization of a pH-sensing regulatory factor that modulates transport activity of the human H⁺/peptide cotransporter, PEPT1. *Biochem Biophys Res Commun* **237**:577-82.
189. **Saito, H., M. Okuda, T. Terada, S. Sasaki, and K. Inui.** 1995. Cloning and characterization of a rat H⁺/peptide cotransporter mediating absorption of beta-lactam antibiotics in the intestine and kidney. *J Pharmacol Exp Ther* **275**:1631-7.
190. **Sakata, K., T. Yamashita, M. Maeda, Y. Moriyama, S. Shimada, and M. Tohyama.** 2001. Cloning of a lymphatic peptide/histidine transporter. *Biochem J* **356**:53-60.
191. **Sato, H., A. Shiiya, M. Kimata, K. Maebara, M. Tamba, Y. Sakakura, N. Makino, F. Sugiyama, K. Yagami, T. Moriguchi, S. Takahashi, and S. Bannai.** 2005. Redox imbalance in cystine/glutamate transporter-deficient mice. *J Biol Chem* **280**:37423-9.
192. **Schnackenberg, L. K., R. C. Jones, S. Thyparambil, J. T. Taylor, T. Han, W. Tong, D. K. Hansen, J. C. Fuscoe, R. D. Edmondson, R. D. Beger, and Y. P. Dragan.** 2006. An integrated study of acute effects of valproic acid in the liver using metabolomics, proteomics, and transcriptomics platforms. *Omics* **10**:1-14.
193. **Schultheis, P. J., L. L. Clarke, P. Meneton, M. L. Miller, M. Soleimani, L. R. Gawenis, T. M. Riddle, J. J. Duffy, T. Doetschman, T. Wang, G. Giebisch, P. S. Aronson, J. N. Lorenz, and G. E. Shull.** 1998. Renal and intestinal absorptive defects in mice lacking the NHE3 Na⁺/H⁺ exchanger. *Nat Genet* **19**:282-5.
194. **Seal, C. J., and D. S. Parker.** 1991. Isolation and characterization of circulating low molecular weight peptides in steer, sheep and rat portal and peripheral blood. *Comp Biochem Physiol B* **99**:679-85.
195. **Seifert, M., M. Scherf, A. Epple, and T. Werner.** 2005. Multievidence microarray mining. *Trends Genet* **21**:553-8.
196. **Sekura, R., and A. Meister.** 1974. Glutathione turnover in the kidney; considerations relating to the gamma-glutamyl cycle and the transport of amino acids. *Proc Natl Acad Sci U S A* **71**:2969-72.
197. **Seltmann, M., M. Horsch, A. Drobyshv, Y. Chen, M. H. de Angelis, and J. Beckers.** 2005. Assessment of a systematic expression profiling approach in ENU-induced mouse mutant lines. *Mamm Genome* **16**:1-10.
198. **Seow, H. F., S. Broer, A. Broer, C. G. Bailey, S. J. Potter, J. A. Cavanaugh, and J. E. Rasko.** 2004. Hartnup disorder is caused by mutations in the gene encoding the neutral amino acid transporter SLC6A19. *Nat Genet* **36**:1003-7.
199. **Sheikh, K., G. Camejo, B. Lanne, T. Halvarsson, M. Ryden-Landergren, and N. D. Oakes.** 2006. Beyond lipids, pharmacological PPAR{alpha} activation has important effects on amino acid metabolism as studied in the rat. *Am J Physiol Endocrinol Metab*.
200. **Shen, H., D. E. Smith, and F. C. Brosius, 3rd.** 2001. Developmental expression of PEPT1 and PEPT2 in rat small intestine, colon, and kidney. *Pediatr Res* **49**:789-95.
201. **Shen, H., D. E. Smith, R. F. Keep, and F. C. Brosius, 3rd.** 2004. Immunolocalization of the proton-coupled oligopeptide transporter PEPT2 in developing rat brain. *Mol Pharm* **1**:248-56.

202. **Shen, H., D. E. Smith, R. F. Keep, J. Xiang, and F. C. Brosius, 3rd.** 2003. Targeted disruption of the PEPT2 gene markedly reduces dipeptide uptake in choroid plexus. *J Biol Chem* **278**:4786-91.
203. **Shen, H., D. E. Smith, T. Yang, Y. G. Huang, J. B. Schnermann, and F. C. Brosius, 3rd.** 1999. Localization of PEPT1 and PEPT2 proton-coupled oligopeptide transporter mRNA and protein in rat kidney. *Am J Physiol* **276**:F658-65.
204. **Shi, L., L. H. Reid, W. D. Jones, R. Shippy, J. A. Warrington, S. C. Baker, P. J. Collins, F. de Longueville, E. S. Kawasaki, K. Y. Lee, Y. Luo, Y. A. Sun, J. C. Willey, R. A. Setterquist, G. M. Fischer, W. Tong, Y. P. Dragan, D. J. Dix, F. W. Frueh, F. M. Goodsaid, D. Herman, R. V. Jensen, C. D. Johnson, E. K. Lobenhofer, R. K. Puri, U. Schrf, J. Thierry-Mieg, C. Wang, M. Wilson, P. K. Wolber, L. Zhang, S. Amur, W. Bao, C. C. Barbacioru, A. B. Lucas, V. Bertholet, C. Boysen, B. Bromley, D. Brown, A. Brunner, R. Canales, X. M. Cao, T. A. Cebula, J. J. Chen, J. Cheng, T. M. Chu, E. Chudin, J. Corson, J. C. Corton, L. J. Croner, C. Davies, T. S. Davison, G. Delenstarr, X. Deng, D. Dorris, A. C. Eklund, X. H. Fan, H. Fang, S. Fulmer-Smentek, J. C. Fuscoe, K. Gallagher, W. Ge, L. Guo, X. Guo, J. Hager, P. K. Haje, J. Han, T. Han, H. C. Harbottle, S. C. Harris, E. Hatchwell, C. A. Hauser, S. Hester, H. Hong, P. Hurban, S. A. Jackson, H. Ji, C. R. Knight, W. P. Kuo, J. E. LeClerc, S. Levy, Q. Z. Li, C. Liu, Y. Liu, M. J. Lombardi, Y. Ma, S. R. Magnuson, B. Maqsodi, T. McDaniel, N. Mei, O. Myklebost, B. Ning, N. Novoradovskaya, M. S. Orr, T. W. Osborn, A. Papallo, T. A. Patterson, R. G. Perkins, E. H. Peters, R. Peterson, et al.** 2006. The MicroArray Quality Control (MAQC) project shows inter- and intraplatform reproducibility of gene expression measurements. *Nat Biotechnol* **24**:1151-61.
205. **Shi, L., W. Tong, H. Fang, U. Scherf, J. Han, R. K. Puri, F. W. Frueh, F. M. Goodsaid, L. Guo, Z. Su, T. Han, J. C. Fuscoe, Z. A. Xu, T. A. Patterson, H. Hong, Q. Xie, R. G. Perkins, J. J. Chen, and D. A. Casciano.** 2005. Cross-platform comparability of microarray technology: intra-platform consistency and appropriate data analysis procedures are essential. *BMC Bioinformatics* **6 Suppl 2**:S12.
206. **Shimakura, J., T. Terada, T. Katsura, and K. Inui.** 2005. Characterization of the human peptide transporter PEPT1 promoter: Sp1 functions as a basal transcriptional regulator of human PEPT1. *Am J Physiol Gastrointest Liver Physiol* **289**:G471-7.
207. **Shimakura, J., T. Terada, H. Saito, T. Katsura, and K. Inui.** 2006. Induction of intestinal peptide transporter 1 expression during fasting is mediated via peroxisome proliferator-activated receptor alpha. *Am J Physiol Gastrointest Liver Physiol* **291**:G851-6.
208. **Shimakura, J., T. Terada, Y. Shimada, T. Katsura, and K. Inui.** 2006. The transcription factor Cdx2 regulates the intestine-specific expression of human peptide transporter 1 through functional interaction with Sp1. *Biochem Pharmacol* **71**:1581-8.
209. **Shiraga, T., K. Miyamoto, H. Tanaka, H. Yamamoto, Y. Taketani, K. Morita, I. Tamai, A. Tsuji, and E. Takeda.** 1999. Cellular and molecular mechanisms of dietary regulation on rat intestinal H⁺/Peptide transporter PepT1. *Gastroenterology* **116**:354-62.

210. **Silbernagl, S., V. Ganapathy, and F. H. Leibach.** 1987. H⁺ gradient-driven dipeptide reabsorption in proximal tubule of rat kidney. Studies in vivo and in vitro. *Am J Physiol* **253**:F448-57.
211. **Sitaraman, S., X. Liu, L. Charrier, L. H. Gu, T. R. Ziegler, A. Gewirtz, and D. Merlin.** 2004. Colonic leptin: source of a novel proinflammatory cytokine involved in IBD. *Faseb J* **18**:696-8.
212. **Snell, E. E.** 1945. THE VITAMIN B6 GROUP. VII. REPLACEMENT OF VITAMIN B6 FOR SOME MICROORGANISMS BY d(-)-ALANINE AND AN UNIDENTIFIED FACTOR FROM CASEIN. *J. Biol. Chem.* **158**:497-503.
213. **Song, W., H. Y. Steiner, L. Zhang, F. Naider, G. Stacey, and J. M. Becker.** 1996. Cloning of a second Arabidopsis peptide transport gene. *Plant Physiol* **110**:171-8.
214. **Steiner, H. Y., F. Naider, and J. M. Becker.** 1995. The PTR family: a new group of peptide transporters. *Mol Microbiol* **16**:825-34.
215. **Suliman, M. E., J. C. Divino Filho, P. Barany, B. Anderstam, B. Lindholm, and J. Bergstrom.** 1999. Effects of high-dose folic acid and pyridoxine on plasma and erythrocyte sulfur amino acids in hemodialysis patients. *J Am Soc Nephrol* **10**:1287-96.
216. **Sweet, D. H., D. S. Miller, J. B. Pritchard, Y. Fujiwara, D. R. Beier, and S. K. Nigam.** 2002. Impaired organic anion transport in kidney and choroid plexus of organic anion transporter 3 (Oat3 (Slc22a8)) knockout mice. *J Biol Chem* **277**:26934-43.
217. **Tachibana, K., N. Anzai, C. Ueda, T. Katayama, T. Kirino, R. Takahashi, D. Yamasaki, K. Ishimoto, T. Tanaka, T. Hamakubo, Y. Ueda, H. Arai, J. Sakai, T. Kodama, and T. Doi.** 2006. Analysis of PPAR alpha function in human kidney cell line using siRNA. *Nucleic Acids Symp Ser (Oxf)*:257-8.
218. **Terada, T., M. Irie, M. Okuda, and K. Inui.** 2004. Genetic variant Arg57His in human H⁺/peptide cotransporter 2 causes a complete loss of transport function. *Biochem Biophys Res Commun* **316**:416-20.
219. **Terada, T., K. Sawada, T. Ito, H. Saito, Y. Hashimoto, and K. Inui.** 2000. Functional expression of novel peptide transporter in renal basolateral membranes. *Am J Physiol Renal Physiol* **279**:F851-7.
220. **Terada, T., K. Sawada, H. Saito, Y. Hashimoto, and K. Inui.** 1999. Functional characteristics of basolateral peptide transporter in the human intestinal cell line Caco-2. *Am J Physiol* **276**:G1435-41.
221. **Terada, T., Y. Shimada, X. Pan, K. Kishimoto, T. Sakurai, R. Doi, H. Onodera, T. Katsura, M. Imamura, and K. Inui.** 2005. Expression profiles of various transporters for oligopeptides, amino acids and organic ions along the human digestive tract. *Biochem Pharmacol* **70**:1756-63.
222. **Teuscher, N. S., H. Shen, C. Shu, J. Xiang, R. F. Keep, and D. E. Smith.** 2004. Carnosine uptake in rat choroid plexus primary cell cultures and choroid plexus whole tissue from PEPT2 null mice. *J Neurochem* **89**:375-82.
223. **Thamotharan, M., S. Z. Bawani, X. Zhou, and S. A. Adibi.** 1999. Functional and molecular expression of intestinal oligopeptide transporter (Pept-1) after a brief fast. *Metabolism* **48**:681-4.
224. **Thamotharan, M., S. Z. Bawani, X. Zhou, and S. A. Adibi.** 1998. Mechanism of dipeptide stimulation of its own transport in a human intestinal cell line. *Proc Assoc Am Physicians* **110**:361-8.

225. **Theis, S., B. Hartrodt, G. Kottra, K. Neubert, and H. Daniel.** 2002. Defining minimal structural features in substrates of the H(+)/peptide cotransporter PEPT2 using novel amino acid and dipeptide derivatives. *Mol Pharmacol* **61**:214-21.
226. **Theis, S., I. Knutter, B. Hartrodt, M. Brandsch, G. Kottra, K. Neubert, and H. Daniel.** 2002. Synthesis and characterization of high affinity inhibitors of the H+/peptide transporter PEPT2. *J Biol Chem* **277**:7287-92.
227. **Thwaites, D. T., C. D. Brown, B. H. Hirst, and N. L. Simmons.** 1993. H(+)-coupled dipeptide (glycylsarcosine) transport across apical and basal borders of human intestinal Caco-2 cell monolayers display distinctive characteristics. *Biochim Biophys Acta* **1151**:237-45.
228. **Thwaites, D. T., C. D. Brown, B. H. Hirst, and N. L. Simmons.** 1993. Transepithelial glycylsarcosine transport in intestinal Caco-2 cells mediated by expression of H(+)-coupled carriers at both apical and basal membranes. *J Biol Chem* **268**:7640-2.
229. **Thwaites, D. T., D. J. Kennedy, D. Raldua, C. M. Anderson, M. E. Mendoza, C. L. Bladen, and N. L. Simmons.** 2002. H/dipeptide absorption across the human intestinal epithelium is controlled indirectly via a functional Na/H exchanger. *Gastroenterology* **122**:1322-33.
230. **Torrents, D., R. Estevez, M. Pineda, E. Fernandez, J. Lloberas, Y. B. Shi, A. Zorzano, and M. Palacin.** 1998. Identification and characterization of a membrane protein (γ +L amino acid transporter-1) that associates with 4F2hc to encode the amino acid transport activity γ +L. A candidate gene for lysinuric protein intolerance. *J Biol Chem* **273**:32437-45.
231. **Toyomizu, M., K. Hayashi, K. Yamashita, and Y. Tomita.** 1988. Response surface analyses of the effects of dietary protein on feeding and growth patterns in mice from weaning to maturity. *J Nutr* **118**:86-92.
232. **Toyomizu, M., S. Kimura, K. Hayashi, Y. Tomita, and K. Yamashita.** 1989. Body protein and energy accretion in response to dietary protein level in mice from weaning to maturity. Response surface analyses of the effects of dietary protein on feeding and growth patterns in mice from weaning to maturity. *J Nutr* **119**:1028-33.
233. **Tramonti, G., P. Xie, E. I. Wallner, F. R. Danesh, and Y. S. Kanwar.** 2006. Expression and functional characteristics of tubular transporters: P-glycoprotein, PEPT1, and PEPT2 in renal mass reduction and diabetes. *Am J Physiol Renal Physiol* **291**:F972-80.
234. **Vavricka, S. R., M. W. Musch, M. Fujiya, K. Kles, L. Chang, J. J. Eloranta, G. A. Kullak-Ublick, K. Drabik, D. Merlin, and E. B. Chang.** 2006. Tumor necrosis factor- α and interferon- γ increase PepT1 expression and activity in the human colon carcinoma cell line Caco-2/bbe and in mouse intestine. *Pflugers Arch* **452**:71-80.
235. **Verri, T., G. Kottra, A. Romano, N. Tiso, M. Peric, M. Maffia, M. Boll, F. Argenton, H. Daniel, and C. Storelli.** 2003. Molecular and functional characterisation of the zebrafish (*Danio rerio*) PEPT1-type peptide transporter. *FEBS Lett* **549**:115-22.
236. **Vizcaino, J. A., R. E. Cardoza, M. Hauser, R. Hermosa, M. Rey, A. Llobell, J. M. Becker, S. Gutierrez, and E. Monte.** 2006. ThPTR2, a di/tri-peptide transporter gene from *Trichoderma harzianum*. *Fungal Genet Biol* **43**:234-46.

237. **Wada, M., S. Miyakawa, A. Shimada, N. Okada, A. Yamamoto, and T. Fujita.** 2005. Functional linkage of H⁺/peptide transporter PEPT2 and Na⁺/H⁺ exchanger in primary cultures of astrocytes from mouse cerebral cortex. *Brain Res* **1044**:33-41.
238. **Walker, D., D. T. Thwaites, N. L. Simmons, H. J. Gilbert, and B. H. Hirst.** 1998. Substrate upregulation of the human small intestinal peptide transporter, hPepT1. *J Physiol* **507 (Pt 3)**:697-706.
239. **Wang, X., and B. Seed.** 2003. A PCR primer bank for quantitative gene expression analysis. *Nucleic Acids Res* **31**:e154.
240. **Watahiki, A., K. Waki, N. Hayatsu, T. Shiraki, S. Kondo, M. Nakamura, D. Sasaki, T. Arakawa, J. Kawai, M. Harbers, Y. Hayashizaki, and P. Carninci.** 2004. Libraries enriched for alternatively spliced exons reveal splicing patterns in melanocytes and melanomas. *Nat Methods* **1**:233-9.
241. **Watanabe, C., Y. Kato, S. Ito, Y. Kubo, Y. Sai, and A. Tsuji.** 2005. Na⁺/H⁺ exchanger 3 affects transport property of H⁺/oligopeptide transporter 1. *Drug Metab Pharmacokinet* **20**:443-51.
242. **Watanabe, K., T. Jinriki, and J. Sato.** 2006. Effects of progesterone and norethisterone on cephalixin transport and peptide transporter PEPT1 expression in human intestinal cell line Caco-2. *Biol Pharm Bull* **29**:90-5.
243. **Watanabe, K., K. Terada, and J. Sato.** 2003. Intestinal absorption of cephalixin in diabetes mellitus model rats. *Eur J Pharm Sci* **19**:91-8.
244. **Waterston, R. H., K. Lindblad-Toh, E. Birney, J. Rogers, J. F. Abril, P. Agarwal, R. Agarwala, R. Ainscough, M. Alexandersson, P. An, S. E. Antonarakis, J. Attwood, R. Baertsch, J. Bailey, K. Barlow, S. Beck, E. Berry, B. Birren, T. Bloom, P. Bork, M. Botcherby, N. Bray, M. R. Brent, D. G. Brown, S. D. Brown, C. Bult, J. Burton, J. Butler, R. D. Campbell, P. Carninci, S. Cawley, F. Chiaromonte, A. T. Chinwalla, D. M. Church, M. Clamp, C. Clee, F. S. Collins, L. L. Cook, R. R. Copley, A. Coulson, O. Couronne, J. Cuff, V. Curwen, T. Cutts, M. Daly, R. David, J. Davies, K. D. Delehaunty, J. Deri, E. T. Dermitzakis, C. Dewey, N. J. Dickens, M. Diekhans, S. Dodge, I. Dubchak, D. M. Dunn, S. R. Eddy, L. Elnitski, R. D. Emes, P. Eswara, E. Eyra, A. Felsenfeld, G. A. Fewell, P. Flicek, K. Foley, W. N. Frankel, L. A. Fulton, R. S. Fulton, T. S. Furey, D. Gage, R. A. Gibbs, G. Glusman, S. Gnerre, N. Goldman, L. Goodstadt, D. Grafham, T. A. Graves, E. D. Green, S. Gregory, R. Guigo, M. Guyer, R. C. Hardison, D. Haussler, Y. Hayashizaki, L. W. Hillier, A. Hinrichs, W. Hlavina, T. Holzer, F. Hsu, A. Hua, T. Hubbard, A. Hunt, I. Jackson, D. B. Jaffe, L. S. Johnson, M. Jones, T. A. Jones, A. Joy, M. Kamal, E. K. Karlsson, et al.** 2002. Initial sequencing and comparative analysis of the mouse genome. *Nature* **420**:520-62.
245. **Weckwerth, W.** 2003. Metabolomics in systems biology. *Annu Rev Plant Biol* **54**:669-89.
246. **Weckwerth, W., M. E. Loureiro, K. Wenzel, and O. Fiehn.** 2004. Differential metabolic networks unravel the effects of silent plant phenotypes. *Proc Natl Acad Sci U S A* **101**:7809-14.
247. **Weckwerth, W., and K. Morgenthal.** 2005. Metabolomics: from pattern recognition to biological interpretation. *Drug Discov Today* **10**:1551-8.
248. **Weckwerth, W., K. Wenzel, and O. Fiehn.** 2004. Process for the integrated extraction, identification and quantification of metabolites, proteins and RNA to reveal their co-regulation in biochemical networks. *Proteomics* **4**:78-83.

249. **Wenzel, U., D. Diehl, M. Herget, S. Kuntz, and H. Daniel.** 1999. Regulation of the high-affinity H⁺/peptide cotransporter in renal LLC-PK1 cells. *J Cell Physiol* **178**:341-8.
250. **Whitedouble dagger, B. D., M. H. Porter, and R. J. Martin.** 2000. Protein selection, food intake, and body composition in response to the amount of dietary protein. *Physiol Behav* **69**:383-9.
251. **Wishart, D. S., D. Tzur, C. Knox, R. Eisner, A. C. Guo, N. Young, D. Cheng, K. Jewell, D. Arndt, S. Sawhney, C. Fung, L. Nikolai, M. Lewis, M. A. Coutouly, I. Forsythe, P. Tang, S. Shrivastava, K. Jeroncic, P. Stothard, G. Amegbey, D. Block, D. D. Hau, J. Wagner, J. Miniaci, M. Clements, M. Gebremedhin, N. Guo, Y. Zhang, G. E. Duggan, G. D. Macinnis, A. M. Weljie, R. Dowlatabadi, F. Bamforth, D. Clive, R. Greiner, L. Li, T. Marrie, B. D. Sykes, H. J. Vogel, and L. Querengesser.** 2007. HMDB: the Human Metabolome Database. *Nucleic Acids Res* **35**:D521-6.
252. **Wolfer, D. P., W. E. Crusio, and H. P. Lipp.** 2002. Knockout mice: simple solutions to the problems of genetic background and flanking genes. *Trends Neurosci* **25**:336-40.
253. **Wood, P. A.** 2000. Phenotype assessment: are you missing something? *Comp Med* **50**:12-5.
254. **Wren, J. D., and T. Conway.** 2006. Meta-analysis of published transcriptional and translational fold changes reveals a preference for low-fold inductions. *Omics* **10**:15-27.
255. **Xiang, J., Y. Hu, D. E. Smith, and R. F. Keep.** 2006. PEPT2-mediated transport of 5-aminolevulinic acid and carnosine in astrocytes. *Brain Res* **1122**:18-23.
256. **Xie, Y., W. Pan, and A. B. Khodursky.** 2005. A note on using permutation-based false discovery rate estimates to compare different analysis methods for microarray data. *Bioinformatics* **21**:4280-8.
257. **Yamashita, T., S. Shimada, W. Guo, K. Sato, E. Kohmura, T. Hayakawa, T. Takagi, and M. Tohyama.** 1997. Cloning and functional expression of a brain peptide/histidine transporter. *J Biol Chem* **272**:10205-11.
258. **Yang, X. D., J. Y. Ma, M. W. Barger, and J. K. Ma.** 2002. Transport and utilization of arginine and arginine-containing peptides by rat alveolar macrophages. *Pharm Res* **19**:825-31.
259. **Yang, Y. H., S. Dudoit, P. Luu, D. M. Lin, V. Peng, J. Ngai, and T. P. Speed.** 2002. Normalization for cDNA microarray data: a robust composite method addressing single and multiple slide systematic variation. *Nucleic Acids Res* **30**:e15.
260. **Yeung, A. K., S. K. Basu, S. K. Wu, C. Chu, C. T. Okamoto, S. F. Hamm-Alvarez, H. von Grafenstein, W. C. Shen, K. J. Kim, M. B. Bolger, I. S. Haworth, D. K. Ann, and V. H. Lee.** 1998. Molecular identification of a role for tyrosine 167 in the function of the human intestinal proton- coupled dipeptide transporter (hPepT1). *Biochem Biophys Res Commun* **250**:103-7.
261. **Ziegler, T. R., C. Fernandez-Estivariz, L. H. Gu, N. Bazargan, K. Umeakunne, T. M. Wallace, E. E. Diaz, K. E. Rosado, R. R. Pascal, J. R. Galloway, J. N. Wilcox, and L. M. Leader.** 2002. Distribution of the H⁺/peptide transporter PepT1 in human intestine: up-regulated expression in the colonic mucosa of patients with short-bowel syndrome. *Am J Clin Nutr* **75**:922-30.

Erklärung

Hiermit versichere ich, dass ich die vorliegende Arbeit

**Phenotypic characterization of peptide transporter PEPT2
deficient mice: assessing complex metabolic alterations by
profiling techniques**

selbständig verfasst und keine anderen als die angegebenen Quellen und Hilfsmittel benutzt habe. Die den benutzten Quellen wörtlich oder inhaltlich entnommenen Stellen sind als solch kenntlich gemacht

Diese Arbeit hat in gleicher oder ähnlicher Form noch keiner anderen Prüfungsbehörde vorgelegen.

Freising,

Isabelle Frey

Teile dieser Arbeit wurden vorab veröffentlicht:

Rubio-Aliaga I, **Frey I**, Boll M, Groneberg D, Eichinger HM, Balling R, Daniel H
Targeted disruption of the peptide transporter *Pept2* gene in mice defines its
physiological role in the kidney
Molecular and Cellular Biology 23, 3247-3252 (2003)

Frey IM, Rubio-Aliaga I, Klempt M, Wolf E, Daniel H
Phenotype analysis of mice deficient in the peptide transporter PEPT2 in response to
alterations in dietary protein intake
Plügeres Archiv – European Journal of Physiology, 452(3), 300-306 (2006)

Frey IM, Rubio-Aliaga I, Siewert A, Sailer D, Drobyshev A, Beckers J, Aubert J,
Bar Hen A, Fiehn O, Eichinger HM, Daniel H
Comprehensive molecular profiling at mRNA, protein and metabolite level reveals
alterations in renal amino acid handling and glutathione metabolism in kidney tissue
of *Pept2*^{-/-} mice
Physiological genomics 2007 Feb 12; 28(3): 301-310

Manuskript in Vorbereitung:

Frey IM, Rubio-Aliaga I, Scheundl R, Eichinger HM, Daniel H
Renal amino acid and dipeptide handling and corresponding alterations in kidney
protein expression in response to alterations in dietary protein intake in *Pept2*^{-/-} mice

Curriculum Vitae

Name: Isabelle Maria Anna Frey
Date of Birth: 23rd December 1974
Place of Birth: Augsburg, Germany
Current address: Viktoriastr. 55
CH-8050 Zurich, Switzerland
Phone: +41-44-3101350
E-mail: Isabelle.Frey@usz.ch
Civil status: Single
Nationality: German

School Education

1981 – 1985 primary school Neusäß Westheim
1985 – 1994 Gymnasium A. B. v. Stettensches Institut Augsburg
July 1994 Abitur (general qualification for university entrance)

University Education

1994 – 1998 Food Chemistry, State Exam

1999 – 2000 Postgraduate Studies in Human Nutrition, ETH Zurich,
Zurich, Switzerland, graduated as first of class
Thesis: Biomarkers of Bone Turnover: Applications and
Limitations in Diagnosis and Treatment of Osteoporosis
Additional Thesis: Critical Evaluation of Pro- and Prebiotics
on the Basis of Human Studies

2001 – 2007 PhD in Nutrition Physiology in the group of Prof. Dr. Hannelore
Daniel, Molecular Nutrition Unit, Technical University of Munich,
Weihenstephan, Germany

since 05/2007 Postdoc in the group of Prof. Dr. Dr. Gerhard Rogler,
Departement of Internal Medicine, Gastroenterology,
University Hospital Zurich, Zurich, Switzerland

Additional Qualifications

1999 Internship at the Norwich Institute of Food Research (UK)
Implementation and evaluation of a colorimetric method for
for analysis of serum iron and transferrin saturation
Assistance in human studies for mineral resorption

List of Scientific Publications

Peer reviewed original papers

- 1999 Tauer A, Hasenkopf K, Kislinger T, **Frey I**, Pischetsrieder M
Determination of N- ϵ -carboxymethyllysine in heated milk products
by immunochemical methods
Zeitschrift für Lebensmittel-Untersuchung und Forschung A:
Food Research and Technology 209(1), 72-76 (1999)
- 2001 **Frey I**, Arrigoni E, Amadò R
Kritische Betrachtung von Pro- und Präbiotika anhand von Humanstudien
Ernährung/Nutrition 25, 485-501 (2001)
- 2003 Rubio-Aliaga I, **Frey I**, Boll M, Groneberg D, Eichinger HM, Balling R, Daniel H
Targeted disruption of the peptide transporter *Pept2* gene in mice defines its
physiological role in the kidney
Molecular and Cellular Biology 23, 3247-3252 (2003)
- 2005 Rühl A, Hoppe S, **Frey I**, Daniel H, Schemann M
Functional expression of the peptide transporter PEPT2 in the mammalian
enteric nervous system
Journal of Comparative Neurology 490, 1-11 (2005)
- 2006 **Frey IM**, Rubio-Aliaga I, Klempt M, Wolf E, Daniel H
Phenotype analysis of mice deficient in the peptide transporter PEPT2 in
response to alterations in dietary protein intake
Pflügeres Archiv – European Journal of Physiology, 452(3), 300-306 (2006)
- 2007 **Frey IM**, Rubio-Aliaga I, Siewert A, Sailer D, Drobyshev A, Beckers J,
Aubert J, Bar Hen A, Fiehn O, Eichinger HM, Daniel H
Comprehensive molecular profiling at mRNA, protein and metabolite level
reveals alterations in renal amino acid handling and glutathione metabolism in
kidney tissue of *Pept2*^{-/-} mice
Physiological genomics 2007 Feb 12; 28(3): 301-310
- Font-Llitjos M, Feliubadalo L, Espino M, Cleries R, Manas S, **Frey IM**,
Puertas S, Colell G, Palomo S, Aranda J, Visa J, Palacin M, Nunes V
Slc7a9 knockout mouse is a good cystinuria model for anti-lithiasic
pharmacological studies
American Journal of Physiology Renal Physiology, 2007 Jun 27; [Epub
ahead of print]

Oral Presentations

- 2003 **Frey I**, Drobyshev A, Beckers J, Eichinger HM, Daniel H
Pept2 knockout mice show altered renal handling of amino acids
8th International Congress on Amino Acids and Proteins, Rome, 2003
- Frey I**, Drobyshev A, Beckers J, Eichinger HM, Daniel H
Pept2 knockout mice show altered renal handling of peptides
3rd Masterclass Nutrigenomics, University of Wageningen, Wageningen, 2003
- 2005 **Frey I**, Siewert A, Rubio-Aliaga I, Drobyshev A, Beckers J, Fiehn O, Eichinger HM, Daniel H
Transcriptome, proteome and metabolome of *Pept2*^{-/-} mouse kidney
NuGO week 2005 – 2nd European Nutrigenomics Conference, Castelvecchio Pascoli, 2005
- 2006 **Frey I**, Siewert A, Rubio-Aliaga I, Drobyshev A, Beckers J, Aubert J, Bar Hen A, Fiehn O, Eichinger HM, Daniel H
Transcriptome, proteome and metabolome profiling of *Pept2*^{-/-} mouse kidney tissue
Young FEPS at the Joint Meeting of the German Society of Physiology and the Federation of European Physiological Societies, Munich, 2006
Award for the best presentation
- Frey I**, Rubio-Aliaga I, Siewert A, Sailer D, Drobyshev A, Beckers J, Aubert J, Bar Hen A, Fiehn O, Eichinger HM, Daniel H
Comprehensive molecular profiling reveals novel phenotypic alterations in mice deficient for the high affinity peptide transporter PEPT2
Transporters 2006, Parma, 2006
- 2007 **Frey I**, Rubio-Aliaga I, Siewert A, Sailer D, Drobyshev A, Beckers J, Aubert J, Bar Hen A, Fiehn O, Eichinger HM, Daniel H
Application of profiling techniques to *Pept2*^{-/-} mice reveals novel phenotypic alterations
Annual meeting of the German physiological society, Hannover, 2007

Selected Poster Contributions

- 2002 **Frey I**, Rubio-Aliaga I, Danier J, Eichinger HM, Daniel H
Renal phenotype of the *Pept2* knockout mouse
Transporters 2002, Seon, 2002
- 2003 **Frey I**, Rubio-Aliaga I, Danier J, Eiching HM, Balling R, Daniel H
Targeted disruption of the peptide transporter PEPT2 in mice leads to altered renal handling of peptides
17th International Mouse Genome Conference, Braunschweig 2003
Award of an IMGC travel scholarship
- 2004 **Frey I**, Sailer D, Rubio-Aliaga I, Drobyshev A, Beckers J, Daniel H,
Analysis of differentially expressed genes in kidneys of PEPT2 knockout mice
1st International qPCR & Application Workshop, Freising, 2004
- 2005 **Frey I**, Rubio-Aliaga I, Siewert A, Letzel T, Eichinger HM, Daniel H
Altered renal handling of dipeptides in *Pept2*^{-/-} mice
Experimental Biology 2005 Annual Meeting and the XXXV International Congress of Physiological Sciences, San Diego (CA), 2005
- Frey I**, Siewert A, Rubio-Aliaga I, Drobyshev A, Beckers J, Fiehn O, Eichinger HM Daniel H
Transcriptome, proteome and metabolome of *Pept2*^{-/-} mouse kidney
6th EMBL Mouse Molecular Genetics Meeting, Heidelberg, 2005

Danksagung

An dieser Stelle möchte ich mich ganz herzlich bei allen, die auf vielfältige Weise zum Gelingen dieser Doktorarbeit beigetragen haben, bedanken.

Mein besonderer Dank gilt:

Frau Prof. H. Daniel, die mir die Doktorarbeit in Ihrer Arbeitsgruppe ermöglicht und mich dabei fortwährend gefordert und gefördert hat. Mit Ihrer Kompetenz, Begeisterungsfähigkeit und den vielen Freiheiten, die Sie mir gewährt hat, hat Sie entscheidend dazu beigetragen, dass ich sehr gerne an meiner Doktorarbeit gearbeitet habe.

Dr. Isabel Rubio-Aliaga für Ihre hervorragende Einführung in das Experimentieren mit Mäusen und viele weitere Techniken. Auch nach Ihrem Wechsel in eine andere Arbeitsgruppe stand Sie für alle meine Mäusefragen stets zur Verfügung und hat durch Ihre konstruktive Kritik so manche Überlegung angestoßen.

Prof. H. Eichinger für die unkomplizierte Bereitstellung seines Aminosäureanalyzers. Dr. J. Beckers, Dr. A. Drobyshev, Dr. A. Bar Hen, Dr. J. Aubert und Dr. O. Fiehn für die Durchführung der Transkriptom- und Metabolitanalysen und Unterstützung bei der Datenauswertung. Vielen Dank vor allem für die stete Bereitschaft mir diese Techniken zu erläutern.

Ronny Scheundl, der mir durch zuverlässige Versorgung der Mäuse und maßgebliche Unterstützung bei der Proteomanalyse eine große Hilfe war.

Helene Prunkl, die stets Zeit hatte, wenn bei den Mäusen Not am Mann war und Elmar Jocham für den Bau der Stoffwechselkäfige und Hilfe bei allen technischen Fragen.

Anne Siewert und Daniela Sailer, die bei der Erstellung Ihrer Zulassungsarbeiten wichtige Ergebnisse zu meinen Projekten beigesteuert haben.

Anne Nässl, die die Projekte mit großem Enthusiasmus weiterführt.

Birgit Kindermann, Maja Klapper, Angelika Herzog, Ladislav Raschka, Carolin Heim, Dietmar Weitz und Annika Helbig für die schönen Zeiten am Institut, bei sportlichen Aktivitäten und kulinarischen Experimenten.

Katja Bühlmeyer, die mir als Mitbewohnerin in allen Lebenslagen zur Seite stand.

Allen Mitarbeitern der Arbeitsgruppe Daniel. Die gute Atmosphäre im Labor und die gemeinsamen Feste lassen mich die Zeit in Freising immer als sehr schöne Zeit in Erinnerung behalten.

Meinem Freund Carsten Wagner, der meiner Begeisterung für Mäuse noch mal neuen Aufwind gegeben hat.

Meiner Mutter Sibylle Frey für ihre Unterstützung, ihr Vertrauen und ihre Geduld.